Fakultät für Medizin

Institut für Molekulare Immunologie- Experimentelle Onkologie

Establishing mRNA Delivery Systems for Conversion of Cell Differentiation Status

Zohreh Sadat Badieyan

Vollständiger Abdruck der von der Fakultät für Medizin der Technischen Universität München zur Erlangung des akademischen Grades eines

Doktor der Naturwissenschaften (Dr. rer. nat.)

genehmigten Dissertation.

Vorsitzender: Prof. Dr. Percy Knolle

Prüfer der Dissertation:

1. apl. Prof. Dr. Christian Plank

2. Prof. Dr. Friedrich Simmel

Die Dissertation wurde am 14.03.2016 bei der Technischen Universität München eingereicht und durch die Fakultät für Medizin am 03.08.2016 angenommen.

Table of contents

Figures

Figures

Figures

Tables

Acknowledgement

"This dissertation is dedicated to God, the beneficent the merciful, who helped me to make it through against all odds."

Though only my name appears on the cover of this dissertation, a great many people have contributed to its production. I owe my gratitude to all those people who have made this dissertation possible.

First and foremost, I offer my sincerest gratitude to my supervisor, Prof. Dr. Christian Plank, who has supported me throughout my thesis with his patience and knowledge, whilst giving me the freedom to explore on my own. His patience and support helped me overcome many crises and hardships to complete this dissertation. His effort on revision of this manuscript and the German translation of the thesis summary is much appreciated. I hope that one day I would be as fair, knowledgeable and patient to my students, as he was to me.

My sincere gratitude to Prof. Dr. Percy A. Knolle and Prof. Dr. Bernd Gänsbacher the heads of Institute of Molecular Immunology and the Institute of Experimental Oncology and Therapy Research, respectively, for giving me the opportunity to pursue my graduate studies in the medical faculty of Technical University Munich.

I would like to truly acknowledge PD. Dr. Carsten Rudolph for our numerous discussions on this topic, which helped me to uncover new ideas and improve my knowledge in my research area.

I am also thankful to Dr. Manish Aneja, who has always been there to listen and give advice. I am deeply grateful to him for the long discussions that helped me through the complicated situation

that I experienced. His consistent notations in my writings, and carefully reading and commenting on this manuscript is truly appreciated.

A special thanks goes to my second supervisor and my mentor, Prof. Dr. Friedrich Simmel and Prof. Dr. Axel Haase, respectively, for their insightful comments and constructive feedback at different stages of my research. This feedback was thought-provoking and helped me focus my ideas.

During my daily work, I have been blessed with a friendly and cheerful group of fellow students. I want to thanks all my friends, especially the members of "SPASS BOX" for all the joy and fun we have had throughout these years. The special thanks goes to Mehrije Ferizi, who helped me spiritually and technically throughout my PhD. Her help with German translation of my thesis summary as well as my CV is also truly appreciated.

I would like to thank the Ethris team for all their help, and for the friendly and scientific atmosphere they fostered. Namely, I want to thank Taras Berezhanskyy for his assistance with animal experiments.

My sincere thanks goes to Mrs. Gerlinde Stejskal who helped me to settle in Germany and to find accommodation in Munich (which is not an easy job!) when I first started my PhD.

I am also grateful to my supervisors and colleagues at my former university, "Mashhad University of Medical Sciences" in Iran, for their teaching and training during my Pharm.D. studies, which provided a good basis for my graduate studies.

Most importantly, none of this would have been possible without the love and patience of my family. I would like to express my heart-felt gratitude to my loving and caring parents, who have made me the person I am becoming. I am also deeply grateful to my parents-in-law who always

supported me and encouraged me with their best wishes. Last but not least, I want to thank my husband, Shahab; my divine gift, who came to my life exactly at the right time, and helped me to forget difficulties and forgive unfairness. Shahab, thanks for your endless love, care and patience. Thanks for being you.

Zohreh Sadat Badieyan
Munich, Germany
March 2016

Zusammenfassung

Transkript-Therapien mit chemisch modifizierten Boten-RNAs (cmRNAs) werden als vielversprechende und sichere Alternative zu Gen- und Proteinersatztherapien entwickelt. In Patientenzellen zu einem therapeutischen Protein translatierte cmRNAs sollten im Vergleich zu rekombinanten Proteinen ein geringeres Risiko von adoptiver Immunogenität bergen, und im Vergleich zu Gentherapien bergen sie nicht das Risiko der insertionellen Mutagenese. In dieser Dissertation wurden effiziente Methoden zum Transport von cmRNAs in Zellen etabliert, die für die Zelldifferenzierung und Dedifferenzierung verwendbar sind. Um den Differenzierungsstatus einer Zelle zu ändern, sollten in der Regel ein oder mehrere Transkriptions- bzw. Wachstumsfaktoren über einen bestimmten Zeitraum in Zielzellen von cmRNA translatiert werden, um Dedifferenzierung bzw. Differenzierung hervorzurufen. Dazu kann entweder ein verbesserter Transport von cmRNAs in Zielzellen oder eine verlängerte Abgabe von cmRNAs an Zielzellen aus einem Depot heraus hilfreich sein.

Für eine zukünftige Verwendung zur Zell-Dedifferenzierung wurde in dieser Dissertation die Magnetofektion von gleichzeitig mehreren cmRNAs als verbesserte Transportmethode entwickelt. Zuerst wurde die Magnetofektion unter Verwendung von verschiedenen magnetischen Nanopartikeln mit unterschiedlichen Eisen-zu-RNA-Verhältnissen, mit der normalen Lipofektion und Polyfektion unter der Verwendung von Luciferase (Luc) cmRNA verglichen, um ein optimales Protokoll für die Transfektion von cmRNAs zu etablieren. Anschließend wurde dieses Protokoll für die Co-Transfektion von bis zu drei Reporter cmRNAs (Luc, eGFP und RFP) in Monokultur von primären embryonalen murinen Fibroblasten (PMEF) oder Co-Kultur von PMEF und fötalen Fibroblasten vom Schwein (PFF) getestet. Parallel dazu wurde eine Kinetikstudie durchgeführt, um die Wirkung der Magnetofektion auf die Translation von d2eGFP cmRNA zu untersuchen.

Schließlich, wurde das Protokoll auch für die Co-Transfektion verschiedener cmRNAs auf Mono-und-Co-Kulturen von unterschiedlichen Zellen optimiert. Dies ist in der Forschung und in therapeutischen Anwendungen relevant, wenn eine gleichzeitige Wirkung von mehreren in der mRNA kodierten Proteinen erforderlich ist, wie beispielsweise zur Reprogrammierung zu induzierten pluripotenten Stammzellen (iPS) mit cmRNAs von Yamanaka-Faktoren.

Im zweiten Teil dieser Dissertation wurden vakuum-getrocknete, mit cmRNA beladene Kollagenschwämme als Transkript-aktivierte Matrizen (TAMs) für einen nachhaltigen mRNA Transport entwickelt, die eine anhaltend hohe Protein-Translation über sechs Tage hinweg ermöglichten. Ein besonderer Vorteil der entwickelten Technologie ist ihre hohe Transfektionseffizienz von bis zu 100% transfizierte Zellen bei geringer Zelltoxizität. Auf den TAM geladene cmRNAs in Lipid-Nanopartikelformulierung waren mindestens 6 Monate lang bei Raumtemperatur stabil. Zum Ende dieser Arbeit wurden optimierte TAMs mit cmRNA hergestellt, welche für humanes Bone Morphogenetic Protein 2 (hBMP2) kodieren. Mit diesen TAMs wurde in vitro osteogene Differenzierung mit MC3T3-E1-Zellen und mesenchymalen Stammzellen erzielt. Schließlich konnte in einem nicht kritischen Femurknochen-Defektmodell in der Ratte eine durch diese TAMs induzierte verbesserte Knochenheilung nachgewiesen werden und so die Eignung des Systems in einer präklinischen therapeutischen Anwendung demonstriert werden.

In dieser Dissertation wurden zusammengefasst zwei hoch effiziente Methoden für den Transport von cmRNAs in Zellen entwickelt. Die erste Methode empfiehlt sich für die weitere Verwendung zur Reprogrammierung von differenzierten Zellen zu Stammzellen, die zweite Methode ist nachweislich für die Induktion einer osteogenen Differenzierung und damit zur Knochenheilung geeignet. Beide Methoden bringen die Transkript-Therapie einen Schritt näher an die klinische Anwendung heran.

Summary

Transcript therapies, using chemically modified messenger RNAs (cmRNAs), are emerging as safer yet promising substitutes for gene and recombinant protein therapies. cmRNAs do not harbor the risk of insertional mutagenesis which is normally associated with DNA-based gene delivery. In addition, adoptive immunogenicity accompanied with recombinant protein therapy is less likely to happen when using cmRNAs. In this thesis, efficient methods for cmRNAs delivery, which are useful for cell differentiation and dedifferentiation, were established. To change a cell's differentiation status, normally one or more transcription factors should over-express for a defined period. Therefore, either enhanced delivery or prolonged delivery of cmRNAs can be helpful to reach the goal.

In this thesis, magnetofection of cmRNAs has been introduced as an enhanced cmRNA delivery method for future use in cell dedifferentiation. First, magnetofection, using different magnetic nanoparticles with various iron-to-RNA ratios, was compared to normal lipofection and polyfection to find an optimized protocol for single cmRNA delivery, using Luciferase (Luc) cmRNA. Then the established protocol was tested for cotransfection of up to three reporter cmRNAs (Luc, eGFP and RFP) in the mono-culture of Primary Mouse Embryonic Fibroblasts (PMEFs), or the coculture of PMEFs and Porcine Fetal Fibroblasts (PFFs). In parallel, kinetics studies were performed to investigate the effect of magnetofection on kinetics of expression of d2eGFP cmRNA. As a result, the protocol was well optimized for cotransfection of different cmRNAs on mono-and-co-cultures of different cells. This is relevant in research and therapeutic applications when simultaneous translation of several cmRNA-encoded proteins is required, such as reprogramming to induced pluripotent Stem Cells (iPSCs) with cmRNAs encoding Yamanaka factors.

Summary

In the second part of this study, vacuum-dried cmRNA-loaded collagen sponges were used as transcript-activated matrices (TAMs). TAMs served as depots for sustained cmRNA delivery, providing steady state protein production for six consecutive days. A particular advantage of this technology was high cell transfection efficacy (close to 100%) and low cell toxicity. Considering stability issues, cmRNAs loaded on the TAMs were stable for at least 6 months at room temperature. At the end, osteogenic differentiation *in vitro* (with MC3T3-E1 cells and mesenchymal stem cells), and bone regeneration *in vivo* (in rat femur defects), using hBMP2 cmRNAs, confirmed the ability of the system in a preclinical application.

Summarizing, two highly efficient methods for mRNA transfection were developed in this thesis. The first one will be useful for reprogramming differentiated cells to stem cells. The second one was proven to be suitable for inducing osteogenic differentiation and bone regeneration. Both methods bring transcript therapy a step closer to clinical applications.

1 Introduction

1.1 Messenger RNA (mRNA)

1.1.1 mRNA; transcription and transcript

Messenger RNA (mRNA) is a large family of RNA molecules that transfers genetic information from DNA to the ribosome, where the genetic information is translated into a specific protein (Figure 1).

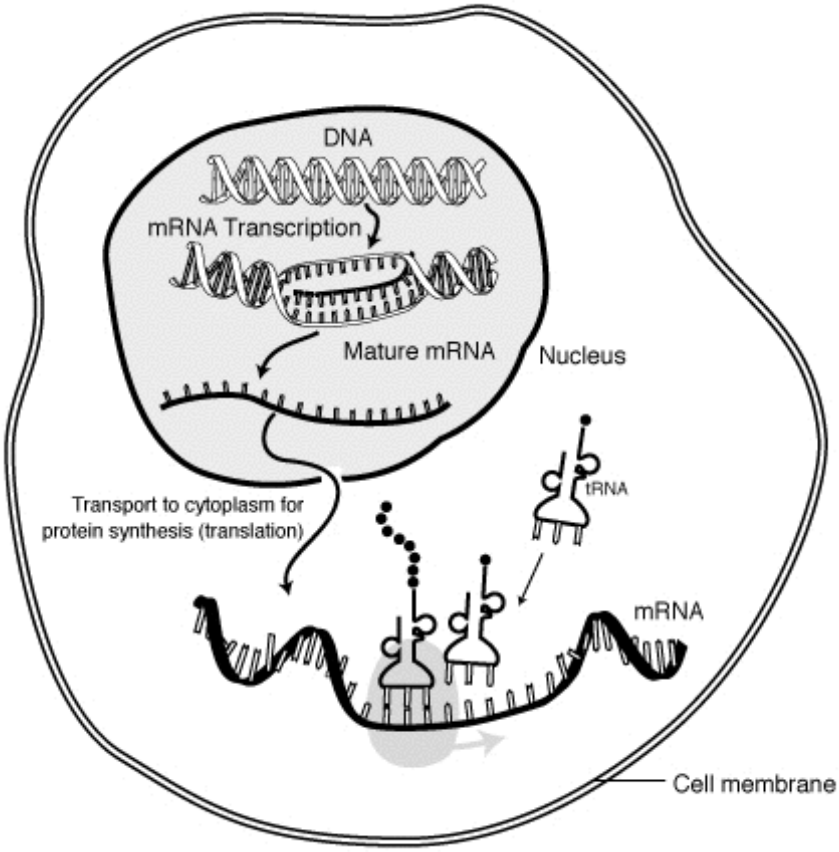

Figure 1 From DNA to protein; mRNA convey the information from nucleus to ribosomal machinery (resource: Wikipedia)

Following DNA transcription by RNA polymerase, the precursor mRNA, known as primary transcript, is created. The precursor mRNA is further subjected to post-transcriptional modifications namely, addition of a 5´ cap, polyadenylation at the 3´ end, and RNA splicing. The final product, so called mature mRNA, can be translated into the final protein with the help of ribosome's protein-manufacturing machinery [1].

1.1.2 mRNA structure

The general structure of a mature eukaryotic mRNA is illustrated in Figure 2.

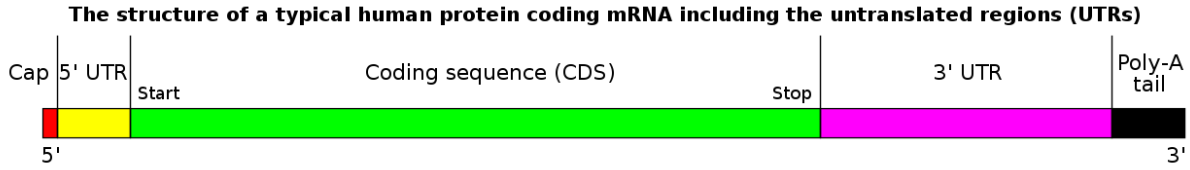

Figure 2 Structure of a mature eukaryotic mRNA (resource: Wikipedia)

A fully processed mRNA includes a 5' cap, 5' untranslated region (5´UTR), coding region, a 3' UTR, and a poly(A) tail. The coding region, also known as open reading frame (ORF), contains the genetic information for protein production. ORF starts with the start codon AUG, and terminates with one of the stop codons UAA, UAG, or UGA.

UTRs, on the other hand, often contain regulatory regions that affect translation efficiency, localization, and stability of the mRNA [2-4]. For example, incorporation of UTRs of β-globin mRNA greatly improves RNA stability and leads to more than a 1,000-fold increase in reporter gene expression than mRNAs lacking these elements [5].

In addition to UTRs, the 5´cap and the 3´poly(A) tail protect the mRNA molecules from enzymatic degradation, and are also essential for nuclear export and translation of mRNA [6-9].

1.2 mRNA therapeutics: a versatile substitute for protein and gene therapy

In recent decades, recombinant protein and gene therapy have been considered as impressive remedies for life-threatening genetic diseases. However, despite all progress, considerable implications have accompanied these approaches thus far. In protein therapy, the recombinant proteins can elicit an immune response, as they were not produced in the host's protein machinery, and are recognized as foreign antigens [10]. In gene therapy, on the other hand, entry of DNA into the nucleus is well known to be a success-limiting step, especially for non-viral delivery systems. Delivery into the nucleus is even more problematic for transfection of non-dividing cells, as these cells rarely have cell cycle-dependent breakdown of the nuclear membrane [11, 12]. The other significant drawback of DNA-based delivery is potential mutagenicity, due to the risk of insertion of DNA into the host genome and the subsequent induction / suppression of endogenous gene expression [13, 14].

The limitations of DNA-based gene therapy have led to intense research focus on messenger RNAs, a promising alternative, which neither needs to enter the nucleus, nor harbors the risk of insertional mutagenesis. Moreover mRNA transfection results in rapid but transient production of the protein of interest, which might serve as an additional safety aspect in regenerative medicine [15, 16]. Accordingly, mRNAs are emerging as promising therapeutics in a broad variety of medical indications [17-19].

1.2.1 Difficulties in applications of mRNA therapeutics; solutions and modifications

Although the idea of RNA-based transfection is associated with a great number of advantages in gene therapy, the strong immunogenicity and limited stability of conventional mRNA hamper its widespread utilities [20]. Recently, these problems have been overcome, using chemically modified mRNA (cmRNA), in which 5 – 50% of the uridines and cytidines is replaced with thio-uridine and 5-methyl-cytidine, respectively. This type of cmRNA, also called stabilized non-immunogenic mRNA (SNIM RNA), is prepared by *in vitro* transcription [21, 22].

1.3 mRNA delivery: current methods and future perspectives

1.3.1 Current methods for mRNA delivery

Mechanical methods, such as gene gun delivery of mRNA have been investigated for transgene expression to elicit immunity [23]. Electroporation, as another example of mechanical methods, has been used to deliver mRNA-encoding tumor antigens to transfect human dendritic cells for dendritic cell-based tumor vaccines [24]. Naked mRNA also has been shown to successfully transfect dendritic cells *in vitro* [25].

Numerous studies have established cationic lipids as efficient non-viral vectors for mRNA delivery, whereas polycations have not been so intensely investigated with respect to their potential as mRNA delivery agents [5, 26-29].

1.3.2 Magnetofection: enhanced nucleic acid delivery

In 2000, the generic term “magentofection” was introduced for the first time [30], and has since been independently developed by a number of different research groups [31-35]. Recently,

magnetofection has been widely used as a dependable and efficient transfection method for localized enhanced delivery of nucleic acids [36].

In this method, nucleic acids, along with viral and non-viral vectors, are associated with magnetic nanoparticles. The resulting magnetic complexes can then be concentrated on the target cells' membranes, using a magnetic field [37] to attain targeted and/or enhanced delivery (Figure 3) [36, 38, 39].

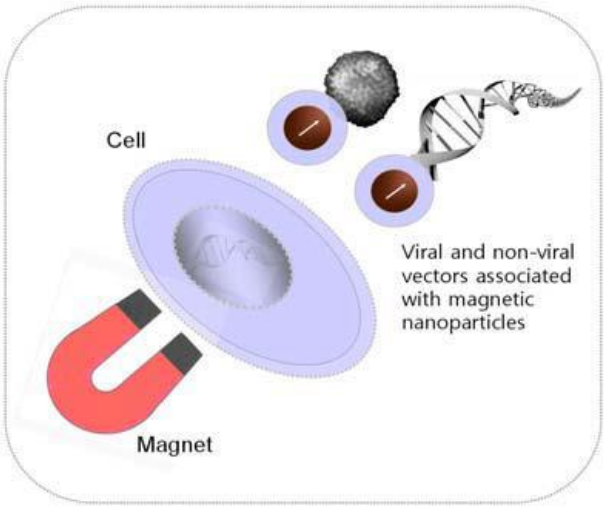

Figure 3 Magnetofection; magnetic field force the nucleic acid / vector to the target cell (C. Plank et al. / Adv. Drug Deliv. Rev. 63 (2011) 1300–1331)

Magnetofection accelerates vector sedimentation on the surface of the target cells, and hence overcomes the slow diffusion and time-dependent inactivation of vectors under cell culture conditions [40]. Nevertheless, the mechanism of vector uptake by magnetofection is probably the same as for a conventional transfection, namely endocytosis [37]. In addition, it has been previously shown that the magnetic nanoparticles are fully biocompatible and biodegradable after *in vivo* applications [41].

Magnetofection has been well established for DNA as well as for small interfering RNA (siRNA) delivery to the target cells *in vitro* [39, 42-44]. Several studies have also proved the *in vivo* functionality of magnetofection for delivery of DNA plasmid [40, 45], short hairpin RNA (shRNA) [46], and antisense oligodesoxynucleotides [47]. The magnetofection of messenger RNA, however, has been demonstrated and established for the first time in the current work.

1.3.3 Transcript-activated matrices (TAMs): sustained mRNA delivery

1.3.3.1 3D cell culture versus conventional 2D cell culture

2D "petri dish"-based cell culture on polystyrene or glass materials has been, and still is, the most common method for culturing eukaryotic cells [48]. However, recent studies have shown that, compared to 'petri dish'-based 2D cell cultures, the culturing of cells within 3D scaffolds more closely resembles the *in vivo* situation with regard to cell shape, cell signaling and cellular behavior, which in turn can influence gene expression in the cells [49, 50]. Therefore, 3D cell culture models can bridge the gap between conventional 2D cell culture systems and *in vivo* tissues. Such 3D models can, therefore, reduce the number of animal studies needed for efficacy and toxicity screening [51].

1.3.3.2 3D culture models-Scaffold free systems

Based on use or non-use of scaffolds, 3D culture models can be divided into two groups. The most common examples of 3D culture without scaffolds are organotypic explant cultures and cell spheroids (Figure 4) [48, 51].

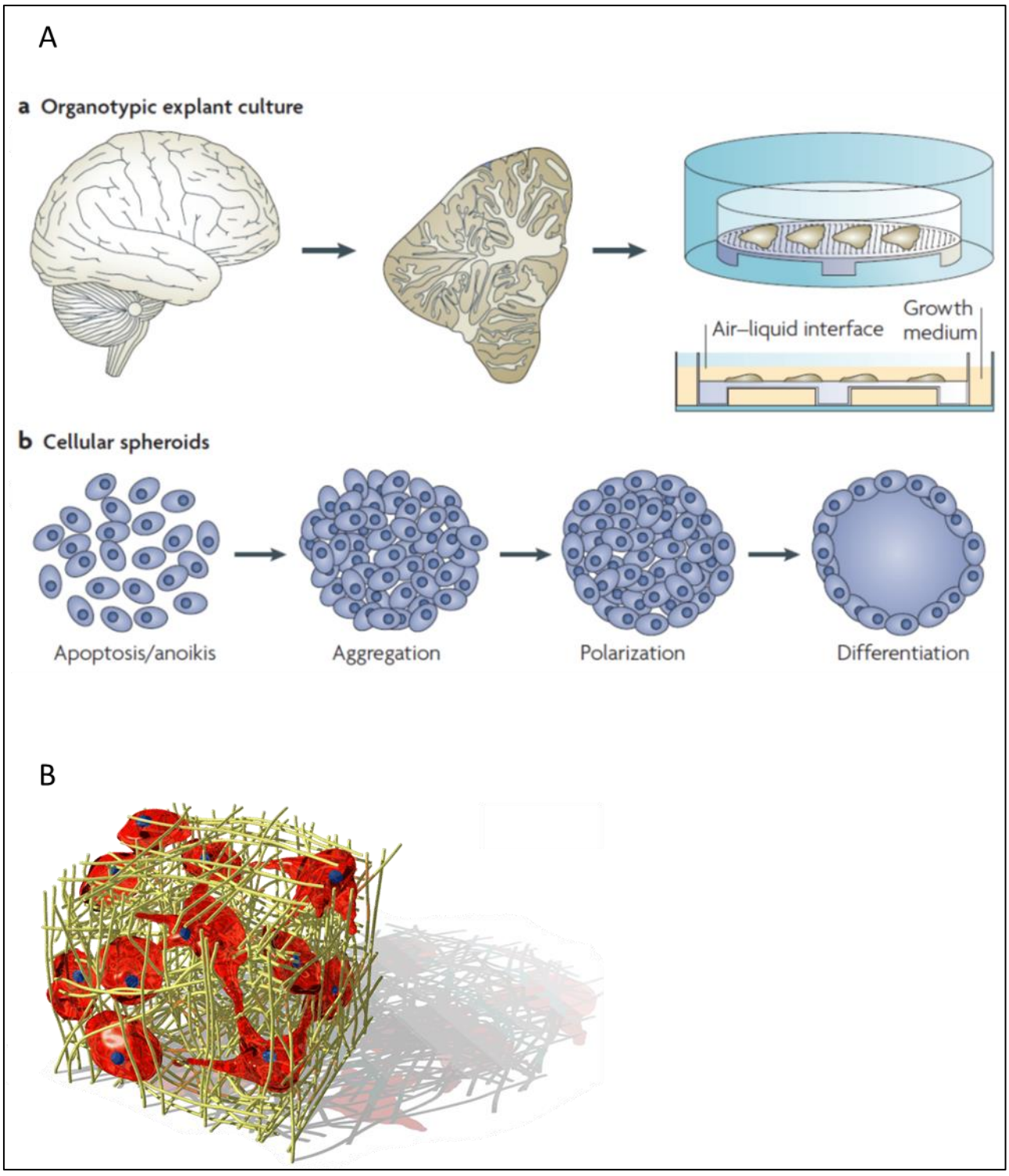

Figure 4 Models for 3D cultures. (A) Without using scaffolds. (a) Organotypic explant culture. (b) Cellular spheroids (figures taken from Pmpaloni F. et al./ Nature Rev Mol cell biol. 2007;8:839-45) [51]. (B) Using 3D scaffold (Figure provided by http://www.medibena.at)

Organotypic explant culture, in which organ slices are cultured either on a semiporous membrane or within a collagen gel, preserves the original tissue architecture very well. Such a model has been widely used for studies of brain and neural physiology [52, 53]. The heterogeneity and low transparency of organ explants are the main drawbacks associated with this model.

Cellular spheroids are the reductionist simple 3D models that benefit from the tendency of adherent cells to aggregate. Similar to organotypic culture, spheroids do not require scaffolds. However, their higher transparency makes them good candidates for imaging with light, fluorescence and confocal microscopy [48]. Spheroid models have been widely used for solid tumor studies [54]. Despite all these advantages, applications of spheroids are limited by the size of 3D cultures. When cell aggregation mass exceeds 1-2 mm, toxicity problems arise due to lack of transfer of nutrition and waste metabolites into and out of the spheroid [51, 55]. This problem has been overcome by the use of highly porous scaffolds, which allow the flow of gases, nutrition and metabolites [56].

1.3.3.3 3D culture scaffolds; collagen polymers

Within the metals, glasses, polymers, and ceramics that can be used as 3D scaffold for 3D cell culture, polymers have received the most interest due to the possibility of controlling their chemical and structural properties. Polymer matrices are subdivided further into synthetic (e.g. poly glycolic acid (PGA) and poly lactic acid (PLA)), and natural polymers (e.g. collagen and chitosan) [56, 57].

A substantial requirement of all biomaterial scaffolds is that they provide an extracellular matrix environment for supporting cell growth. In addition, an ideal 3D scaffold for clinical purposes should be biocompatible and biodegradable [58]. Natural polymers, such as collagen, tend to be more biocompatible than synthetic ones [58].

Collagen is one of the abundant and highly biocompatible natural polymers for 3D cell culture. Collagen, a fibrous, triple-stranded helical protein, which serves as a mechanical support for

connective tissues, is involved in cell distribution and different functional expressions in the cells [59]. Collagen sponges, as 3D scaffolds for cell culture, can modify migration, attachment, adhesion, and in certain cases the differentiation of cells, as described in detail by Chevallay *et.al.* [60]. Although there are at least 19 different types of collagen, collagen type I (located in skin and bone), type II (cartilage), and type III (blood-vessel walls) are considered the main types [57, 59].

1.3.3.4 Collagen scaffolds; biomedical applications

Collagen has been successfully investigated for tissue engineering as well as drug/protein/gene delivery (Figure 5) [59, 61-63].

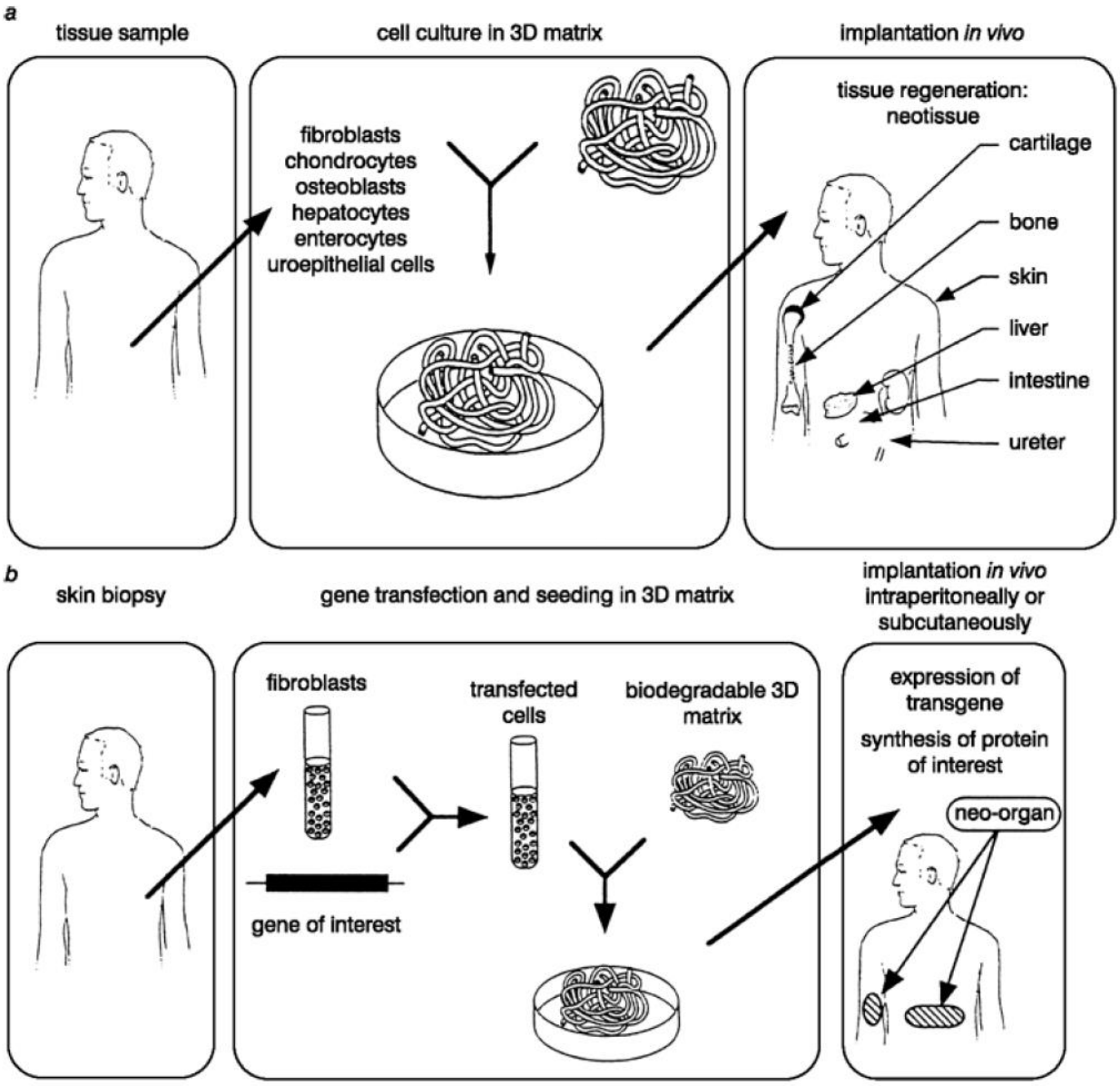

Figure 5 Collagen sponges serves as suitable 3D scaffolds for (a) tissue engineering and (b) gene therapy. Figure taken form Chevallay et al./ Med Bio Eng Comput, 2000, 38: 211-8 [60].

Extra strength and stability of collagen fibers, which come from their self-aggregation and cross-linking, make them excellent scaffolds for biomedical uses. Indeed, the degree of *in vivo* biodegradability of collagen scaffolds can be controlled with the help of crosslinking agents such as glutaraldehyde [59]. Regarding tissue engineering, collagen-based implants have been evaluated for dermal tissues and burn wounds [64, 65], bone regeneration [66, 67], blood vessels and heat

valves [68, 69], periodontal tissues [70], and peripheral nerve regeneration [71]. In addition, collagen in the form of films, shields, sponges, gels, and tablets has been successfully used for gene, protein and drug delivery [59, 63, 72-74]. Currently, collagen is the only FDA approved carrier for recombinant bone morphology protein 2 (BMP2), which is useful for bone healing [75].

1.3.3.5 Collagen sponges for sustained cmRNA delivery

For years, sustained gene or drug delivery systems have been the subject of intense research as they provide patients with a steady state concentration of their cargos and reduce multiple dosing schedules. As a result, patient compliance is increased, which in turn can lead to a better acceptance of therapeutic approaches [76, 77]. In case of cmRNA therapy, such retard delivery systems can be particularly suitable when long-term protein expression is the aim. Nevertheless, efficient methods for sustained delivery of mRNAs are lacking so far. Therefore, collagen sponges have been tested for the first time in this project as carriers for sustained cmRNA delivery.

1.4 Cell fate conversion: changing cell differentiation status

Transcription factors are able to modify or even change the cells' fates. The ability to convert a stem cell to a somatic cell (differentiation), or a somatic cell to a stem cell (dedifferentiation) holds great promise for cell-based therapy and regenerative medicine [78, 79] (Figure 6).

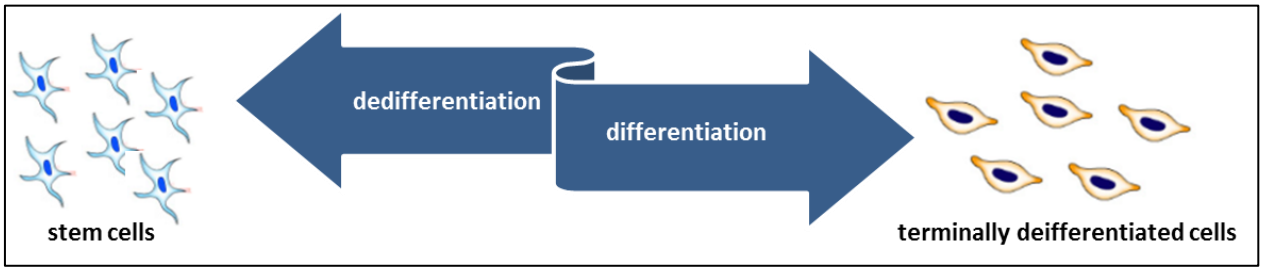

Figure 6 Genetically modified cells can undergo differentiation or dedifferentiation

1.4.1 Differentiation

Cell differentiation refers to a process in which a less specialized cell, such as a stem cell, changes to the more specialized one. This process finally leads to the terminally differentiated cells, which are not able to further differentiate [1].

Differentiation of cells to osteoblasts by using BMPs is one example of cell differentiation application in regenerative medicine. Several studies have shown that BMP2 can trigger differentiation to osteoblasts, and thus is a suitable tool for bone healing *in vitro* and *in vivo*, using either protein or gene therapy approaches [80-82]. Bone regeneration with BMP2 cmRNA has been established within this thesis.

1.4.2 Dedifferentiation

Cell dedifferentiation, also known as cell reprogramming, is a relatively new approach in biotechnology, where a specialized cell reverts to a simpler state of stem cell. The self-renewal properties along with their capability to give rise to multiple differentiated cell types make stem cells unique tools for regenerative medicine (Figure 7) [83].

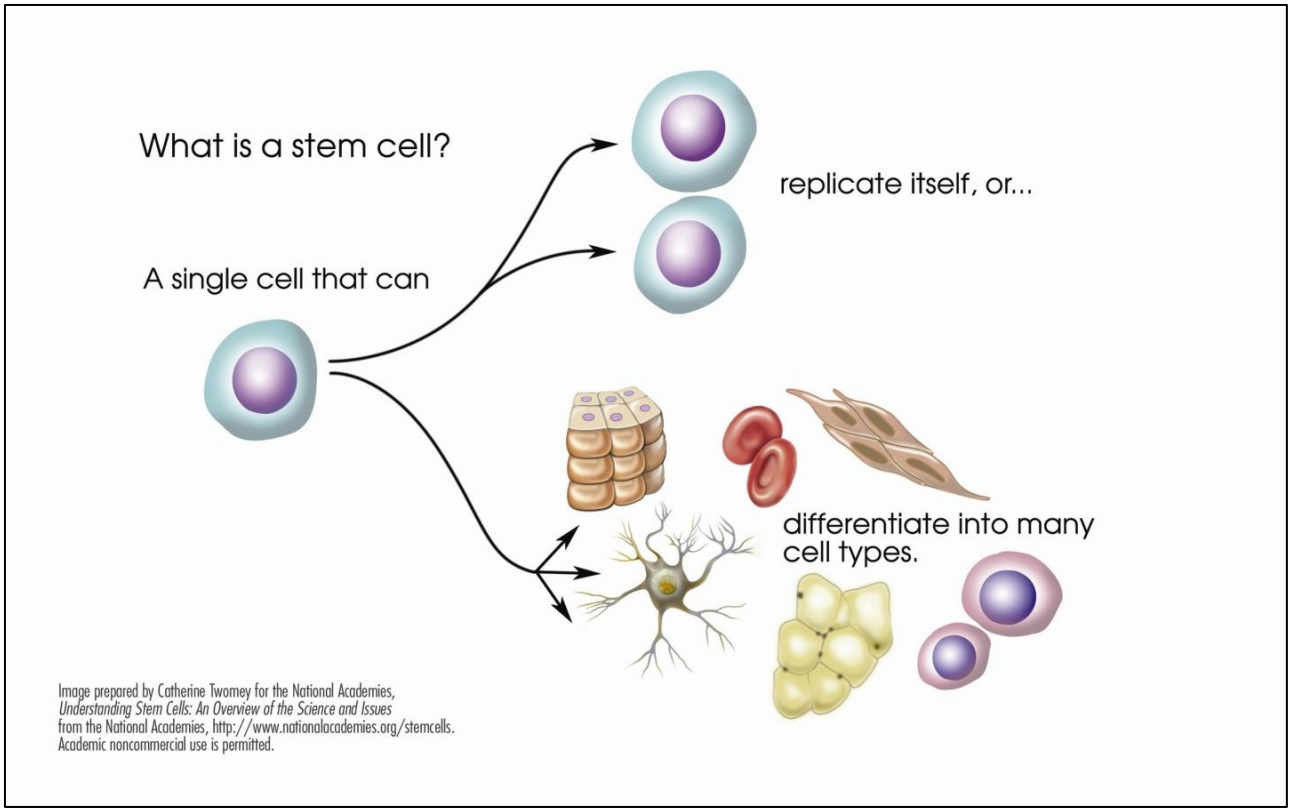

Figure 7 Self-renewal and the capability of differentiation to other cell types are the unique stem cells' properties

In 2006, Shinya Yamanaka proved that over-expression of four transcription factors, OCT3/4, SOX2, KLF4 and cMYC (also known as Yamanaka factors), can reprogram mature fibroblasts to pluripotency [84]. He was awarded the 2012 Nobel Prize for the discovery that mature cells can reprogram into induced pluripotent stem cells (iPSCs) [85].

The discovery of iPSCs was a remarkable achievement in biotechnology and regenerative medicine, since iPSCs can be generated from one's own cells, and thus do not harbor the risk of genetic incompatibility or immune rejection. From the ethical side, too, iPSCs are more favourable than the embryonic stem cells [83].

In 2010, successful reprogramming from fibroblasts to iPSCs with cmRNAs encoding Yamanaka factors was performed for the first time [86]. In this protocol, coculture of fibroblasts underwent a

"daily transfection regime" for 14 days, and iPSC colonies were picked up at day 18 (Figure 8) [87].

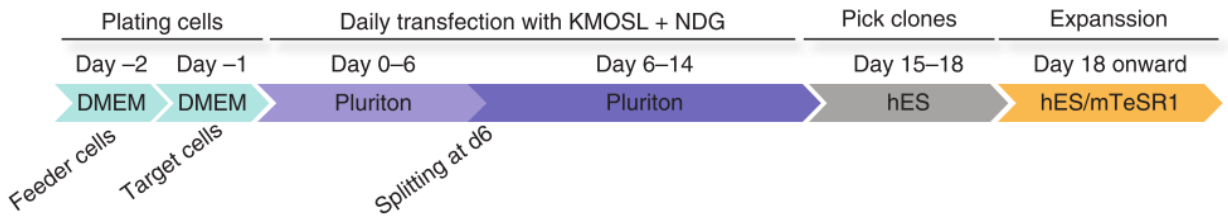

Figure 8 Schematic of step-wise protocol for reprogramming to iPS, using cmRNAs. Figure from Mandal et al./ Nat. Protoc. 2013; 8: 568-82 [87]

Different reprogramming kits based on the above mentioned protocol are commercially available. However, the protocol suffers from limitations such as low reprogramming efficiency (0.04-4.4%) and high sensitivity to even minor changes [86, 87].

Therefore, an efficient and robust reprogramming protocol is still lacking.

1.5 Thesis objectives

The main goal of this thesis was to establish efficient methods for cmRNA delivery that are useful for cell differentiation and dedifferentiation. To change a cell's fate, normally one or more transcription factors should be over-expressed for a defined period. Therefore, either enhanced delivery or prolonged delivery of cmRNAs can be helpful to reach our goal.

In this report, magnetofection of cmRNAs has been introduced as an enhanced cmRNA delivery method, more efficient than conventional lipofection or polyfection. The goal in this part was simplification and enhancement of the current protocol for iPSC reprogramming with cmRNAs encoding Yamanaka factors [87]. However, the reprogramming to pluripotency was not performed in this thesis.

In the second part of this study, vacuum-dried cmRNA-loaded collagen sponges have been used as transcript-activated matrices (TAMs) for sustained cmRNA delivery (Figure 9), providing steady state protein expression for six consecutive days.

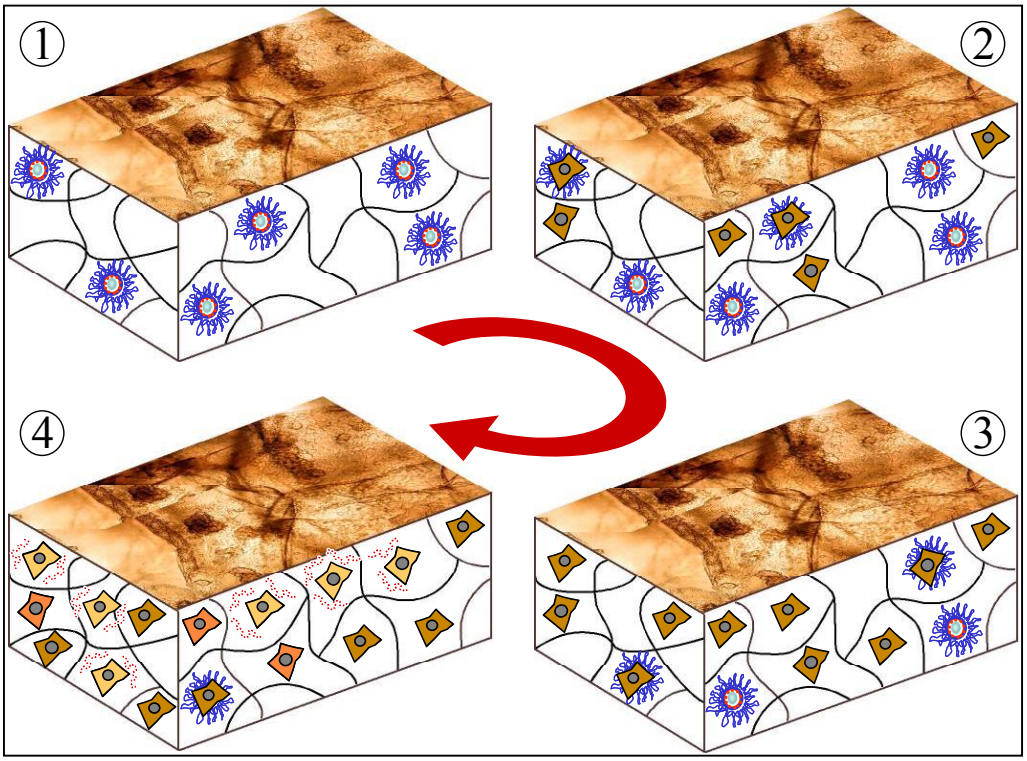

Figure 9 Schematic of sustained cmRNA delivery system using collagen sponges. (1) Trans-activated matrix: collagen sponges pre-loaded with cmRNA complexes. (2) Cell seeding on trans-activated matrix. (3) By the time cell grow, proliferate and reach the complexes, and (4) Cells are transfected with complexes of cmRNAs and produced protein of interest (Picture prepared by Christian Koch)

At the end, osteogenic differentiation *in vitro* (with MC3T3-E1 cells and MSCs) and *in vivo* (in rat femur defects), using hBMP2 cmRNAs, confirmed the ability of the transcript-activated matrices in a preclinical application.

2 Materials and Methods

2.1 Materials

2.1.1 Cell culture reagents

Dulbecco's Modified Eagle's Medium (DMEM), alpha Minimum essential medium (α-MEM), Dulbecco's Phosphate-Buffered Saline without Calcium and Magnesium (DPBS), Fetal Bovine Serum (FBS), Penicillin/Streptomycin (P/S), 0.05% Trypsine-EDTA and collagenase type I and II were purchased from Gibco by Life Technologies GmbH (Darmstadt, Germany). Collagen sponges, with the trade name "KOLLAGEN *resorb*^{TM}", were provided by Resorba (Nürenburg, Germany).

2.1.2 Chemicals and reagents

Helper lipids including 1,2-dipalmitoyl-*sn*-glycero-3-phosphocholine (DPPC) and Cholesterol were supplied by Avanti Polar Lipids INC (AL, USA). Other required materials for complex preparation, such as ethanol and 1,2-Dimyristoyl-sn-glycerol, methoxypolyethylene Glycol (DMG-PEG) 2kD were purchased from CarlRoth (Karlsruhe, Germany) and Nof America Corporation (NY,USA), respectively.

D-luciferin was obtained from Roche Diagnostics (Unterhaching, Germany). Liposomal transfection reagent Dreamfect-gold (DF-Gold), and 96-well magnetic plates was acquired from OZ Biosciences (Marseille, France). methylthiazoyldiphenyl-tetrazolium (MTT) was provided by Trevigen (MD, USA). BioRAD protein assay reagent was purchased from Bio-Rad Laboratories (Hercules, USA).

Non-viral vectors for cmRNA delivery including PAA20k-EPE and C12EPE were also provided by Ethris GmbH (Planegg, Germany).

Magnetic nanoparticles (MNPs), i.e. PEI Mag2 and SO-Mag5, were supplied by Dr. Olga Mykhaylyk in the medical faculty of Technical University Munich.

Anti-rat CD45-FITC, CD90-FITC, CD29-FITC, CD31-PE, CD106-PE, and also isotype controls including IgM,k-FITC, IgG1,k-FITC, IgG1,k-PE were supplied by BD Pharmingen™ (San Jose, CA, USA).

Other reagents and materials were obtained from Sigma-Aldrich, unless specified otherwise.

2.2 cmRNA production

The chemically modified mRNAs encoding for d2eGFP, RFP, SOX2, KLF, cMYC, and OCT3/4 have been produced in this thesis. Other cmRNAs were supplied by Ethris GmbH.

An *in vitro* transcription (IVT) was performed using RiboMax Large Scale RNA production System-T7 (Promega, Madison, WI, USA) to produced cmRNAs. Shortly, plasmid vectors were linearized with Not I and purified using chloroform/ethanol precipitation. Prior to transcription, ribonucleotide mixture was prepared using adenosine-triphosphate (ATP), guanosine-triphosphate (GTP), uridine-triphosphate (UTP) and cytosine-triphosphate (CTP) as well as the chemically modified ribonucleotides methyl-CTP and thio-UTP (Jena Bioscience, GmbH, Jena, Germany) with a final concentration of ATP: GTP: UTP: CTP: methyl-CTP: thio-UTP of 7.13mM: 1.14mM: 5.36mM: 5.36 mM:0.536 mM: 0.536 mM. 20 µl IVT mixture was then prepared by adding anti-reverse cap analog (ARCA), T7 RNA polymerase and linearized template DNA, and incubated for 2 h at 37°C to complete the transcription procedure. Next, DNA template was digested during 20 min incubation at 37°C with DNase I. The cmRNA product was precipitated during 30 min

incubation on ice with pre-cooled ammonium-acetate with a final concentration of 2.5 M. After centrifugation, the pallet was washed twice with 70% ethanol and re-suspend in water for injection (WFI). The precipitation step with ammonium-acetate and washing with ethanol were repeated again, and final cmRNA pallet was re-suspended in WFI. cmRNA concentration and purity were determined with NanoDrop 2000C spectrophotometer (Thermo Scientific, DE, USA). In addition, further quality control of cmRNA product was performed by loading on the 1% agarose gel.

2.3 Cell culture

Primary Mouse Embryonic Fibroblasts (PMEFs) (PMEF cells strain CF-1/ untreated, Millipore, CA, USA), and Porcine Fetal Fibroblasts (PFFs, provided by Dr. Bartosz F. Grześkowiak) were cultured in complete DMEM high glucose (supplied with 10% FBS (Millipore, CA, USA) and 1% penicillin/streptomycin) and kept at humidified 37 °C supplied with 5% CO2. For both cell types, the plates were coated with Gelatin 0.1% for 30 min at RT prior to cell seeding. Cells splited 1:3 to 1:5 every three to five days. The fibroblast have been used in passage 7 to 15.

NIH 3T3 cell line (ATCC, VA, USA), and rat mesenchymal stem cells (MSCs) were cultured using complete DMEM low glucose (supplied with 10% FBS and 1% penicillin/streptomycin). Mc3T3-E1 cells (ATCC, VA, USA), were cultured in the complete alpha Minimum essential medium (α-MEM). NIH3T3 and MC3T3-E1 cells were splitted every three to five days 1:5 to 1:20, and have been used until passage 20. MSCs were expanded at the density of 1000-3000 cells/cm^2, and have been used until passage 6 in this project.

In all cases, cells were cultured and kept at humidified 37 °C supplied with 5% CO2.

2.4 Preparation of magnetic cmRNA complexes

For magnetofection experiments, three different components were mixed to prepare magnetic complexes: cmRNAs, enhancers (cationic lipids or polymers) and magnetic nanoparticles (Figure 10).

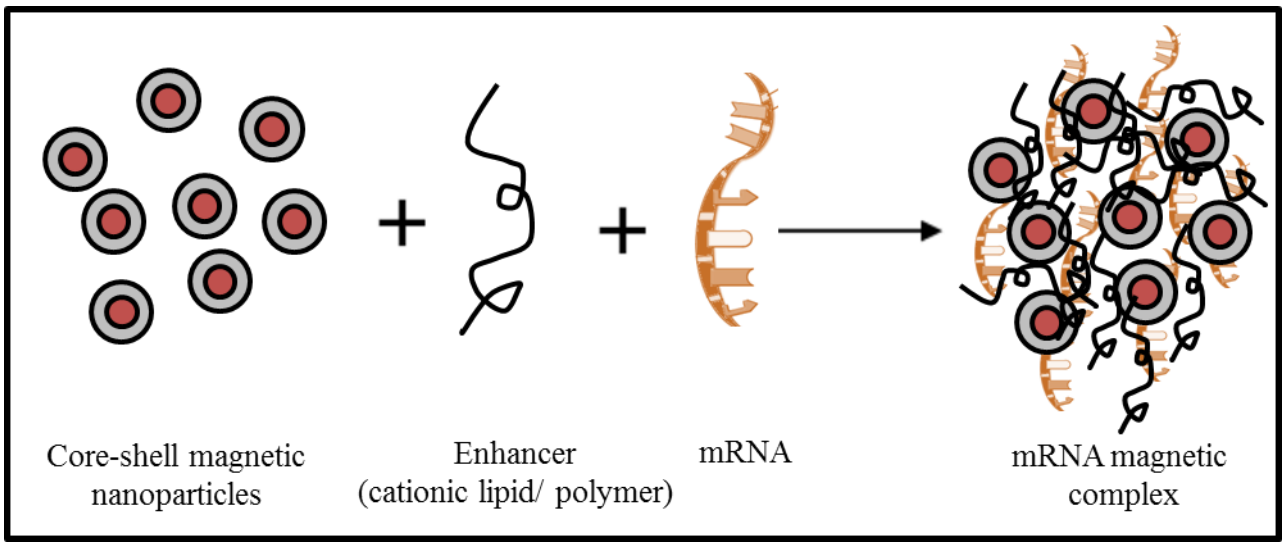

Figure 10 Schematic of non-viral self-assembling magnetic complexes of cmRNA (according to a figure from C. Plank et al. / Advanced Drug Delivery Reviews 63 (2011) 1300–1331)

The magnetic complexes were prepared at cmRNA concentration of 10 µg/ml. Magnetic nanoparticles (PEI Mag2 and SO-Mag5) at different iron to nucleic acid ratios (w:w), Df-Gold with different lipid to nucleic acid ratios (v:w), and PAA20k-EPE in different N:P (nitrogen of amino groups of cationic polymer to phosphate groups of nucleic acid) ratios have been used to optimize the cmRNA magnetic complex preparation. For a conventional lipofection and polyfection, magnetic nanoparticles were replaced with WFI. After mixing the components, the mixture was further incubated at RT for 20 min to allow self-assembling, then 1:2 dilutions with serum- and supplement-free DMEM were performed to set up all the different doses of cmRNAs. The prepared

dilutions then were added to the 70% confluent fibroblasts and the plates were incubated on the magnet for 20-30 min at humidified 37 °C and 5% CO2.

In the 96-well-plate format, complexes were prepared in total volume of 360 µl, from which 50 µl was added to each well of the cell culture plate, to perform three replicates for each sample. For other plates, the final volume of complexes were calculated accordingly.

2.5 cmRNA complexes characterization

Particle size and zeta potential of lipoplexes were measured by laser light scattering, using a Zetasizer (Malvern Instruments, Worcester, UK).750µl of complexes (or 1:5 to 1:10 dilution of complexes in supplement free-media) were filled into a clean disposable cuvette cell, and a total of 30 and 300 runs were performed for particle sizing and estimation of surface charge, respectively.

2.6 Analysis of translation of reporter cmRNAs

2.6.1 Luciferase assay

24 h after transfection, supernatant of the wells of a 96-well-plate was removed, and the cells were washed with DPBS. Next, 100µl lysis buffer (0.1% Triton X-100 in 250 mM Tris pH 7.8) per well was added, and plate incubated for 10-15 min at RT. 50 µl of the cell lysate then were transferred to the wells of a black 96-well plate and mixed with 100 µl of luciferin buffer (35 mM D-luciferin, 60 mM DTT, 10 mM magnesium sulphate, 1 mM ATP and 25 mM glycyl-glycine-NaOH buffer, pH 7.8). Chemiluminescence was recorded using a TopCount instrument (Canberra Packard, Groningen, The Netherlands). The amount of Luciferase was then calculated using a calibration curve.

In the next step, the amount of Luciferase were normalized per total protein in the cell lysate. For that, 150 µl deionized water was added to each well in a 96-well-plate, followed by transferring 10

µl of the cell lysate to the corresponding wells of the protein assay plate. Then 40 µl BioRad protein assay reagent was added to each well, and plate placed on a shaker for 5-10 min. The absorbance was measured at 590 nm using Wallac 1420 Multi-label counter; measuring time set to 0.1 s (Wallac Victor, Perkin–Elmer Life Sciences). The amount of protein was then calculated using a calibration curve.

2.6.2 Fluorescent-activated cell sorting (FACS)

To prepare the FACS samples for the cells in conventional 2D culture, cells were washed with DPBS and detached using 200 µl/well/12-well-plate 0.05% Trypsin-EDTA. To detach the cells cultured in collagen scaffolds however, each sponge was incubated with 300U/ml collagenase type I in Hanks' balanced salt solution (HBSS) with Calcium and Magnesium for 4 to 7 h. During incubation time, sponges were visually investigated for several times to ensure complete collagen digestion. Then, cells were centrifuged at 500g for 5 min, followed by washing with DPBS. In the next step, cells were incubated for 5 min at 37°C with 10 µl 0.05% Trypsin-EDTA to accelerate detachment of cells. Detachment was stopped by adding 90µl of DPBS containing 2% FBS to each well. FACS analysis was carried out using Attune NxT flow cytometer (Life technologies, NY, USA). Before each experiment, the machine was calibrated using calibration beads (Molecular probes, Life technologies, NY, USA). Cell debris was excluded from analysis by using forward- and side-scatter gating. Untransfected cells cultured under 2D and 3D condition were used as negative controls to adjust fluorescence channel. The data, obtained from triplicates, was analyzed with FlowJo_V10 software.

2.6.3 *Metridia* luciferase assay

Kinetics of translation of a reporter cmRNA, *Metridia* luciferase, was used to test the quality of collagen sponges for sustained cmRNA delivery. For this, cell culture supernatant was collected

every 24 h post transfection, and replaced with new media. The collected media was either proceeded immediately for measurement, or frozen at -20 °C until the last day of experiment to measure samples collectively. To quantify Met luc expression, 80µl of supernatant was gently mixed, in black 96-well plates (Costar, NY, USA), with 30 µl of 0.05 mM Coelenterazine (Synchem, Felsberg, Germany) and measured, using a luminescence reader (Wallac Victor, Perkin–Elmer Life Sciences) in triplicates.

2.7 Cell viability assays

2.7.1 Cell viability assay for conventional 2D culture: MTT assay

The MTT assay, based on reduction of the MTT reagent into formazan by superoxide anions produced in the mitochondrial respiratory chain, was performed to assess the cytotoxicity of the cmRNA polyplexes, lipoplexes, and magnetic complexes. 24 h post-transfection, supernatant of cells were discard, and the cells were washed with DPBS. Then cells were incubated for 2 h with 100 µl of 1 mg/mL MTT solution prepared in DPBS with 5 mg/mL glucose. When violet crystals of formazan were observed under the microscope, 100 µl solubilisation solution (10% Triton X-100 in 0.1 N HCL in anhydrous isopropanol) per well was added and plate was incubated at 37°C on the shaker overnight to let the formazan crystals to be dissolved. The optical density was measured at 590 nm. Untransfected cells were used as a reference, and 100 µl MTT solution mixed with 100 µl solubilisation solution used as the background.

2.7.2 Cell viability assay for 3D culture: ATP Glo assay

For assessment of cell viability TAMs loaded with different doses of Met luc cmRNA complexes were used. NIH3T3 cells were inoculated on the sponges at 10,000 cells per sponge, and cultivated in complete DMEM for 48 h. Cells cultivated on collagen sponges not loaded with cmRNA formulations were used as control. Cell viability was evaluated using CellTiter-Glo® according to

manufacturer's instructions (CellTiter-Glo® luminescence cell viability assay, Promega, WI, USA). 70 µl of the final reaction medium was transferred to a white 96-well plate (Costar, NY, USA), and measured using a luminescence reader (Tecan infinite 200 pro, Tecan group Ltd, Switzerland) in triplicates.

2.8 Preparing cmRNA complexes for loading onto collagen sponges

A proprietary cationic lipid (C12EPE) has been used as a non-viral transfection agent, along with DPPC and cholesterol as helper lipids and DMG-PEG2k as PEGylated lipid. Lipoplexes were formed at a final cmRNA concentration of 200µg/ml and N/P ratio of 8 which stand for molar ratios of amino groups of proprietary lipid to phosphate groups of cmRNA using the solvent exchange method [88]. Briefly, lipoplexes were induced to self-assemble by rapid injection of an ethanolic solution of lipid phase into an aqueous solution of cmRNA in10mM citrate / 150 mM sodium chloride using insulin syringes, followed by 15 sec vortexing at high speed and 30 min incubation at RT. The formulated lipoplexes were then dialyzed against double distilled water using dialysis cassettes with molecular weight cut-off of 7 kDa (Pierce, USA).

To prepare cmRNA polyplexes, 500µl of cmRNA solution was added to 500µl of Polyethylenimine (PEI) solution, followed by 30 s vortexing, and 30 min incubation at RT. Polyplexes were prepared at the final cmRNA concentration of 200µg/ml and an N/P ratio of 10.

2.9 Experimental set up for cell transfection on vacuum-dried cmRNA-loaded collagen sponges as transcript-activated matrices (TAMs)

The experimental set up for preparation TAMs with collagen sponges is illustrated in Figure 11.

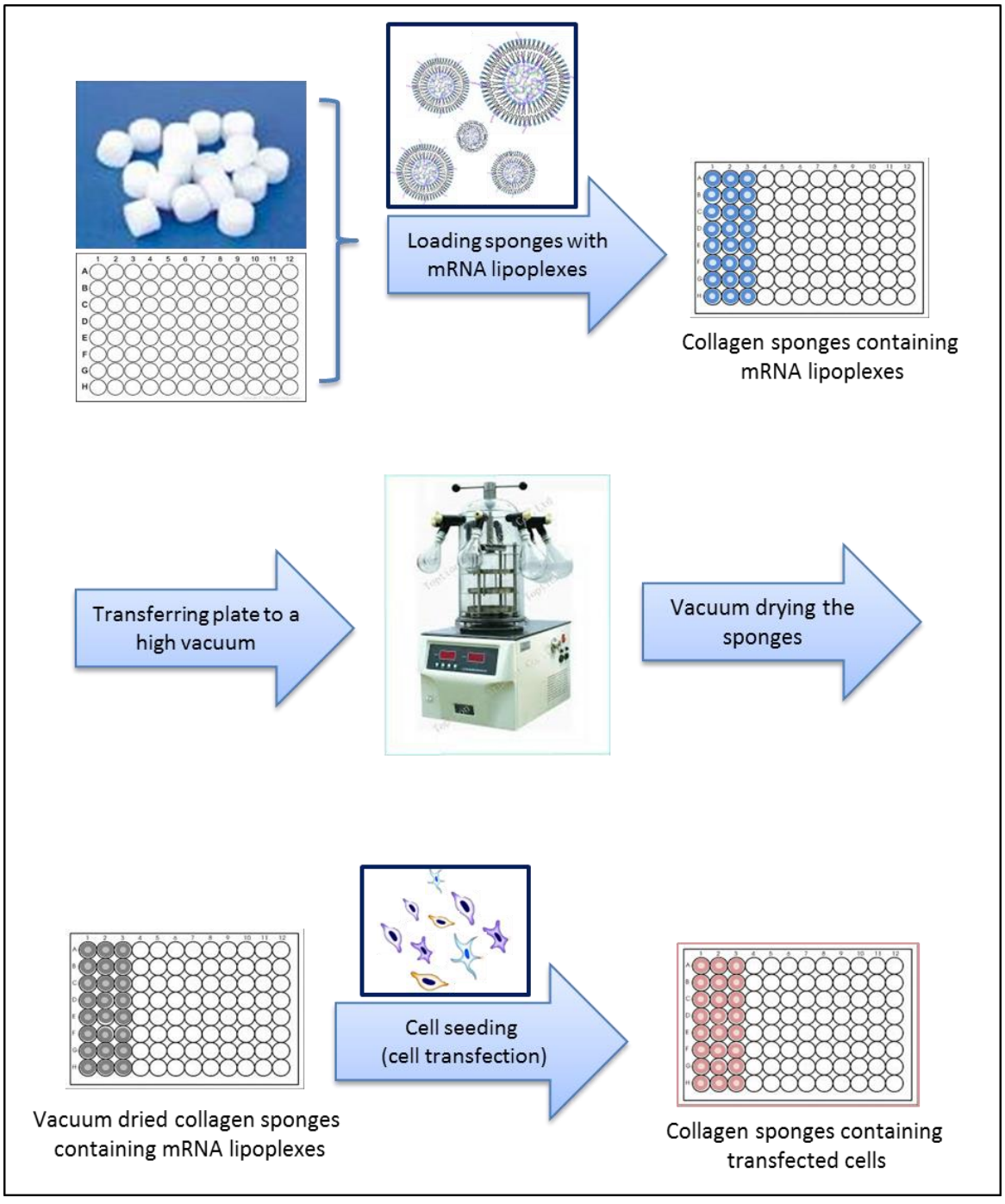

Figure 11 Schematic of preparation transcript-activated matrices (TAMs) using collagen sponges

First, collagen sponges were cut in small pieces (6mm in diameter) using a puncher (VBS Lochzange, Nr. 19970181). The pieces were placed in the wells of a sterile flat bottom, polypropylene uncoated 96-well-plate (Eppendorf, Humburg, Germany). 50 µl of lipoplexes in sucrose (2%), as a lyoprotective, were added drop wise to each piece and incubated for 90 min at

RT to be completely soaked by the sponges. Loaded sponges then were moved to a high vacuum (Martin Christ Gefriertrocknungsanlagen GmbH, Osterode am Harz, Germany) and dried there for at least 2 h at 0.05 mbar. After that, sponges were either used for seeding cells or vacuum-sealed and kept at RT until use. In case of cell seeding, desired cell density in 50 µl complete media (complete DMEM for NIH3T3 and MSC cells) was added to every sponge followed by 30 min incubation at humidified 37 °C and 5% CO2. During incubation time, cells had to be seeded on collagen sponges as they could not adhere and grow on polypropylene uncoated plate. Then, 200 µl complete media was added to the wells and plates incubated in cell culture incubator.

Whole procedure performed under sterile condition using laminar hood (BDK Luft und reinraumtechnik GmbH, Sonnenbühl-Genkingen, Germany). Moreover, plastic materials were avoided due to high electrostatic charge of collagen sponges.

2.10 Scanning Electron Microscopy (SEM)

Scanning electron microscopy was used to characterize the morphology of collagen sponges and evaluate loading cmRNA complexes on that. All samples were coated with Gold and Palladium with ratio of 60/40, using a sputter coater (Edwards sputter coater S150B, HHV Ltd, West Sussex, UK). Then, SEM was carried out using a Zeiss-Leo DSM 982 Gemini (FELMI-ZFE, Graz, Austria) at 5 kV.

2.11 Labeling cmRNAs with FITC

100µg td-Tomato cmRNA was FITC-labeled with 50µl label IT reagent, using the Label IT® Nucleic Acid Labeling kit (mIR3200, Mirus, Madison, WI, USA), according to manufacturers' instruction. The FITC labeled-cmRNAs were then purified with ammonium-acetate precipitation, and the cmRNA pallet was re-suspended in WFI. Labeling degree was calculated as 11 FITC

molecules per cmRNA molecule, using UV-measurement with NanoDrop 2000C spectrophotometer (Thermo Scientific, DE, USA).

2.12 Fluorescence microscopy

Lipoplexes containing FITC-conjugated cmRNAs , as well as transfected cells with tdTomato, eGFP, RFP and d2eGFP cmRNAs were visualized under the fluorescence microscope (Leica DMi8 fluorescent microscope, Leica microsystems, Heerbrugg, Switzerland).

2.13 Hematoxylin-Eosin (HE) staining of cells seeded on the collagen sponges

Cells were fixed with 4% formaldehyde in phosphate-buffered saline (PBS), PH 7.4, overnight at RT. Then collagen sponges were dehydrated and embedded in paraffin. Collagens' sections (7µmm) were deparaffinized, and stained with Hematoxylin and Eosin according to standard protocols.

2.14 Investigation of hBMP2 on the collagen sponges using Immunohistochemistry (IHC)

5 days after transfection, hBMP2 loaded and unloaded collagen sponges containing MC3T3-E1 cells were fixed with 4% formaldehyde in phosphate-buffered saline (PBS) PH 7.4, overnight at RT and kept in 70% ethanol. Then all collagen sponges were dehydrated and embedded in paraffin. Immunohistochemistry was performed for hBMP2 using a polyclonal antibody (ab14933, Abcam, Cambridge, UK). Collagens' sections (7µmm) were deparaffinized, and treated with 1% hydrogen peroxide in PBS for 10 min at RT to inactivate the endogenous peroxidases. After washing with

PBS, the sections were permeabilized with 0.3% Tritone X-100 in PBS for 5min, washed again with PBS and were blocked with 1.5% blocking serum for 1 h in a humid chamber at RT.

Then the slides were incubated with the primary antibody in a humid chamber at 4°C overnight. In the following day, after removing excess of unbound antibody by PBS washing, the sections were incubated with anti-rabbit secondary antibody complexed with avidin-biotin system (Rabbit ABC Staining System: sc-2018, Santa Cruz, CA, USA), and procedure continued following the manufacturer's protocol. Sections were incubated with peroxidase substrate for 3 min, followed by washing in H2O and counterstaining in hematoxylin. At the end, dehydration steps and mounting with Roti Histokitt II medium (CarlRoth, Karlsruhe, Germany) were performed.

2.15 Isolation and expansion of rat mesenchymal stem cells (MSCs)

Rat bone marrow mesenchymal stem cells (BMSCs) were provided by Ethris GmbH.

Adipose mesenchymal stem cells (AMSCs) were isolated form the fat tissue of a male rat. In this procedure, fat tissue was cut into millimeter sized pieces and transferred to a falcon tube (Corning incorporated, NY, USA) containing sterile DPBS and washed several times with DPBS. Next, fat pieces were incubated in a collagenase type II solution (0.4 mg/ml) at humidified 37 °C for 30 min. Then, collagenase activity was stopped by adding complete DMEM culture medium (DMEM containing 10% v/v FBS and 1% v/v Penicillin/streptomycin), and the mixture was centrifuged at 600 g for 10 min. The upper fat layer was collected and re-suspended in complete DMEM culture medium. In the next step, the cell suspension was filtrated through a 40 μm cell strainer (Corning incorporated, NY, USA), and plated in T75 cm^2 flask (Corning incorporated, NY, USA) and placed at humidified 37 °C and 5% CO2 in complete DMEM [89]. To remove the non-adherent cells the media was changed the following day. The cells were expanded with cell densities 1500-3000 cells/$cm^2$and the media changed every three days. In this study, MSCs were used until passage 6.

2.16 Secretion of hBMP-2 by MSCs cultivated on hBMP2-cmRNA loaded collagen matrices

Medium samples from MSC transfected with different doses of hBMP2 cmRNA lipoplexes were collected 24 h after transfection, and the concentration of hBMP-2 was measured with a human BMP-2 ELISA kit following manufacturer's instructions (R&D Systems, Minneapolis, MN). Experiments were performed in triplicates, and the protein content was determined using a standard curve (r^2=0.99)

2.17 *In vitro* osteogenic differentiation

Collagen sponges were loaded with 3µg hBMP2 cmRNA lipoplexes in 2% sucrose and vacuum-dried as described previously. In the next step, 30,000 MC3T3-E1 or freshly isolated rat MSCs, in 50 µl media, were seeded on each collagen sponge and incubated for 30 min at 37 °C in a humidified atmosphere of 5% CO2, to ensure the cell adherence to the collagen sponges. Then, 250µl Osteogenic Medium (DMEM+ 2% FBS+ 10mM ß-Glycerophosphate+ 200µM L-Ascorbic acid+ 1% Pen-Strp for MSCs, and α-MEM+ 10% FBS+ 10mM ß-Glycerophosphate+ 50 µg/ml L-Ascorbic acid+ 1% Pen-Strp for MC3T3-E1) was added to each well. Half of the media was renewed every two to three days. Negative controls including untransfected cells in 3D (seeded on collagen sponges) and 2D (seeded on the normal cell culture flask) were treated exactly like transfected cells in 3D. 7 and 14 days post seeding, cells were investigated for expression of osteogenic markers by RT-PCR.

2.18 RNA isolation, and reverse transcriptase real-time polymerase chain reaction (RT-PCR)

7 and 14 days after seeding cells on the hBMP-2 loaded collagen sponges, appropriate volume of collagenase I in Hanks' balanced salt solution (HBSS) was added to each well to reach the final concentration of 300 U/ml of collagenase type I. Then, plates were incubated for 4 to 7 hours at humidified 37 °C and 5% CO2. When the collagen sponges were entirely dissolved, cells were centrifuged at 500g for 5 min, supernatant removed and cells subsequently lysed by TRIzol reagent (Ambion by life technologies, Darmstadt, Germany) for total RNA isolation, following manufacture's instruction. For each of the hBMP2 transfected and untransfected groups, 15 sponges were used, and the lysed cells were pooled together for RNA isolation.

RNA concentration and purity were determined with NanoDrop 2000C spectrophotometer (Thermo Scientific, DE, USA). First-strand cDNA was reverse-transcribed from 450 ng of total RNA by the use of First Strand cDNA Synthesis Kit (Thermo Scientific, Darmstadt, Germany), following manufacturer's instructions.

To evaluate the expression of osteo-related genes, soAdvanced Universal SYBR Green Supermix (Bio-Rad, Munich Germany) was used to perform quantitative realtime PCR (n = 3). PCR was carried out on a Light Cycler 96 thermal cycler (Roche, Mannheim, Germany). The expression levels of target genes were normalized to that of GAPDH (in case of MC3T3-E1 cells), and beta-tubulin (for MSCs). The data expressed as fold induction relative to controls, i.e. untransfected MC3T3-E1cells in 3D, and untransfected MSCs in 2D culture. Primer sequences were listed from 5' to 3' as follows:

Table 1 Mouse primers for osteogenic differentiation experiment on MC3T3-E1 cells

Gene	Forward primer	Reverse primer
ALP	gtgccctgactgaggctgtc	ggatcatcgtgtcctgctcac
OCN	ccgggagcagtgtgagctta	tagatgcgtttgtaggcggtc
GAPDH	gcacagtcaaggccgagaat	gccttctccatggtggtgaa

Table 2 Rat primers for osteogenic differentiation experiment on MSCs

Gene	Forward primer	Reverse primer
RUNX2	ccgtgtcagcaaaacttcttt	gctcacgtcgctcatcttg
OSX	cccaactgtcaggagctagag	gatgtggcggctgtgaat
OCN	acggcagcttcagctttg	gaggcagagagagggaacag
ALP	tggaacactgggtcccata	gacctggtcttccctccaa
β-tubulin	ctgatgagcagggcgagt	tccgagaagttcttaagcctca

2.19 *In vivo* bone differentiation

An *in vivo* implantation experiment was design, following the Guidelines for The Care and Use of Laboratory Animals provided by District Government of Upper Bavaria. In total 9 Sprague-Dawley rats (6-month-old males, average weight 600 to 700 g; Janvier, Le Genest-St- Isles, France) were used. In each rat, femur defect in the left leg was treated with empty collagen sponge (as negative

control), and the right femur defect was cured with 2.5 μg hBMP2 cmRNA-loaded sponge. To avoid infection and alleviate pain during and after the operation, routine antibiotics and analgesics were prescribed, and animals were anesthetized using a combination of Medetomidin (Domitor®, Orion pharma, Espoo, Finland; 135 µg/kg), Midazolam (Dormicum®, Unterhaching, Germany; 2.5 mg/kg) and Fentanyl (Duragesic®, Beerse, Belgium; 5 µg/kg).

After shaving and disinfecting, a 1.5 cm skin incision on the lateral surface of the thigh of animal was made to generate a mini-invasive access to femur.

A 2-mm dill hole, as a non-critical defect, was created in the middle third of the femur bone, using compressor orthopedic drill machine (Aesculap GA 207 (0-750 1 min); PEP GmbH - Fair and worldwide trade, Dessau, Germany), and a drilling bit (Aesculap GS 4 (Stainless 2) Ø 2 mm; PEP GmbH - Fair and worldwide trade, Dessau, Germany).

After implantation of collagen sponges into drill holes, 4-0 vicryl sutures (Ethicon, USA) were used to close the muscles, fascia and skin. Post operation, a film of silver aluminum aerosol (Henry Schein, Langen, Deutschland) was sprayed on the operated area to provide a protective layer against contaminations and damage of the wound by other animals. The rats were sacrificed at 2 weeks, using natrium pentobarbital (Narcoren®, Merial GmbH, Hallbergmoos, Germany; 400 mg/kg), and samples were collected for μC-T and histology analysis.

2.20 µ-computed tomography (µ-CT) analysis

Three dimensional x-ray micro-computed tomography (µ-CT) imaging was performed to quantify bone formation, using µCT 40 (Scanco Medical, Bassersdorf, Switzerland). Bone volume was measured to compare the amounts of newly formed callus within each specimen (defects treated with empty collagen sponges and defects treated with hBMP2 cmRNA-loaded collagen sponges).

2.21 Histological observation of rat femur defects

Histological evaluations were carried out by Professor Reinhold Erben in the University of Veterinary Medicine Vienna.

Femoral shafts were embedded in a modified methylmethacrylate embedding mixture as described (Erben 1997 J Histochem Cytochem 45:307-313), and 5-µm-thick longitudinal sections were prepared using a Leica SM2500 sledge microtome (Leica Microsysteme, Wetzlar, Germany). Sections were stained with toluidine blue and von Kossa/McNeal (Erben RG, Glösmann M 2012 Histomorphometry in rodents. In: Bone Research Protocols, Methods in Molecular Biology vol. 816. Helfrich MH, Ralston SH (eds) Humana Press, New York, NY, USA, pp 279-303). Histomorphometry of the newly formed callus tissue was performed using OsteoMeasure 3.0 (OsteoMetrics, Decatur, GA, USA) and AxioVision 4.7 (C. Zeiss, Jena, Germany) software for semiautomatic and automatic image analysis, respectively.

2.22 Statistical analysis

All statistical analyses as well as half-life measurements were performed using GraphPad Prism version 6.05 for windows (GraphPad Software Inc., San Diego, CA). Statistical significance was determined using t-test and multiple t-test. $P< 0.05$ was considered significant.

3 Results

3.1 Magnetofection: enhanced cmRNA delivery

3.1.1 Optimum cell density for culture of Primary Mouse Embryonic Fibroblasts (PMEFs)

Cell density plays a critical role in keeping primary cells proliferative and productive in the log phase due to high sensitivity of primary cells to contact inhibition [90]. Therefore, optimum density of PMEFs was determined, using luciferase assay. Different cell densities per well of a 96-well-plate were transfected with various Luc cmRNA doses along with Dreamfect-gold (Df-Gold) as a cationic lipid vector. 24 h later, luciferase and total protein expression were measured, and expression of the luciferase was normalized to that of the protein (Figure 12). Based on the transfection efficacy, 4000 PMEFs per well in a 96-well-plate was chosen as the optimal PMEF density, and number of cells per wells for other cell culture plate formats were calculated accordingly.

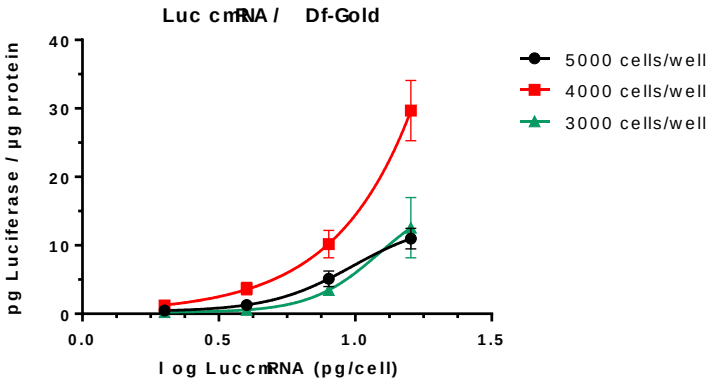

Figure 12 Determination of optimal cell density for PMEFs per well in 96-well-plates. Luciferase assay: transfection efficacies of different doses of Luc cmRNA for various cell densities of PMEFs. All data shown are mean ± SD from the values of three replicates.

3.1.2 Optimizing the ratio of lipid to nucleic acid for Df-Gold as a cationic lipid vector

To find the best transfection reagent for magnetofection of cmRNAs, Df-Gold was tested as an example of lipid vectors. Therefore, Df-Gold with various lipid to nucleic acid (L:N) ratios, either alone or in combination with two different magnetic nanoparticles (SO-Mag5 and PEI Mag2), was used for Luc cmRNA complex preparation. The prepared complexes were then added to the overnight culture of PMEFs. 24 h later, transfection efficacy and cell toxicity were measured using luciferase and MTT assays, respectively. As shown in Figure 13, regardless of the type of magnetic nanoparticle used, magnetofection increased the transfection efficacy of cmRNA, compared to conventional lipofection. The maximum transfection efficacy was observed at L:N of 4:1 and 5:1. In the MTT assay results, increasing lipid to nucleic acid ratio did not yield any enhanced cell toxicity. On the contrary, L:N 6:1 increased cell proliferation.

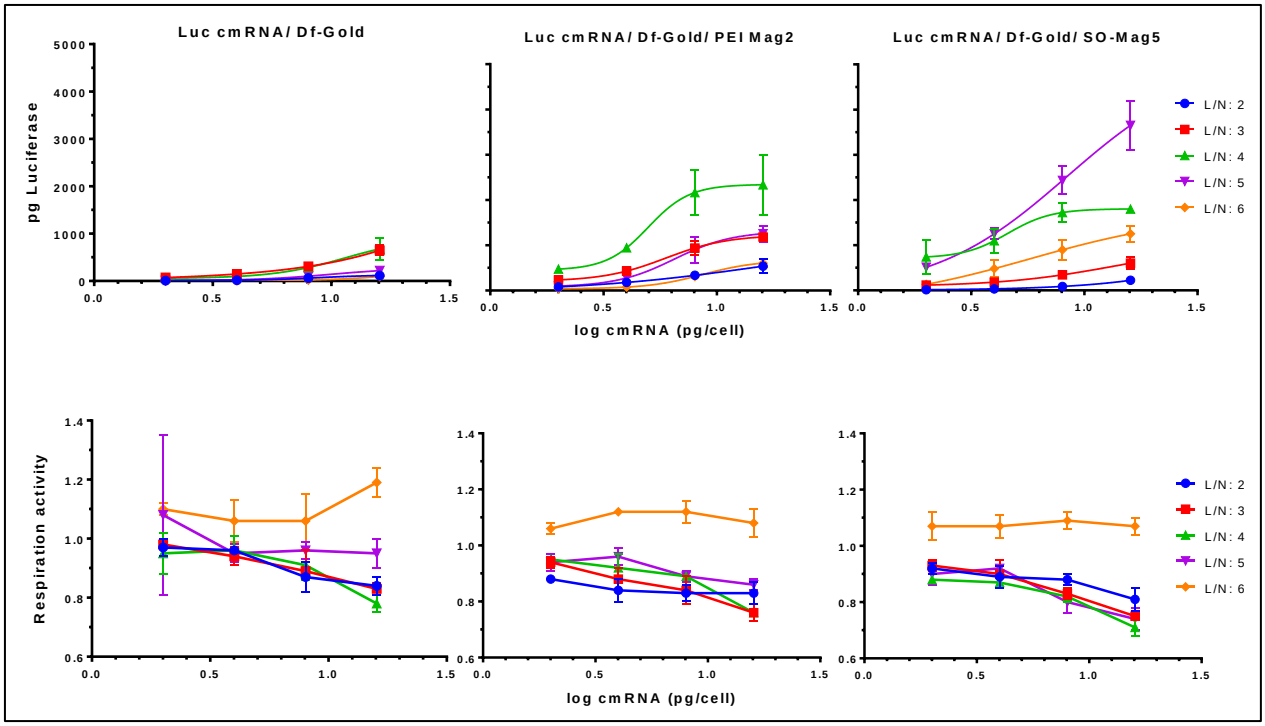

Figure 13 Magnetofection compared to lipofection, optimizing L/N ratio. (A) Luciferase assay: transfection efficacy of Luc cmRNA in PMEFs. (B) MTT assay: toxicity of Luc cmRNA complexes in PMEFs. Untransfected cells were used as control. All data shown are mean ± SD from the values of three replicates.

Based on these results, L:N 4:1 was selected as the optimal ratio, which gave high transfection efficacy as well as low cell toxicity.

3.1.3 Optimizing polymer to nucleic acid ratio for PAA20k-EPE as a cationic polymer vector

To investigate the effect of magnetofection using cationic polymers as transfection reagents, PAA20k-EPE, patented by Ethris GmbH, was used (Figure 14).

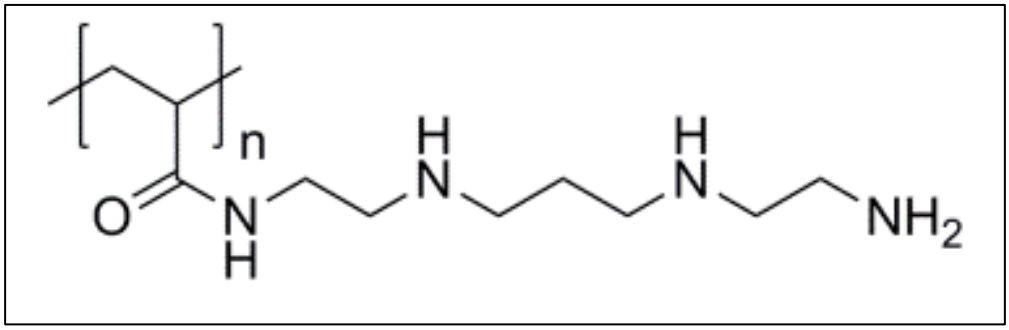

Figure 14 Schematic of PAA20k-EPE, a cationic polymer vector for cmRNA delivery. PAA20k-EPE comprised of an olygo(alkyl amine) with ethylen-propylen-ethylen (EPE) backbone, conjugated to poly(acrylic acid).

24 h after seeding PMEFs, cells were transfected with polyplexes of Luc cmRNA and PAA20k-EPE, with N:P ratios 16:1 and 32:1, which stand for molar ratios of the amino group of cationic polymer to the phosphate group of RNA. Magnetic complexes were prepared using two different magnetic nanoparticles (PEI Mag2 and SO-Mag5). Transfection efficacy and cell toxicity were assessed 24 h post transfection with luciferase and MTT assays, respectively (Figure 15). The results showed that using a higher N:P ratio (32:1) did not result in any significant increase in the transfection efficacy, but negatively affected the cell viability. Therefore, the N:P ratio of 16:1 was chosen for future experiments.

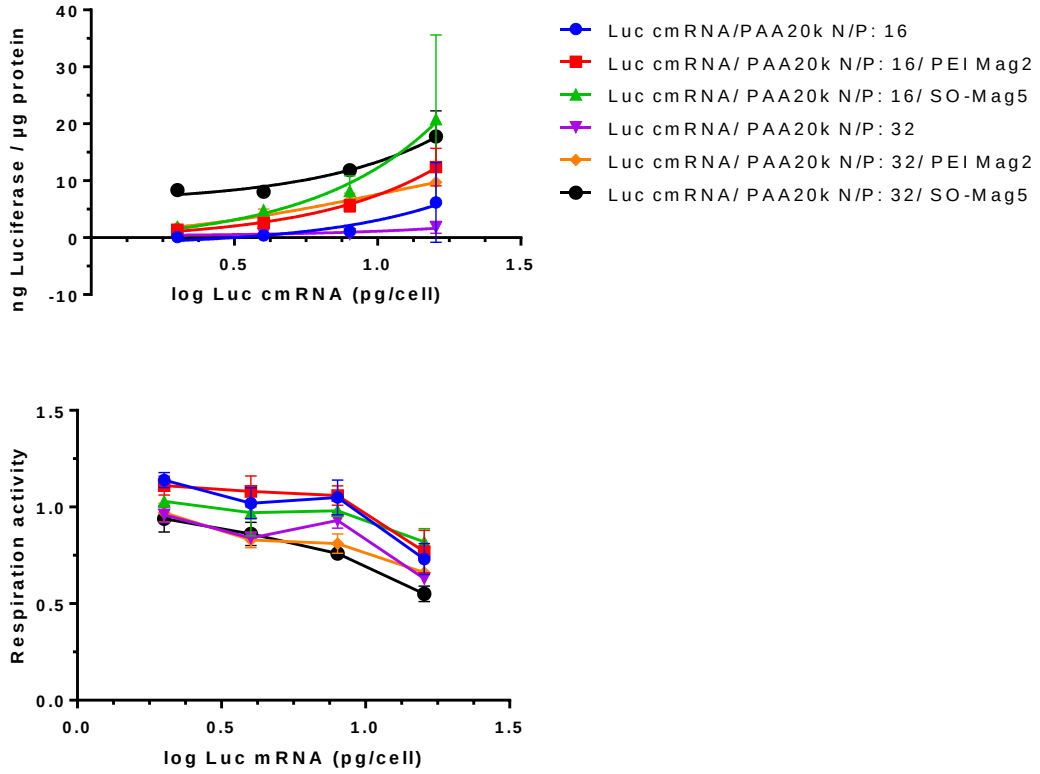

Figure 15 Magnetofection compared to polyfection, optimizing N:P ratio. (A) Luciferase assay: transfection efficacy of Luc cmRNA in PMEFs. (B) MTT assay: toxicity of Luc cmRNA complexes in PMEFs. Untransfected cells were used as control. All data shown are mean ± SD from the values of three replicates.

3.1.4 Evaluation of lipid and polymer vectors for magnetofection

To find the most efficient vector for magnetofection of cmRNAs, transfection efficacy of Df-Gold and PAA20k-EPE were compared, considering all previous optimizations.

cmRNA complexes were self assembled using Luc cmRNA and vectors, alone or along with magnetic nanoparticles (PEI Mag2 and SO-Mag5).

Figure 16 shows the luciferase expression of different Luc cmRNA complexes, 24 h after transfection of PMEFs.

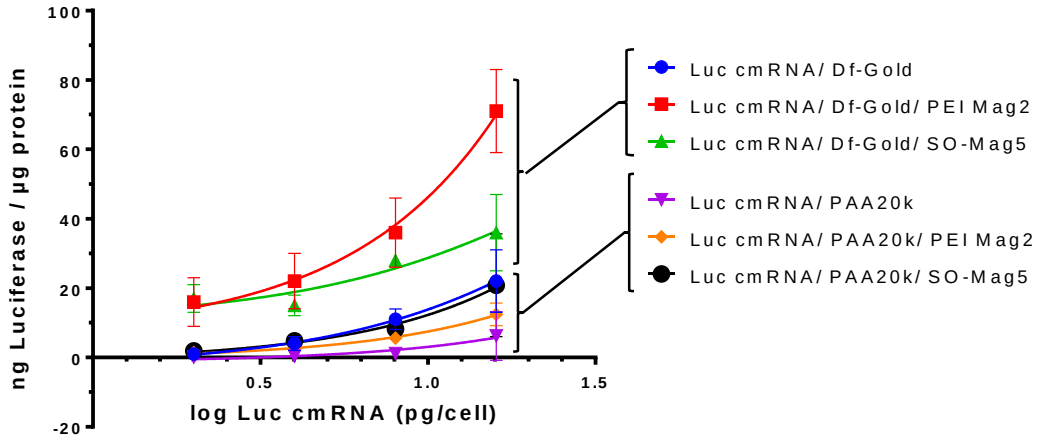

Figure 16 Magnetofection compared to lipofection and polyfection. Luciferase assay: transfection efficacy of Luc cmRNA into PMEFs, using Df-Gold (lipofection), PAA20k-EPE (polyfection), and combination of enhancers with various magnetic nanoparticles (magnetofection). All data shown are mean ± SD from the values of three replicates.

Based on the results, although magnetofection improved the transfection efficacy using both cationic lipids and polymers, Df-Gold, as a lipid vector, was more efficient for magnetofection of cmRNAs.

3.1.5 Optimizing the ratio of iron to nucleic acid

Various iron to nucleic acid (Fe:N) ratios were compared to find the most efficient and lowest toxic amount of iron in the complexes. PMEFs were transfected with different complexes containing Luc cmRNA, Df-Gold, and two magnetic nanoparticles (PEI Mag2 and SO-Mag5) with Fe:N ratios 0.5:1, 1:1, 1.5:1, and 2:1. Luciferase and MTT assays were performed 24 h post transfection (Figure 17).

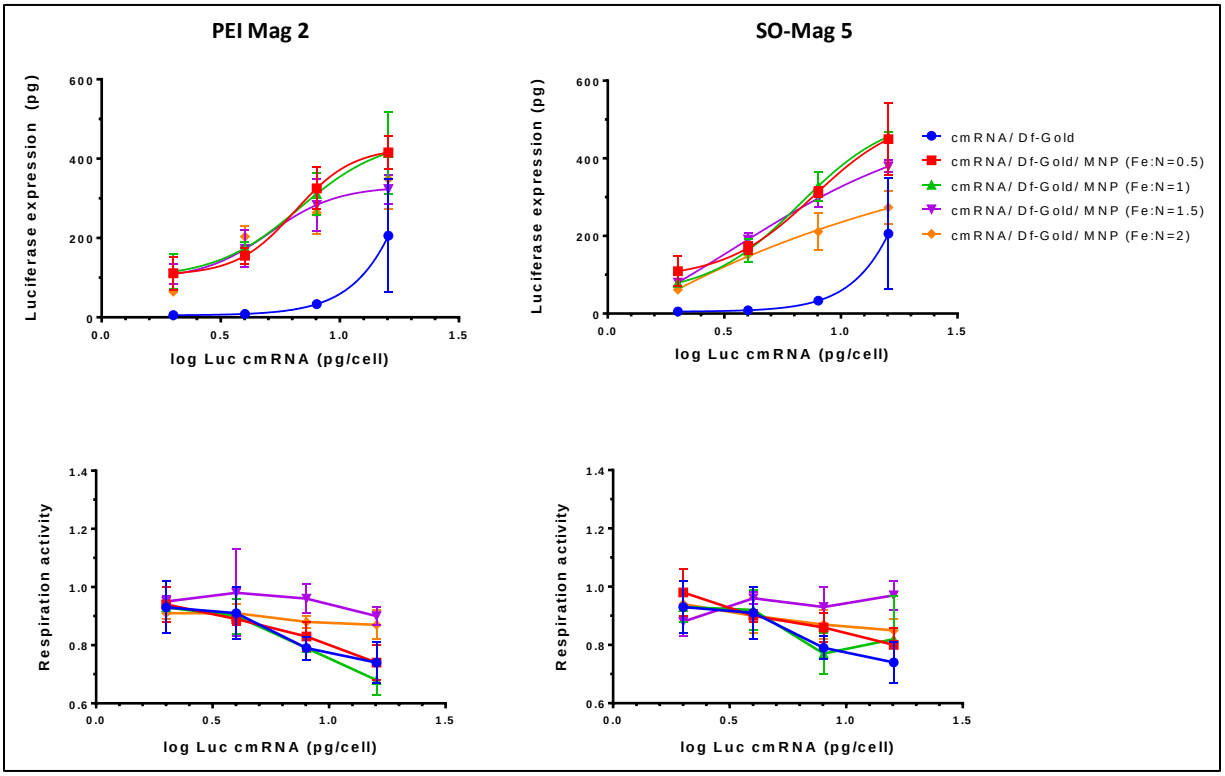

Figure 17 Magnetofection compared to lipofection; optimizing Fe/N ratio.(A) Luciferase assay: transfection efficacy of Luc cmRNA in PMEFs. (B) MTT assay: toxicity of Luc cmRNA magnetic complexes in PMEFs. Untransfected cells were used as controls. All data shown are mean ± SD from the values of three replicates.

Considering transfection efficacy, Fe:N 0.5:1 and 1:1 led to slightly higher cmRNA translation, especially at higher cmRNA doses. Furthermore, according to MTT results, higher concentration of iron in the complexes did not increase cell toxicity. Indeed, cell proliferation was improved using Fe:N 1.5:1.

Based on the transfection efficacy and cell viability results, Fe:N 1:1 was chosen as the optimum Fe:N ratio for transfection of single cmRNA.

3.1.6 Kinetics studies; magnetofection vs. lipofection

Since cmRNAs result in transient protein production, kinetic studies of translation of cmRNAs would be useful to plan retransfection studies, when prolonged protein production for a desired period is aimed at.

To assess kinetics of translation of cmRNA at the protein level, a protein with a short half-life is needed. In this case, the increase or decrease of protein production precisely correlates with the cmRNA translation rate. For this purpose, destabilized eGFP cmRNA, d2eGFP cmRNA, was synthesized. The half-life of this destabilized form of GFP protein has been reported to be 2 hours [91]. Figure 18 compares the kinetics of expression of eGFP cmRNA, with a 26 h half-life, with d2eGFP in PMEFs culture [91]. Due to the long half-life of the eGFP protein, expression of eGFP had a cumulative effect which could not be related to the cmRNA translation, especially at later time points (see T=72 h in Figure 18). However, d2eGFP showed a corresponding translation profile over the time, thanks to its short half-life.

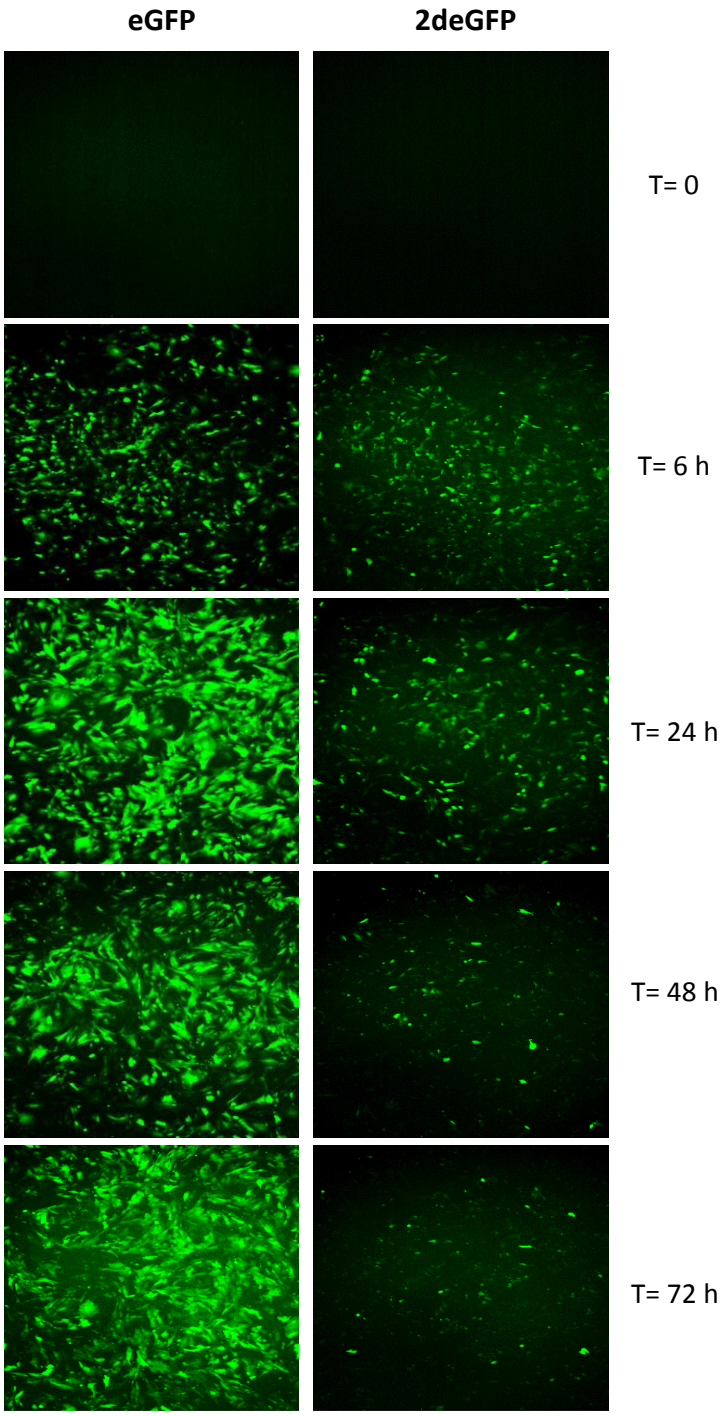

Figure 18 Kinetics studies: comparison of the translation kinetics of eGFP (T ½: 26 h) and 2deGFP (T ½: 2 h) cmRNAs. In each case PMEFs were transfected with SO-Mag5/Df-Gold/cmRNA (16 pg/cell). Pictures were taken at 4× magnification using a Nikon microscope.

FACS analysis was performed to compare translation kinetics of d2eGFP post lipofection (d2eGFP cmRNA/ Df-Gold) and magnetofection (d2eGFP cmRNA/ Df-Gold/ SO-Mag5). For this, both the number of eGFP positive cells (Figure 19 A) and their mean fluorescence intensity were quantified (Figure 19 B). For both the measured parameters, significantly higher values were observed post magnetofection, indicating higher transfection efficiencies coupled with rapid onset of cmRNA translation.

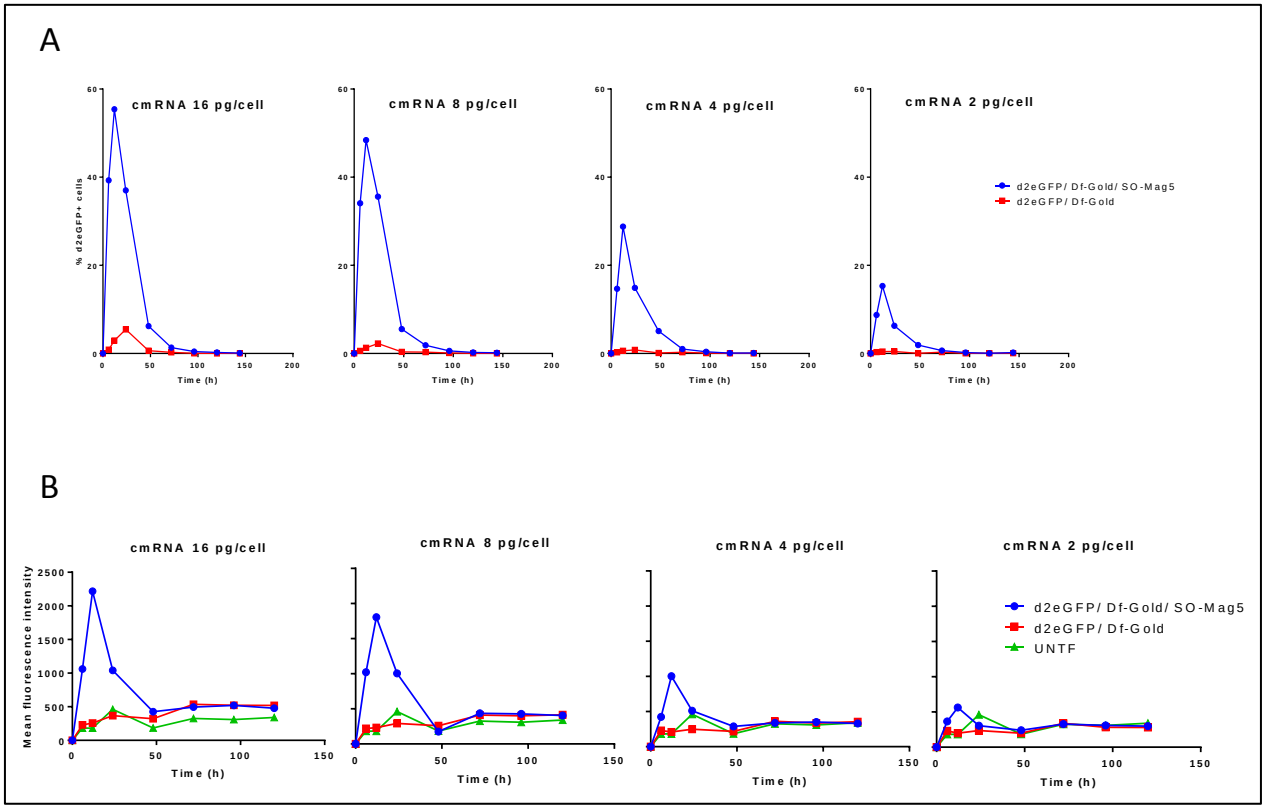

Figure 19 Kinetics studies: translation kinetics of 2deGFP cmRNA using magnetofection and lipofection. (A) Percentage of positive cells. (B) Mean Fluorescence intensity

3.1.7 Cotransfection of two cmRNAs; magnetofection compared to lipofection and polyfection

To evaluate the possibility and effect of magnetofection on cotransfection of different cmRNAs, cotransfection of Luc and eGFP cmRNAs in PMEFs was performed, using Df-Gold and PAA20k-EPE as vectors, and PEI Mag2 and SO-Mag5 as magnetic nanoparticles. All previous optimizations in a single cmRNA transfection (i.e. L:N, N:P, and Fe:N ratios) were applied in this experiment. Figure 20 A, shows the luciferase translation 24 h post luc cmRNA transfection, and luc and eGFP cmRNAs cotransfection, in both of which magnetofection could improve transfection efficacy. Since Df-Gold worked more efficiently than the PAA20k-EPE, it was chosen for the further investigations in cotransfection of cmRNAs.

FACS analysis was also performed to investigate the possible effect of cotransfection on translation of eGFP cmRNA, using magnetofection and lipofection (Figure 20 B). Also in this case, magnetofection could improve the transfection efficacy in transfection as well as cotransfection of cmRNAs. In addition, no considerable differences were observed in translation efficacy of eGFP cmRNA transfection and cotransfection.

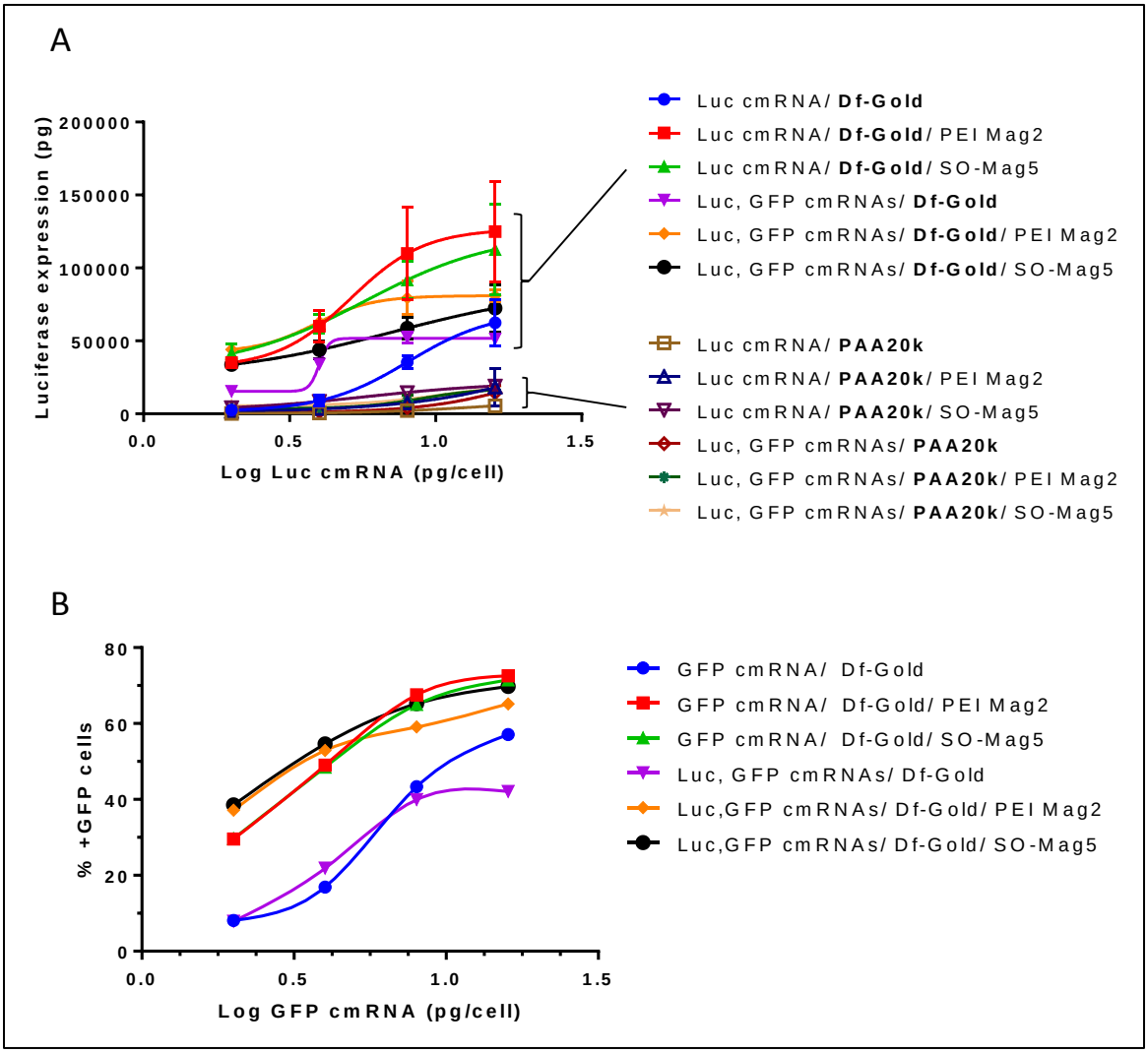

Figure 20 . Magnetofection compared to lipofection and polyfection in cotransfection of two cmRNAs. (A) Luciferase assay: transfection efficacy of Luc cmRNA in cmRNA transfection and cotransfection, using lipofection, polifection, and magentofection. DF-Gold was chosen as vector for further cotransfection experiments. Data are mean ± SD from the values of three replicates. (B) FACS analysis: transfection efficacy of eGFP cmRNA in single mRNA transfection and cotransfection, using lipofection and magentofection.

Regarding luciferase and eGFP translation in this experiment, cotransfection of different cmRNAs was feasible and did not affect the translation of any of the individual cmRNAs.

3.1.8 Cotransfection of three different cmRNAs: lipofection vs magnetofection

To be able to investigate the double positive cells in cotransfection studies, RFP cmRNA was synthesized, and the further optimizations were carried out using Luc, eGFP and RFP cmRNAs.

3.1.8.1 Order of mixing of complexes' components affect cotransfecion efficacy

To prepare cmRNA magnetic complexes, three different components had to be mixed together: cmRNAs, cationic lipids, and magnetic nanoparticles (Figure 21 A). To investigate the effect of order of mixing of these components on cotransfection of cmRNAs, complexes containing the Luc, eGFP and RFP cmRNAs cocktail; Df-Gold; and MNPs (PEI Mag2 or SO-Mag5) were prepared using different orders of mixing (Figure 21).

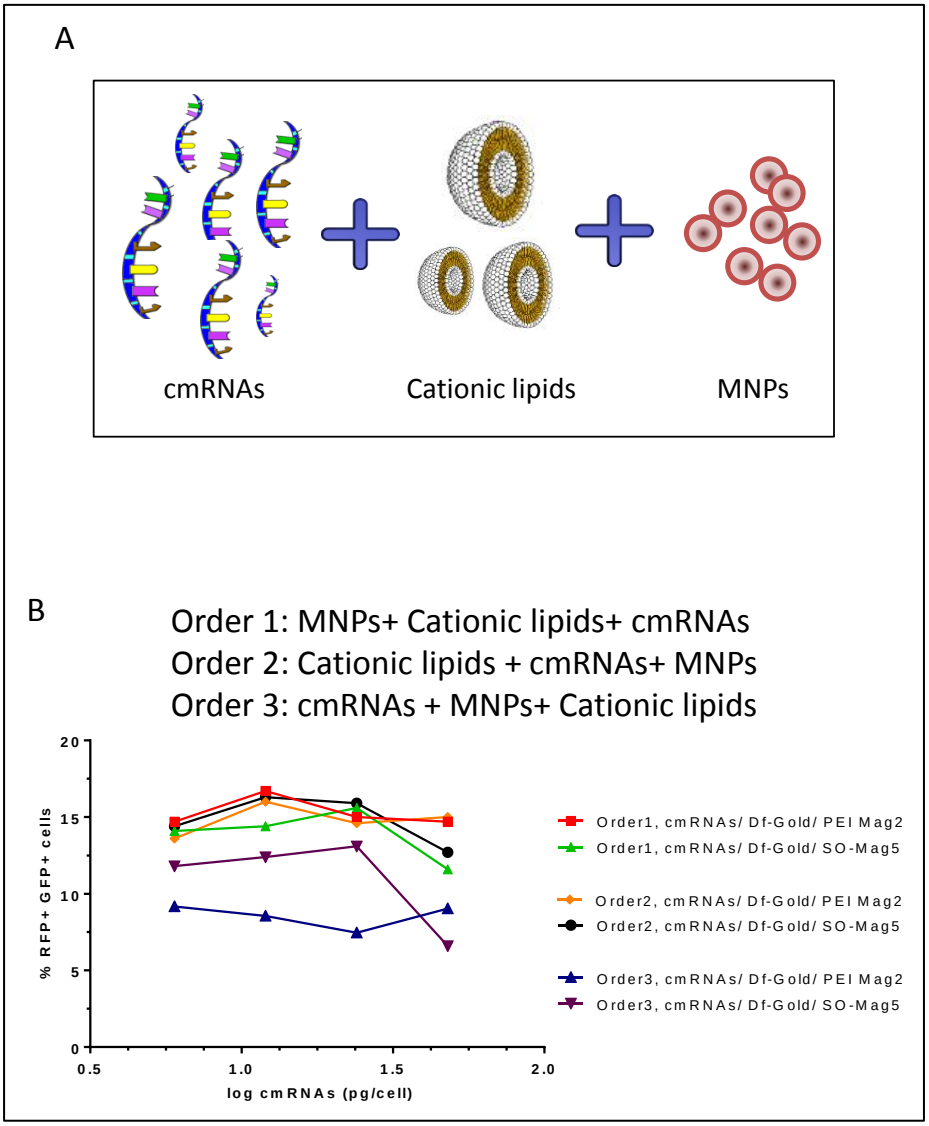

Figure 21 Evaluation of different orders of mixing of components for complex preparation in cotransfection of Luc, eGFP, and RFP cmRNAs. (A) Schematics of complex components. (B) FACS analysis: measuring double positive cells 24 h after cotransfection of PMEFs.

The prepared complexes then were added to the overnight cultured PMEFs. 24 h later, cotransfection efficacy was measured using FACS analysis, with order 3 revealing the lowest cotransfection efficacy. Order 1 was chosen for further experiments in this thesis.

3.1.8.2 Different strategies for adding various cmRNAs in complex preparation creates a dramatic effect on the efficacy of cotransfection

Different strategies of mixing various cmRNAs together and with other components of complexes (vectors and magnetic nanoparticles) were tested to find the most effective combination, resulting in the highest number of cotransfected PMEFs. As illustrated in Figure 22 A, one strategy was to add single cmRNAs, one by one, to the eppi containing Df-Gold and magnetic nanoparticles (strategy 1). Strategy number 2 showed the separate complex preparation for Luc, eGFP and RFP cmRNAs, where the prepared complexes were mixed directly before being added to the cells. Strategy 3, on the other hand, was to make a cocktail of cmRNAs' stocks, and then use this cocktail for complex preparation.

A

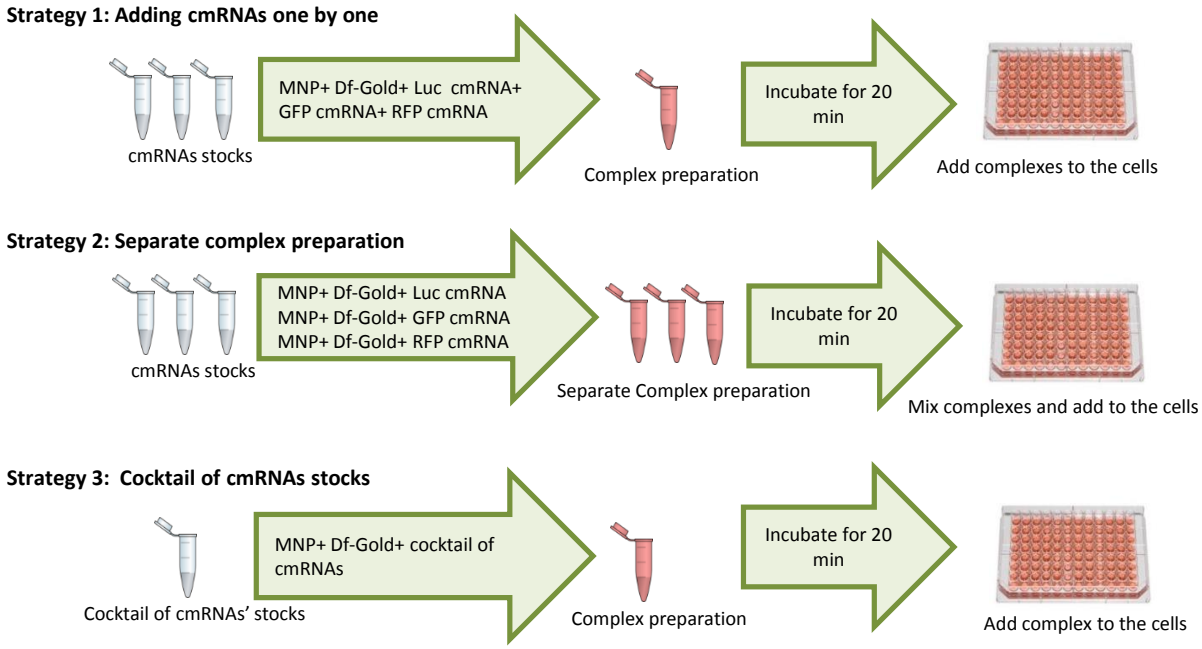
Strategy 1: Adding cmRNAs one by one
cmRNAs stocks
MNP+ Df-Gold+ Luc cmRNA+ GFP cmRNA+ RFP cmRNA
Complex preparation
Incubate for 20 min
Add complexes to the cells
Strategy 2: Separate complex preparation
cmRNAs stocks
MNP+ Df-Gold+ Luc cmRNA
MNP+ Df-Gold+ GFP cmRNA
MNP+ Df-Gold+ RFP cmRNA
Separate Complex preparation
Incubate for 20 min
Mix complexes and add to the cells
Strategy 3: Cocktail of cmRNAs stocks
Cocktail of cmRNAs' stocks
MNP+ Df-Gold+ cocktail of cmRNAs
Complex preparation
Incubate for 20 min
Add complex to the cells

B

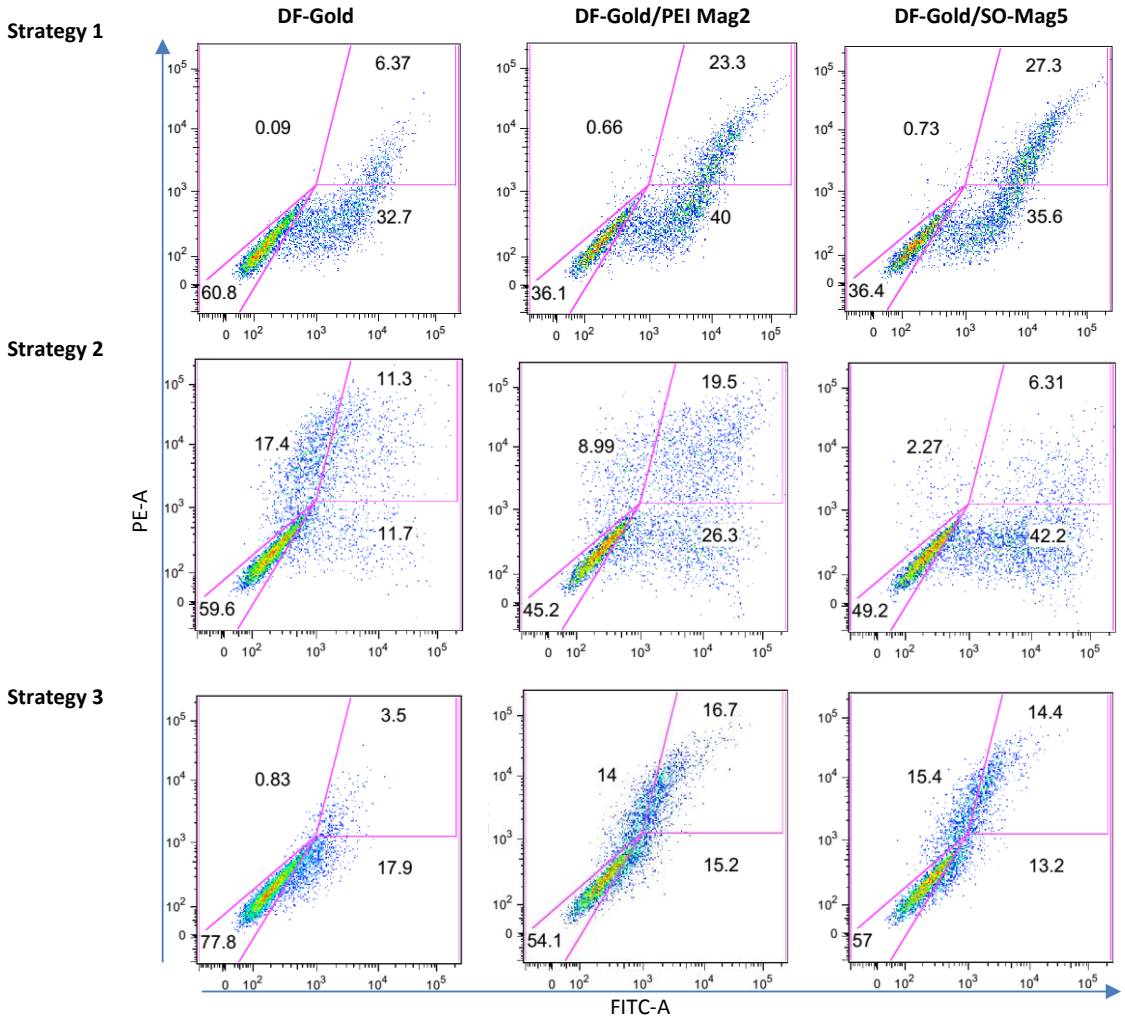
DF-Gold
DF-Gold/PEI Mag2
DF-Gold/SO-Mag5
Strategy 1
Strategy 2
Strategy 3
6.37
0.09
32.7
60.8
23.3
0.66
40
36.1
27.3
0.73
35.6
36.4
11.3
17.4
11.7
59.6
19.5
8.99
26.3
45.2
6.31
2.27
42.2
49.2
3.5
0.83
17.9
77.8
16.7
14
15.2
54.1
14.4
15.4
13.2
57
PE-A
FITC-A

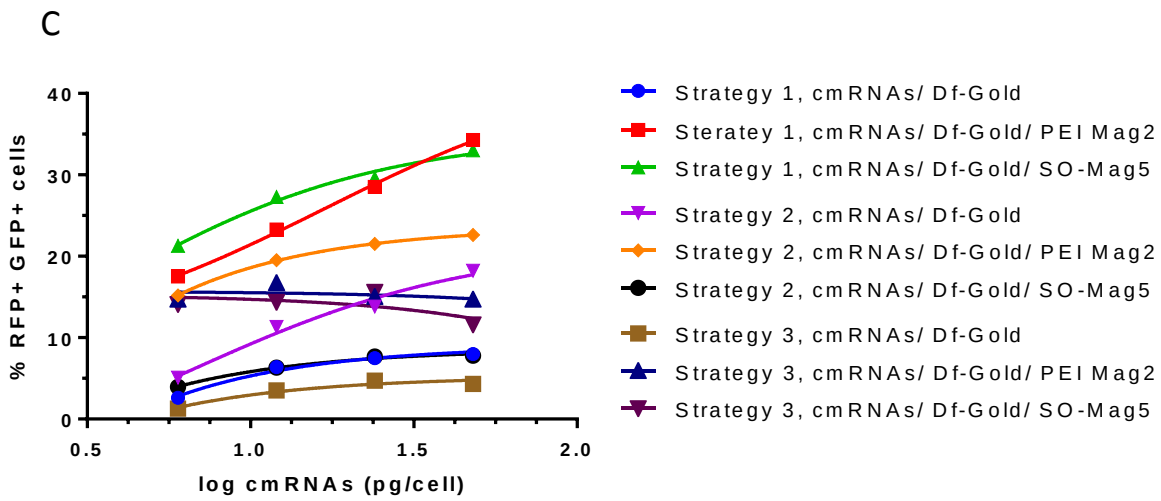

Figure 22 Determining the most efficient strategy of mixing cmRNAs for cotransfection of Luc, eGFP, and RFP cmRNAs. (A) Schematic of three different strategies for complex preparation.(B) FACS analysis: dot plots of single and double positive cells after cotransfetion of cmRNAs, using different strategies. (C) FACS analysis: measuring double positive cells 24 h after cotransfection of PMEFs. X-axis is in logarithmic scale.

All prepared complexes were then added to the overnight culture of PMEFs. 24 h later, FACS analysis was performed to assess the efficacy of cotransfection by measuring double positive cells (RFP+ GFP+). Figure 22 B displays the obvious differences in dispersity of cells in the dot plots of FACS analysis, and Figure 22 C quantifies the number of double positive cells. According to the FACS results, strategy number one was superior to other strategies, especially number 3 (cocktail of cmRNAs). Strategy 1 led to a high number of double positive cells that showed higher mean fluorescence intensity in dot plots than the strategy number 3. To be sure about the efficacy, strategy 1 was repeated but by using different orders when adding various cmRNAs to the solution of Df-Gold and MNPs. Similar results were obtained (data not shown). Cotransfection of just two mRNAs (RFP and eGFP) also did not vary the results (data not shown). Note that Luciferase was efficiently expressed in all different strategies (data not shown).

3.1.8.3 An optimized protocol was used to cotransfect PMEFs

Based on previous optimizations, SO-Mag5 nanoparticles were firstly mixed with Df-Gold, and then Luc, eGFP, and RFP cmRNAs were added stepwise. The mixture then was incubated for 20 min at RT to let the complexes self-assemble. Next, the prepared complexes were added to the semi-confluent culture of PMEFs, and the plate was incubated on the permanent magnetic field (average field and field gradient of 213 mT and 4 Tm^{-1}, respectively) for 20 min at humidified 37 °C and 5% CO2 (Figure 23 A). Then, the magnetic field was removed and double positive cells were visualized with a Nikon fluorescent microscope, 24 h post transfection (Figure 23 B).

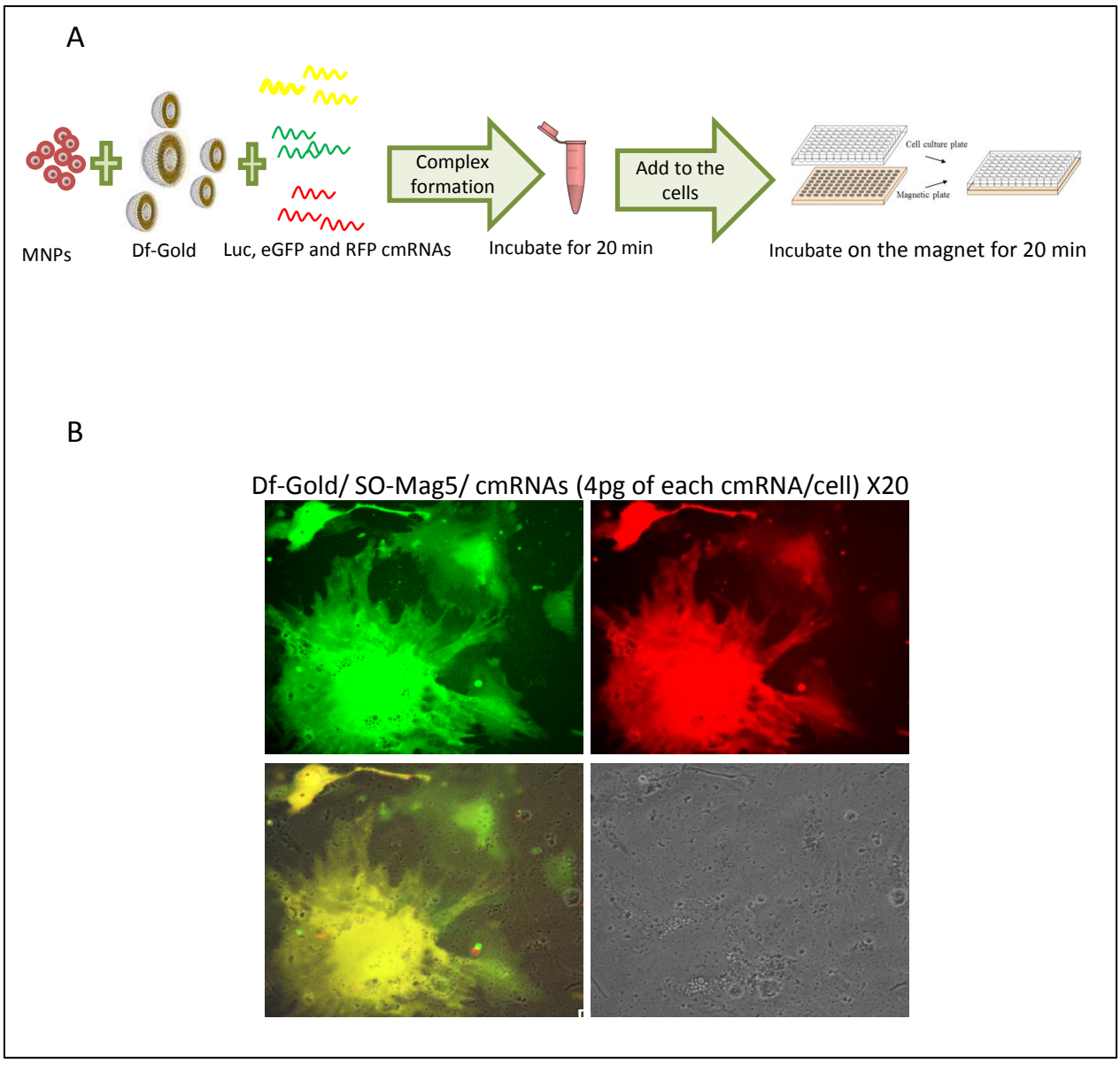

Figure 23 Cotransfection of Luc, eGFP, and RFP cmRNAs in an optimized way (strategy1, order1). (A) Schematic of optimized complex preparation and cotransfection. (B) Double positive PMEFs 24 h after cotransfection.

3.1.8.4 Magnetofection improved the efficacy of cotransfection of cmRNAs

24 h after the cotransfection of PMEFs with Luc, eGFP and RFP cmRNAs, the effect of magnetofection on improvement of cotransfection efficacy was investigated by using fluorescent microscopy, luciferase assay, and FACS analysis. As presented in Figure 24 A, more single and double positive cells were visualized with magnetofection than lipofection. Magnetofection also

had a positive effect on translation of luciferase in cotransfection of Luc, eGFP and RFP cmRNAs in PMEFs (Figure 24 B). In addition, when magnetic nanoparticles were used more double positive cells (eGFP+, RFP+) were detected by FACS analysis (Figure 24 C).

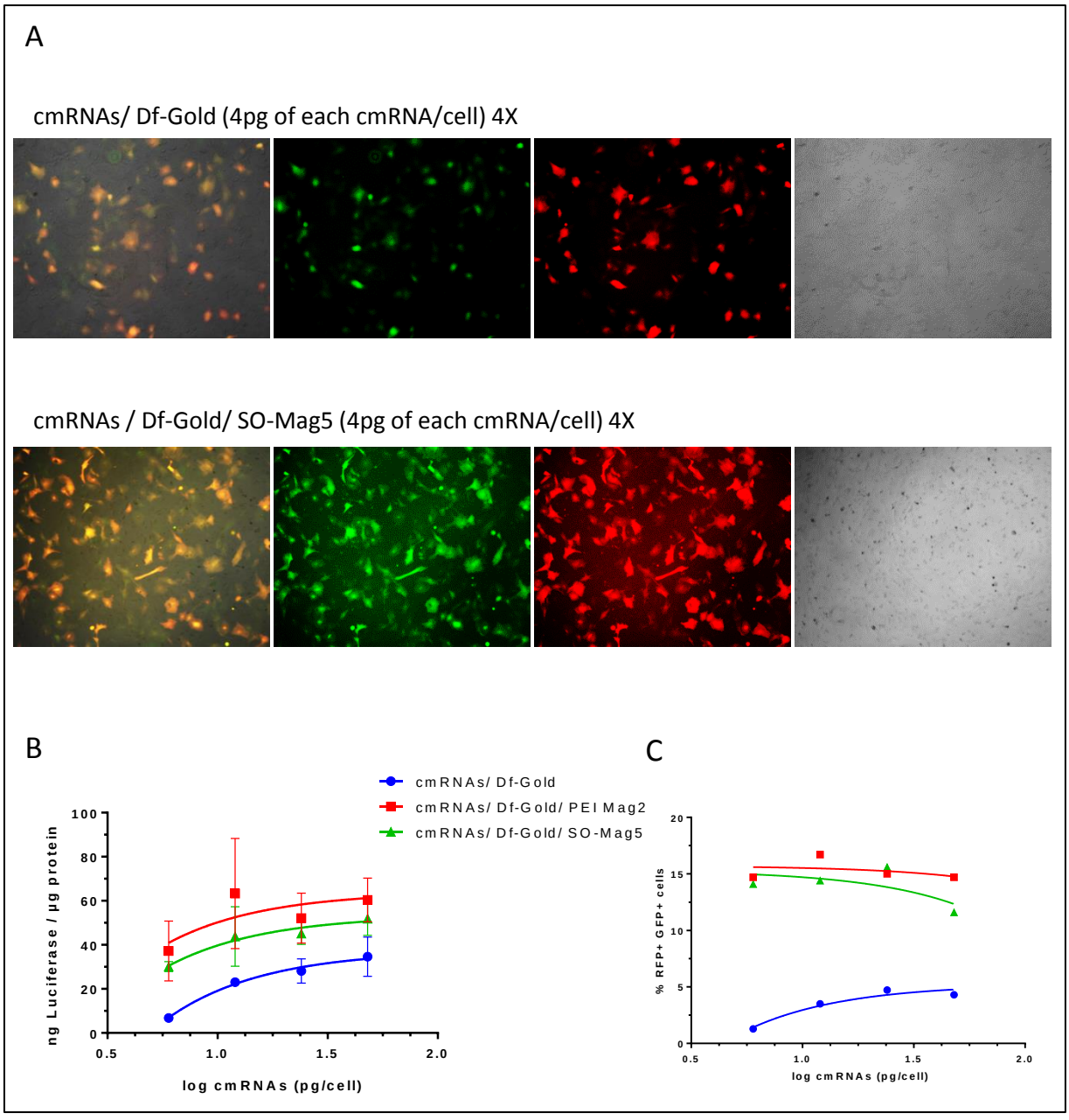

Figure 24 The effect of magnetofection in efficacy of cotransfection of Luc, eGFP, and RFP cmRNAs in PMEFs. (A) Fluorescent microscopy of cotransfected cells. (B) Luciferase assay: translation efficacy of luc cmRNA after cotransfection. Values are mean ± SD from three replicates. (C) FACS analysis: investigation of double positive cells. All data were obtained 24 h after cotransfection. X-axis is in logarithmic scale.

3.1.8.5 Iron content did not increase the toxicity in cotransfection of cmRNAs

According to previous optimizations, Fe:N 1:1 and 0.5:1, showed the highest transfection efficacy as well as low toxicity in single cmRNA transfection (Figure 17). In cotransfection of various cmRNAs however, the high amount of cmRNAs and, consequently, the high amount of iron might increase the risk of iron toxicity. Therefore, an MTT assay was performed to determine a safe iron content for cotransfection of cmRNAs. For this, respiration activities of cells were measured 24 h post cotransfection of PMEFs with Luc, eGFP and RFP cmRNAs, supplied with Df-Gold and magnetic nanoparticles (PEI Mag2 or SO-Mag5) with Fe:N 1:1 and 0.5:1. As shown in Figure 25, higher iron content did not increase the cell toxicity, and indeed, enhanced cell proliferations. According to these results, the cotransfection project was continued using Fe:N 1:1.

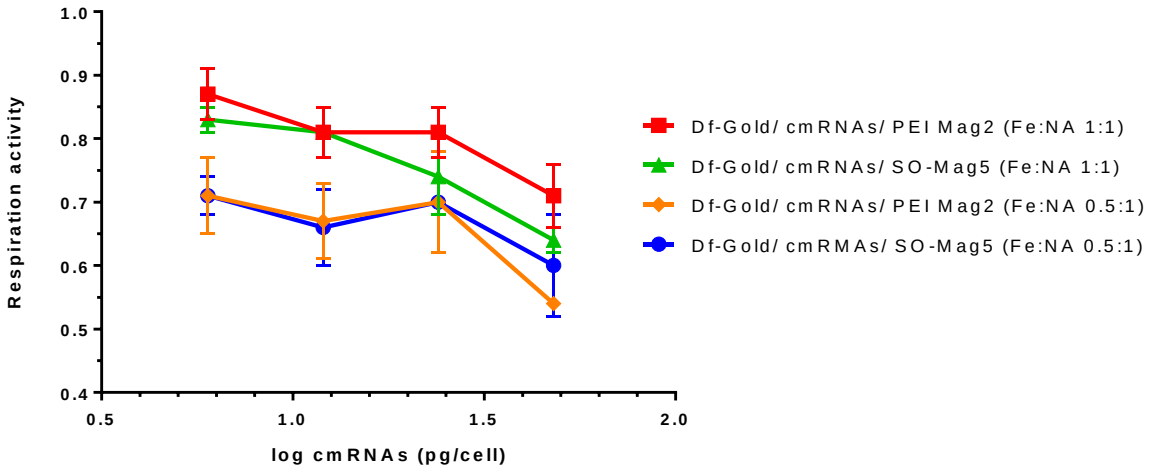

Figure 25 Optimizing iron to nucleic acid ratio in cotransfection of three cmRNAs to PMEFs. MTT assay: evaluation of toxicity of the most efficient concentrations of iron in the magnetic complexes.Untransfected cells were used as control. All data shown are mean ± SD from the values of three replicates. X-axis is in logarithmic scale.

3.1.9 Transfection and cotransfection of cmRNAs into cocultures of different cells; magnetofection compared to lipofection

A coculture of PMEFs and Porcine Fetal Fibroblasts (PFFs) was used to investigate the effect of magnetofection on transfection and cotransfection of cmRNAs in cocultures of different cells. In these experiments, Df-Gold as vector and PEI Mag2 and SO-Mag5 as magnetic nanoparticles were used. First, PMEFs (feeder layer) were seeded in day -2. One day later, PFFs (main layer) were seeded on the feeder layer. Transfection or cotransfection of cmRNAs was done 24 h after seeding the main layer, and a FACS analysis was performed 24 h post transfection/cotransfection (Figure 26). Prior to flow cytometry, PMEFs were stained with anti-feeder-APC (Miltenyi Biotec, Bergisch Gladbach, Germany), and thus could be distinguished from PFFs in the FACS analysis.

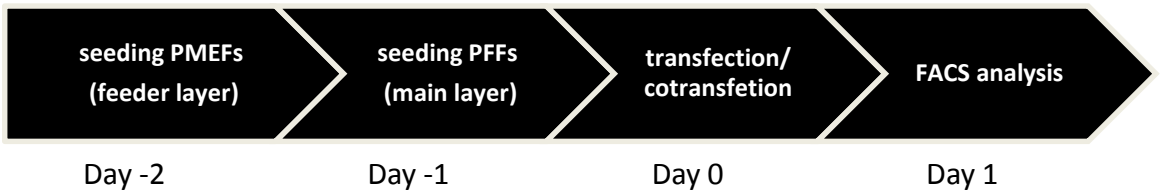

Figure 26 Time schedule for cotransfection of three different cmRNAs in coculture of cells

3.1.9.1 Transfection of single cmRNA into the coculture of PMEFs and PFFs

The effect of magnetofection on the transfection efficacy of single cmRNA in the coculture of PMEFs and PFFs was investigated using magnetofection and lipofection for delivery of RFP cmRNA and delivery of eGFP cmRNA, separately. As shown in Figure 27 A and B, regardless of type of magnetic nanoparticle and cmRNA, magnetofection improved the transfection efficacy in both the main layer (PFFs) and the feeder layer (PMEFs) over that obtained by convetional lipofection.

In general, transfection efficacy in PFFs was lower than PMEFs, which can be due to either different protein production ability in various cells, or higher passage number of PFF in this experiment.

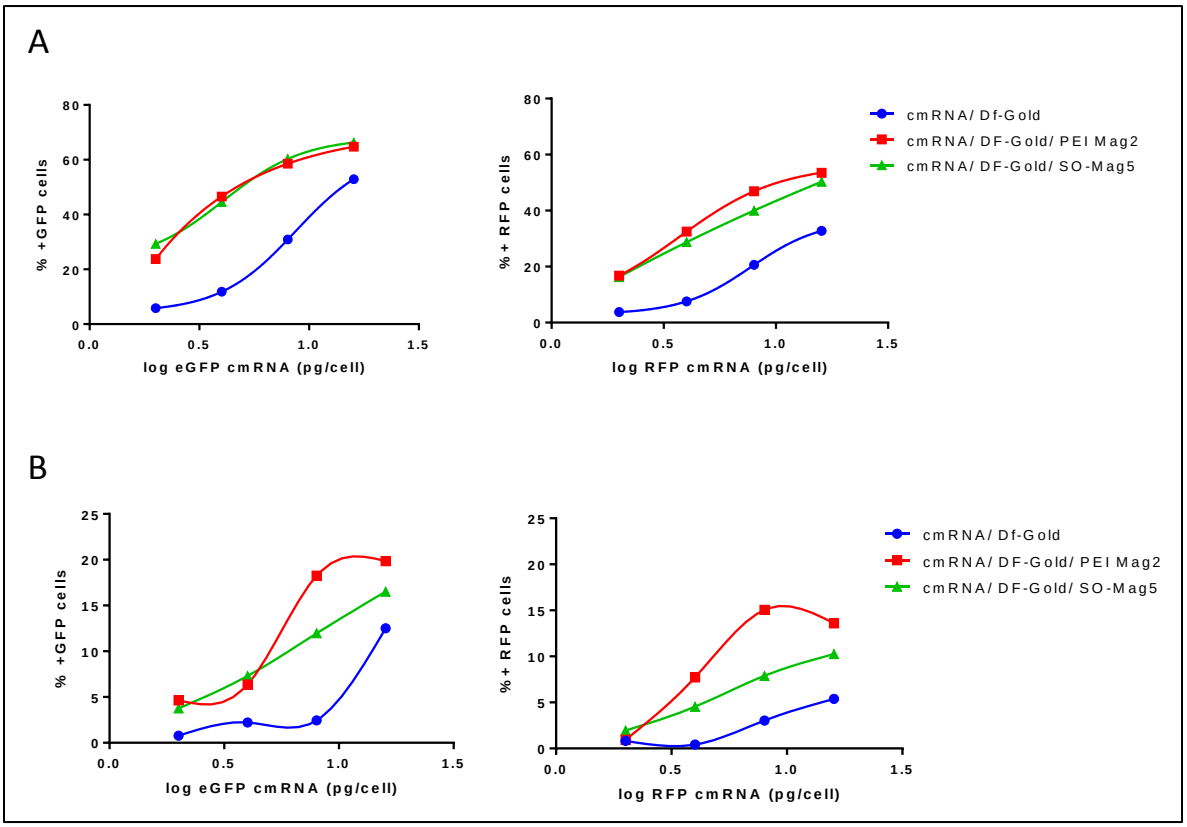

Figure 27 Magnetofection compared to lipofection in single cmRNA transfection into the coculture of PFFs and PMEFs. FACS analysis: quantification of GFP positive cells and RFP positive cells 24 h after transfection. (A) Feeder layer: PMEFs. (B) Main layer: PFFs. X axis is in logarithmic scale.

3.1.9.2 Cotransfection of three different cmRNAs into coculture of PMEFs and PFFs

Cocultures of PMEFs and PFFs were cotransfected with three cmRNAs (Luc, eGFP and RFP). 24 h later, cotransfection efficacy was assessed by measuring double positive cells (Figure 28). According to results, magnetofection improved the cotransfection efficacy of cmRNAs in both feeder and main layers of the coculture of the cells. Luciferase expression was not measured in this experiment.

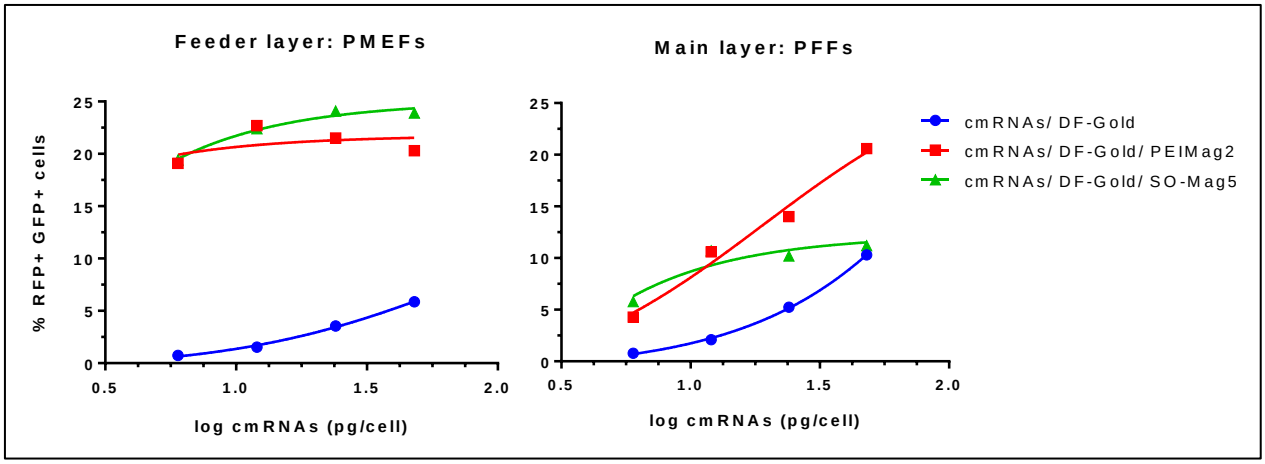

Figure 28 Magnetofection compared to lipofection in cotransfection of Luc, eGFP, and RFP cmRNAs into a coculture of PFFs and PMEFs. FACS analysis: investigation of double positive cells. All data obtained 24 h after cotransfection. X-axis is in logarithmic scale.

3.1.10 Characterizing magnetic lipoplexes of cmRNAs

Size and zeta potential of different complexes were measured using the Malvern instrument (Worcester, UK) (Table 3). All complexes were positively charged; although, the complexes with SO-Mag5 were bigger, the transfection efficacy using SO-Mag5 or PEI Mag2 showed no dramatic differences (Figure 24, Figure 27, and Figure 28).

Table 3 Characterization of cmRNA magnetic lipoplexes

Complex composition	Hydrodynamic diameter (nm)	Zeta potential (mV)
DF-Gold/PEI Mag2/ eGFP cmRNA	155.3	18.23
DF-Gold/PEI Mag2/ RFP cmRNA	192.4	16.17
DF-Gold/PEI Mag2/ Luc cmRNA	138.7	17.63
DF-Gold/So- Mag5/ eGFP cmRNA	1080.0	19.30
DF-Gold/So- Mag5/ RFP cmRNA	998.3	19.33
DF-Gold/So- Mag5/Luc cmRNA	1105.6	18.13

3.1.11 Magnetofection of cmRNA; a well optimized protocol for enhanced cmRNA delivery *in vitro*

In this study, a protocol for enhanced non-viral cmRNA delivery by using magnetofection was established. Among non-viral vectors, Df-Gold (a cationic lipid) enhanced cmRNA delivery more efficiently than PAA20k-EPE (a cationic polymer). With both positively charged (PEI Mag2) and negatively charged (SO-Mag5) magnetic nanoparticles, magnetofection improved the efficacy of transfection as well as cotransfection of cmRNAs in the mono and coculture of primary fibroblasts.

In conclusion, this thesis introduced a well optimized protocol for a safe and efficient cmRNAs transfection *in vitro*. This is relevant in research and therapeutic applications when simultaneous translation of several mRNA-encoded proteins is required, such as reprogramming fibroblasts to iPSCs with cmRNAs encoding for Yamanaka factors.

3.2 cmRNA delivery in 3D matrices of collagen sponges: sustained cmRNA delivery

3.2.1 Preparation and characterization of cmRNAs complexes with a proprietary cationic lipid

The preparation of lipid/RNA complexes is an important prerequisite for cmRNA delivery due to high sensitivity of the mRNA molecule to the ubiquitous nucleases. In this part of the project, a proprietary cationic lipid from Ethris GmbH, C12EPE , was used as a non-viral vector. This cationic lipid is based on a short oligo(alkyl amine), comprising four amino groups in an ethylene-propylene-ethylen (EPE) backbone, as shown in Figure 29.

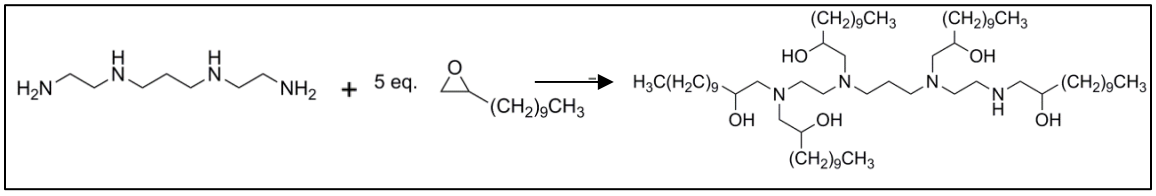

Figure 29 Schematic of C12EPE comprising an olygo(alkyl amine) with ethylen-propylen-ethylen (EPE) backbone and five equivalents of 1,2-epoxydodecane

This alkyl amine was then made to react with 5 equivalents of 1,2-epoxydodecane in order to generate C12EPE [92], which in turn built lipoplex with cmRNAs by means of electrostatic interaction between the positive amino groups of lipid and negative phosphate groups of cmRNA [28]. To stabilize the lipoplex structure and reduce the leakage of encapsulated cmRNAs, C12EPE was further supplied with two helper lipids, namely 1,2-dipalmitoyl-*sn*-glycero-3-phosphocholine (DPPC) and cholesterol [93, 94]. 1,2-Dimyristoyl-sn-glycerol methoxypolyethylene Glycol, (DMG-PEG) 2kD, was also added as shielding lipid. It has been previously demonstrated that PEGylation improves the physico-chemical characteristics of liposome formulation by increasing

water solubility, protecting from enzymatic degradation, and limiting immunogenic and antigenic reactions [95]. Final N/P ratios for the entire ethanolic lipid mixture were 8/ 5.29/ 4.41/ 0.88 for molar ratios of amino groups of C12EPE/ DPPC/ Cholesterol/ DMG-PEG, respectively, to one phosphate group of cmRNA molecule.

Recently, the effect of polyethylenimine (PEI) in cmRNA delivery for bone regeneration has been published [96]. Consequently, cmRNA polyplexes containing PEI were formulated, at an N/P ratio of 10, to compare with cmRNA lipolexes with C12EPE.

Biophysical characteristics of the cmRNA complexes have been tabulated in Table 4. The hydrodynamic diameter for all the products were approximately 50 nm. cmRNA lipoplexes had a polydispersity index close to 0.1, which indicates a homogeneous product. In contrast to highly positive PEI polyplexes, total surface charge for all lipoplexes were slightly positive, close to neutral.

Table 4 Characterization of cmRNA complexes

mRNA Complex	Mean Hydrodynamic Diameter (nm)	SD Hydrodynamic Diameter (nm)	Poly Dispersity Index (PDI)	Zeta Potential (mV)
eGFP/ PEI	49.25	1.15	0.237	32.2
eGFP/C12EPE	45.86	0.34	0.061	0.82
Met luc/C12EPE	69.95	0.26	0.177	0.464
hBMP2/C12EPE	51.84	0.84	0.094	0.27

3.2.2 cmRNA complexes with C12EPE were more efficient and less toxic than cmRNA-PEI complexes

The efficiency and toxicity of cmRNA complexes with PEI and proprietary lipid were then compared in a set of preliminary experiments to find the most efficient vectors for cmRNA delivery on transcript-activated matrices (TAMs). PEI complexes loaded on TAMs showed no effect for cmRNA delivery (Figure 30 A). Indeed, cmRNA lipoplexes with C12EPE showed lower toxicity and higher efficiency than PEI complexes, and thus were used for further experiments (Figure 30 A and B).

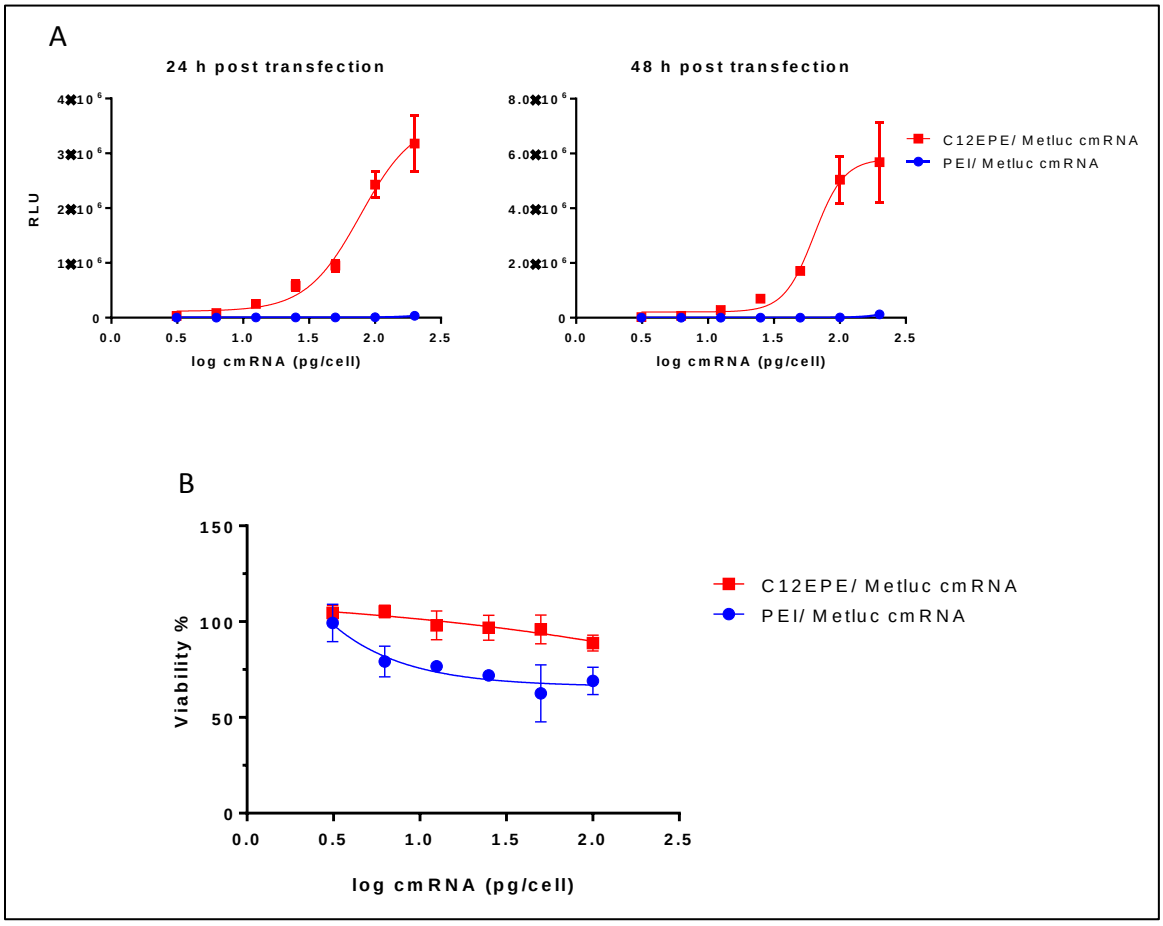

Figure 30 Comparison of PEI and C12EPE as vectors for Met luc cmRNA transfection on TAMs. (A) Expression of Metluc: cmRNA transfection efficacy at 24 h and 48 h post transfection. (B) CellTiter-Glo assay: toxicity measurement at 48 h post transfection. Untransfected cells were used as negative control. All data shown are mean ± SD from the values of three replicates. X-axis is in logarithmic scale.

3.2.3 Collagen sponges as suitable 3D scaffolds for cell culture

For investigation of cell behavior on the 3D matrix, migration of different cells into the collagen sponges was confirmed by Eosin-Hematoxylin (EH) staining of a vertical cut of a sponge several days after cell seeding. Figure 31A shows migration of NIH3T3 cells into the collagen scaffold 7 days after cell seeding. In another experiment, expansion of MC3T3-E1 cells within the collagen matrix was visualized 5 days post cell seeding. Most of the cells appeared on the surface of the collagen sponge one day after seeding, while the sponge was densely populated five days after seeding (Figure 31 B). This indicates that by the time cells colonized the interior of the 3D matrix.

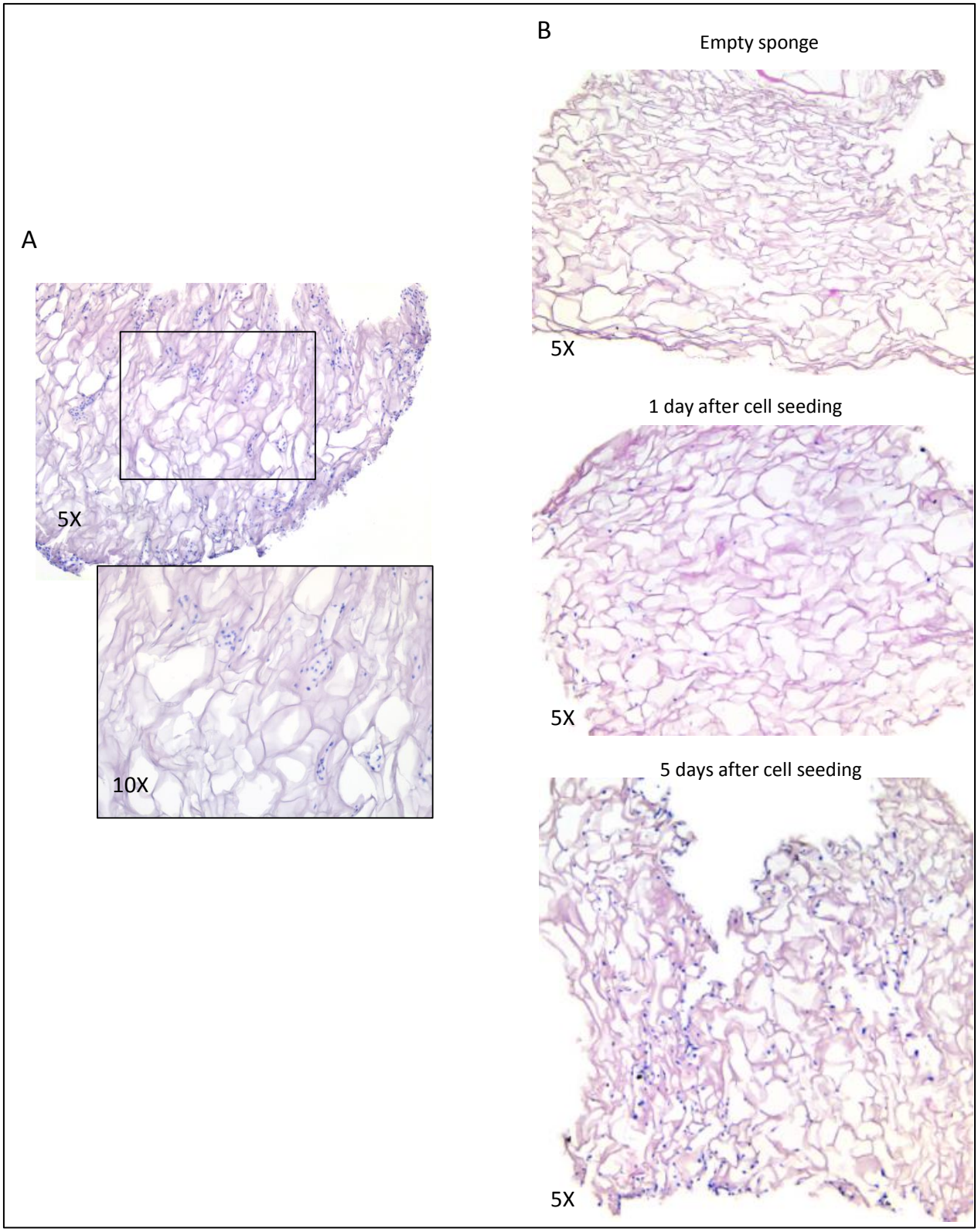

Figure 31 Hematoxylin-Eosin staining: collagen sponges serve as suitable 3D scaffolds for culturing different cells. (A) NIH3T3 cells 7 days after seeding on the collagen sponge. (B) Empty sponge and sponge containing MC3T3-E1 cells, 1 and 5 days after cell seeding. In all pictures the nuclei of the cells were stained in dark blue.

3.2.4 Loading and vacuum-drying of cmRNA lipoplexes onto the collagen sponges

Prior to loading on the collagen sponges, sucrose was added to the lipoplex preparation to a final concentration of 2% w/v as a lyoprotectant. Lyoprotectants maintain the integrity of the biological system during dehydration in the vacuum-drying process [97]. Visualizing the unloaded sponges by scanning electron microscopy (SEM) showed that compared to a native collagen sponge, a vacuum-dried collagen sponge containing 2% sucrose resembled a closed cage with smaller pores, where pores get filled with sucrose film (Figure 32).

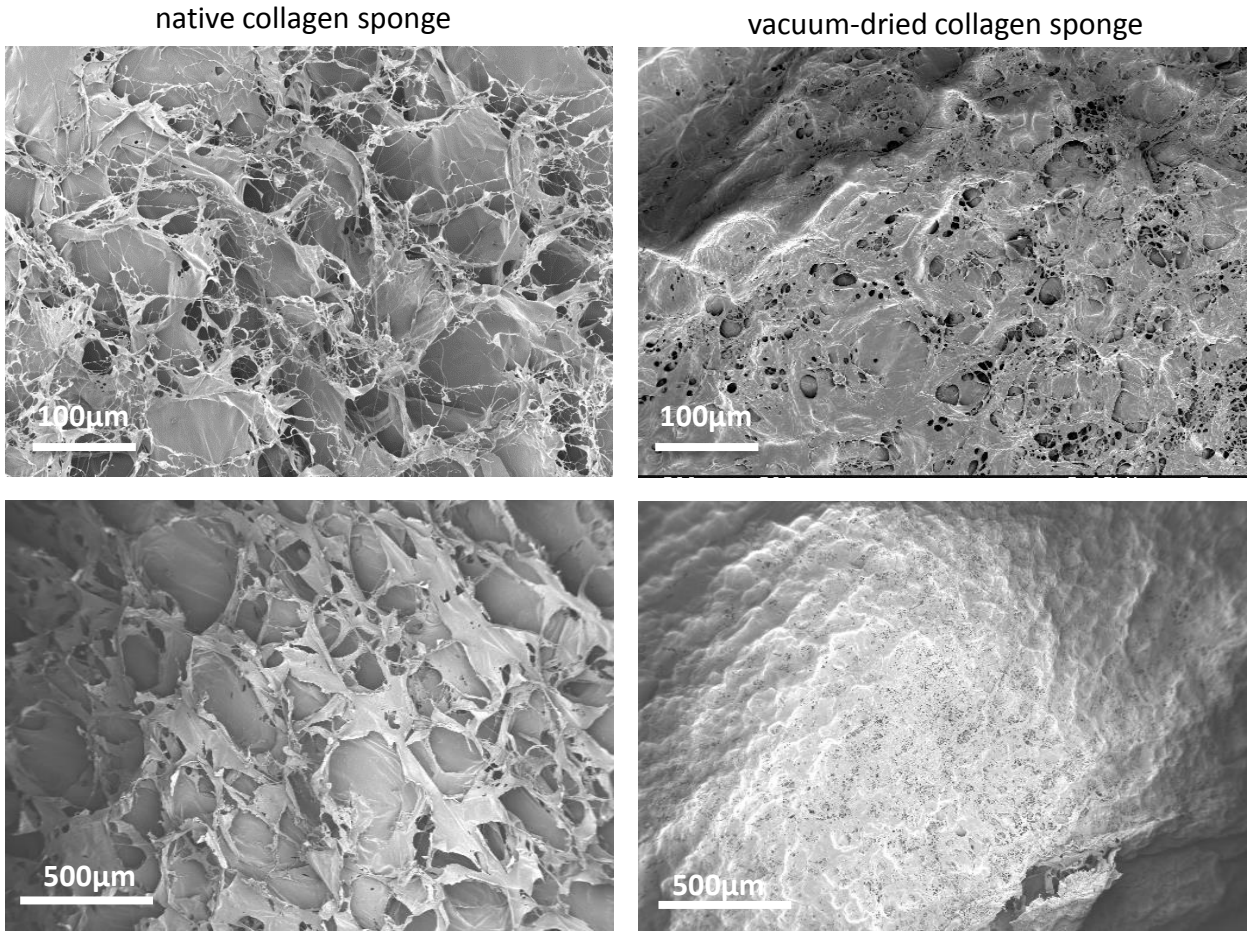

Figure 32 SEM pictures of collagen sponges before and after vacuum drying.

In addition, vacuum-dried cmRNA-loaded sponges were investigated by SEM with higher magnification, and particulate structures were revealed that might represent lipid nanoparticles (Figure 33).

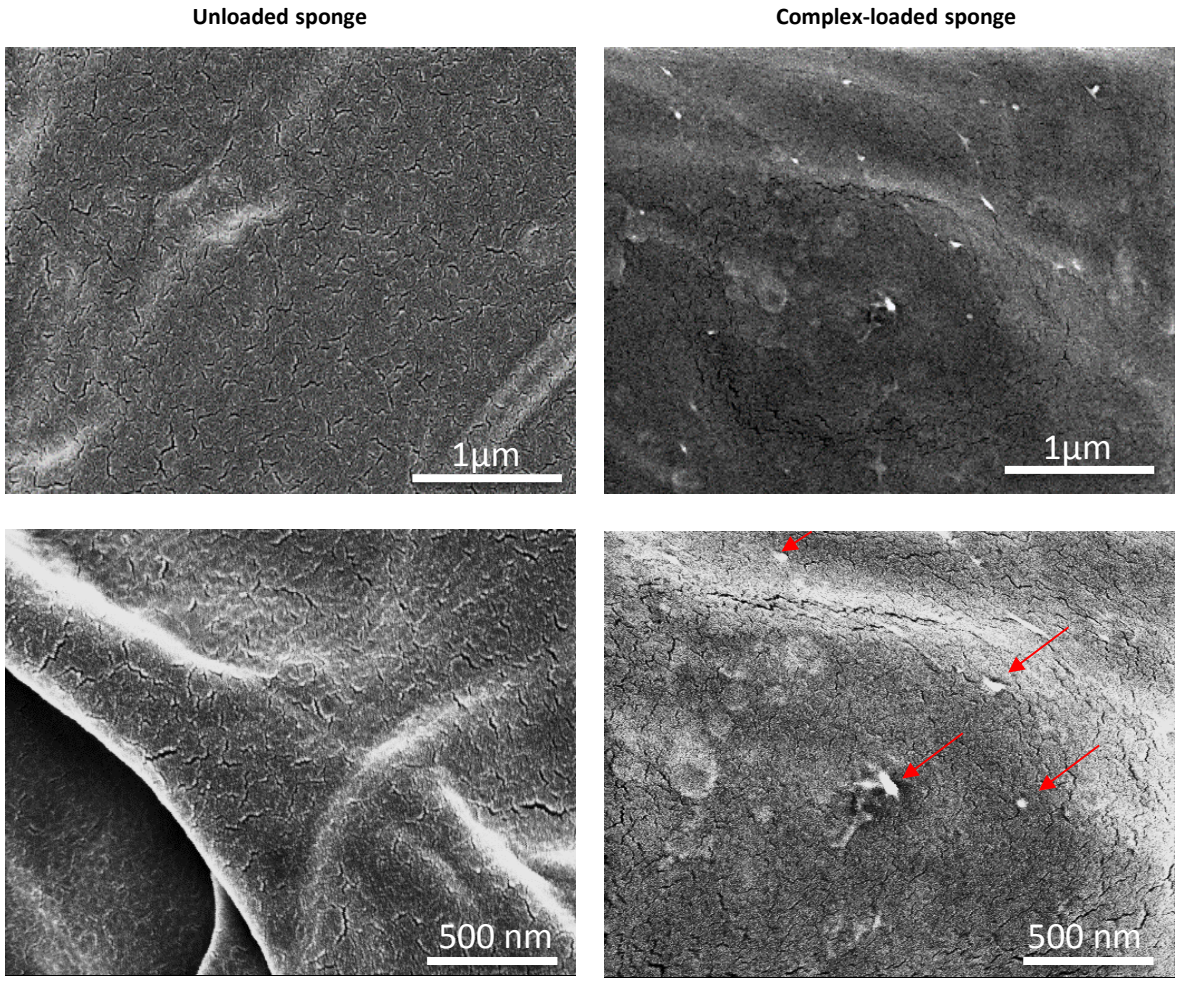

Figure 33 Scanning electron microscopy of vacuum-dried collagen sponges, unloaded and loaded with luciferase cmRNA lipoplexes (mean hydrodynamic diameter of lipoplexes: 65,8 nm).

3.2.5 Cell seeding and cell transfection onto transcript-activated matrices (TAMs)

To investigate cmRNA loading as well as cell transfection on TAMs, collagen sponges were loaded with 2µg of tdTomato cmRNA lipoplexes, in which 10% of tdTomato cmRNA were covalently FITC-conjugated. The dispersity of cells and cmRNA lipoplexes on the sponges, as well as transfection efficacy, was visualized, using a Leica DMi8 fluorescent microscope (Leica microsystems, Heerbrugg, Switzerland) 30 h after seeding NIH3T3 cells. As presented in Figure 34, cells were transfected and expressed tdTomato protein (red spots) mostly in locations with high cmRNA accumulations (green spots).

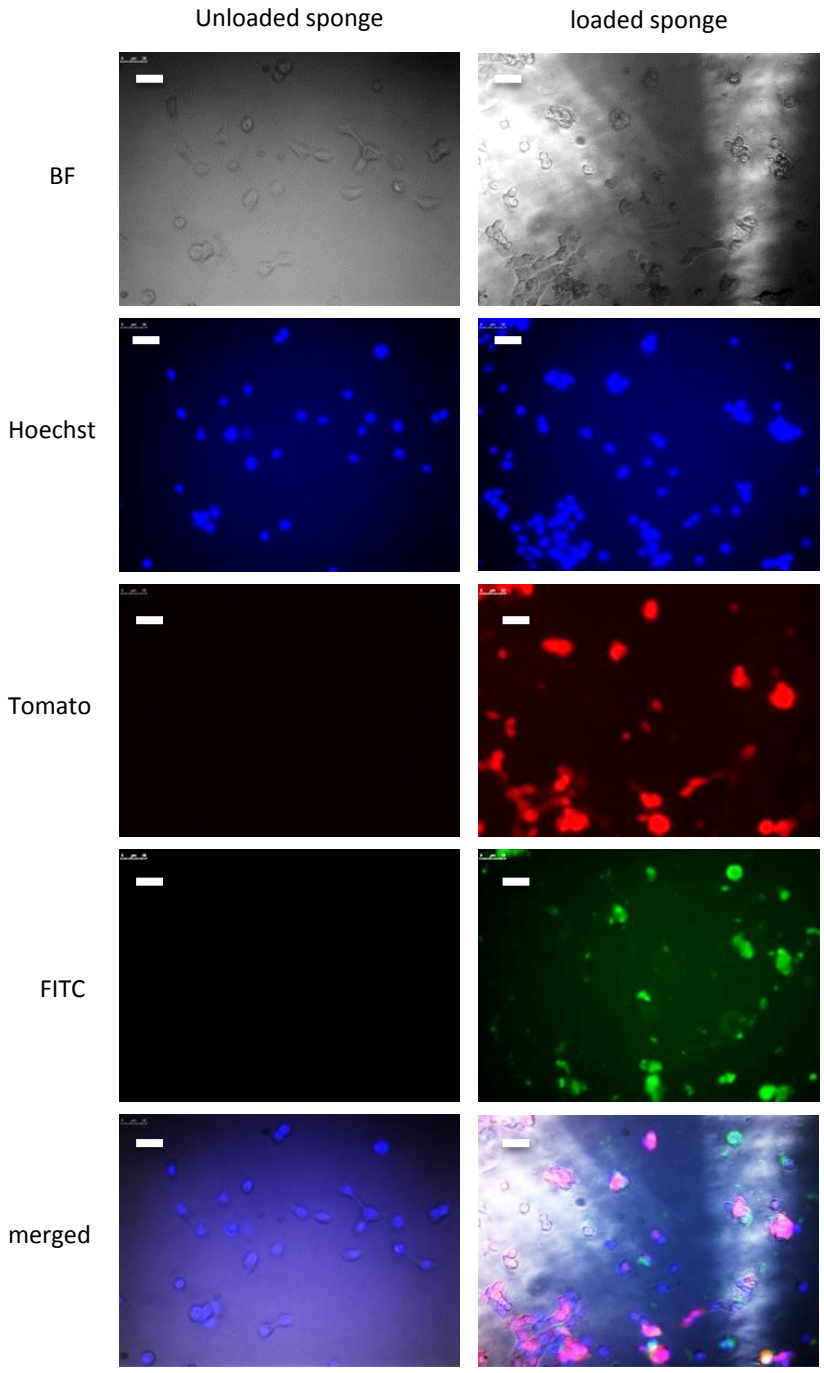

Figure 34 Fluorescence microscopy of NIH3T3 cells 30 h after seeding on the collagen sponges loaded with tdTomato cmRNAs, where 10% tdTomato cmRNAs were FITC labelled. Scale bars show 50 µm.

3.2.6 Transfection efficacy using TAMs

To verify the efficacy of cell transfection in TAMs, transfection efficacy of NIH3T3 cells was assessed 48 h after seeding the cells onto the eGFP-encoding TAMs. Firstly, positive eGFP expressing cells were visualized using a JULY™ fluorescence microscope (Baker and Baker Ruskinn, USA) (Figure 35 A). To quantify these results, a FACS analysis was performed and a significant increase in the mean fluorescence intensity in transfected cells was observed (Figure 35 B). Up to 100% transfection efficiencies were obtained by using higher cmRNA amounts per cell (Figure 35 C).

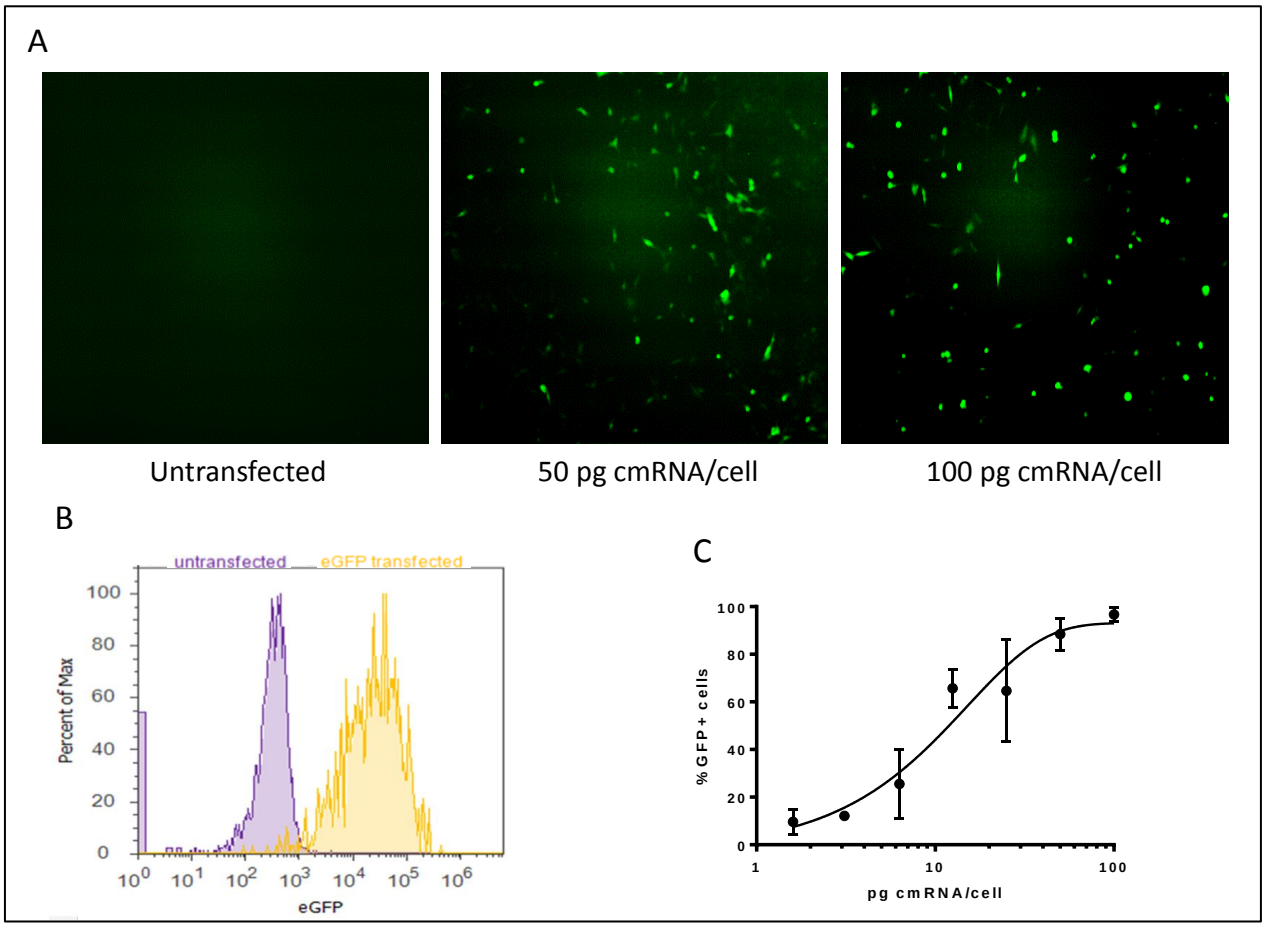

Figure 35 Transfection efficacy 48 h after seeding NIH3T3 cells on eGFP-encoding TAMs. (A) Fluorescence microscopy with 4× magnification (JULY™): expression of eGFP cmRNAs in NIH3T3 cells. (B) FACS analysis: a clear shift of mean fluorescent intensity in NIH3T3 cells transfected with 100 pg/cell eGFP cmRNA, compared to untransfected cells. (C) FACS analysis: correlation of mRNA dose with respect to transfection efficiency. Data shown are mean ± SD from the values of three replicates.

3.2.7 TAMs function as depots for sustained cmRNA delivery

To investigate whether TAMs can provide a sustained cmRNA delivery system, translation kinetics of *Metridia* luciferase (Met luc) cmRNAs in NIH3T3 cells was recorded over 11 days and compared with translation in conventional 2D format (Figure 36).

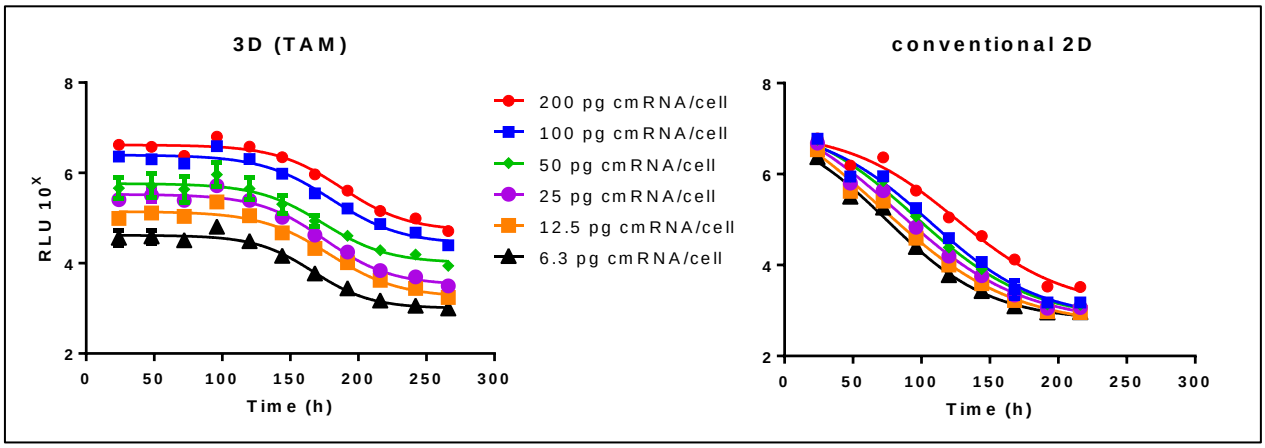

Figure 36 Translation kinetics of Metridia luciferase cmRNAs in 2D versus 3D culture, using NIH3T3 cells. Supernatants were collected every 24 h after transfection, and expression of Met luc was measured immediately in Relative Light Unit (RLU). All data shown are mean ± SD from the values of three replicates. Y-axis is in logarithmic scale

TAMs showed the properties of a sustained cmRNA delivery system with a plateau of protein expression for six consecutive days and substantial residual expression at the higher doses even after 11 days, whereas no expression was detectable after 8 days in the conventional 2D cell culture system.

Similar results were obtained by loading unmodified mRNA-containing lipoplexes onto the collagen sponges (Figure 37).

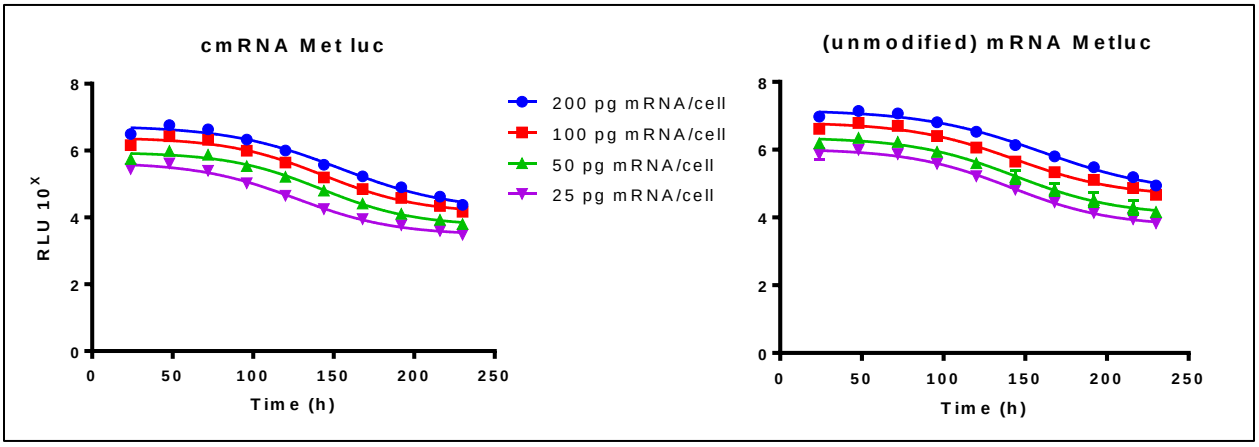

Figure 37 Kinetics of Met luc translation post transfection of chemically modified Met luc mRNA or unmodified Met luc mRNA in NIH3T3 cells on TAMs. Supernatants were collected every 24 h after transfection, and kept at -20 °C. After 10 days, expression of Metridia luciferase was measured for all time points. Data shown are mean ± SD of three replicates. Y axis is in logarithmic scale.

Interestingly, the sustained delivery efficiency was dependent to a significant degree on the vacuum drying step during sponge preparation. When cells were seeded on sponges right after soaking the lipoplexes into the sponges, there was no initial plateau of reporter expression (Figure 38). However, the half-life of expression (18 h) was twice the one upon transfection in 2D format (9 h) but shorter than the signal decay after plateau expression on the dried sponges (23 h). This provides evidence that vacuum-drying is an essential step to provide a sustained cmRNA delivery system in our setting.

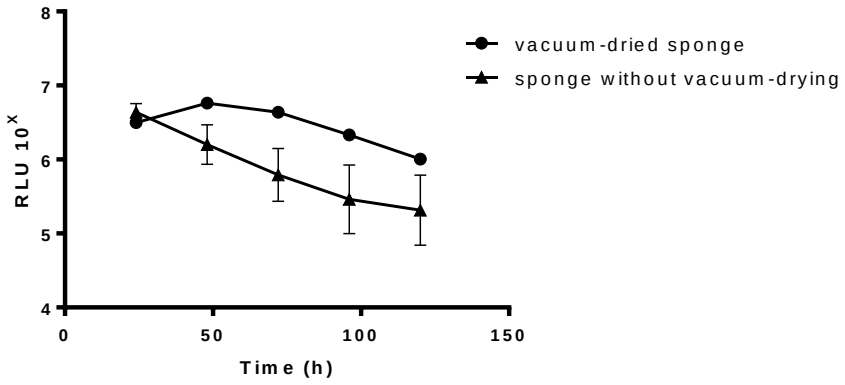

Figure 38 Effect of vacuum drying on kinetics of Metluc translation in NIH3T3 cells on collagen sponges. Supernatants were collected every 24 h after transfection and kept at -20 °C. After 5 days, expression of Metridia luciferase was measured for all time points. Data shown are mean ± SD of three replicates. Y-axis is in logarithmic scale.

In addition, TAM was tested for primary cells, using rat mesenchymal stem cells (MSCs) isolated from bone marrow (BMSCs) and adipose tissue (AMSCs). With both cell types, the kinetics of Met luc translation were determined by seeding an increasing number of cells on lipoplex-loaded collagen sponges (Figure 39.A). The initial plateau of reporter expression was not as pronounced as with NIH3T3 cells. Expression half-life was 15 h for BMSC and 21 h for AMSC. There was a sigmoidal dependence of expression levels on the number of cells seeded per sponge for BMSC reaching a plateau at 20,000 cells per sponge and an EC50 value of 8,000 cells per sponge. In contrast, no cell density-dependent plateau of expression was reached in the examined range of cell densities for AMSC such that no reliable EC50 value could be determined. Summarized, high-level expression was maintained for at least four days at and above 5,000 cells per sponge with both cell types (Figure 39 B).

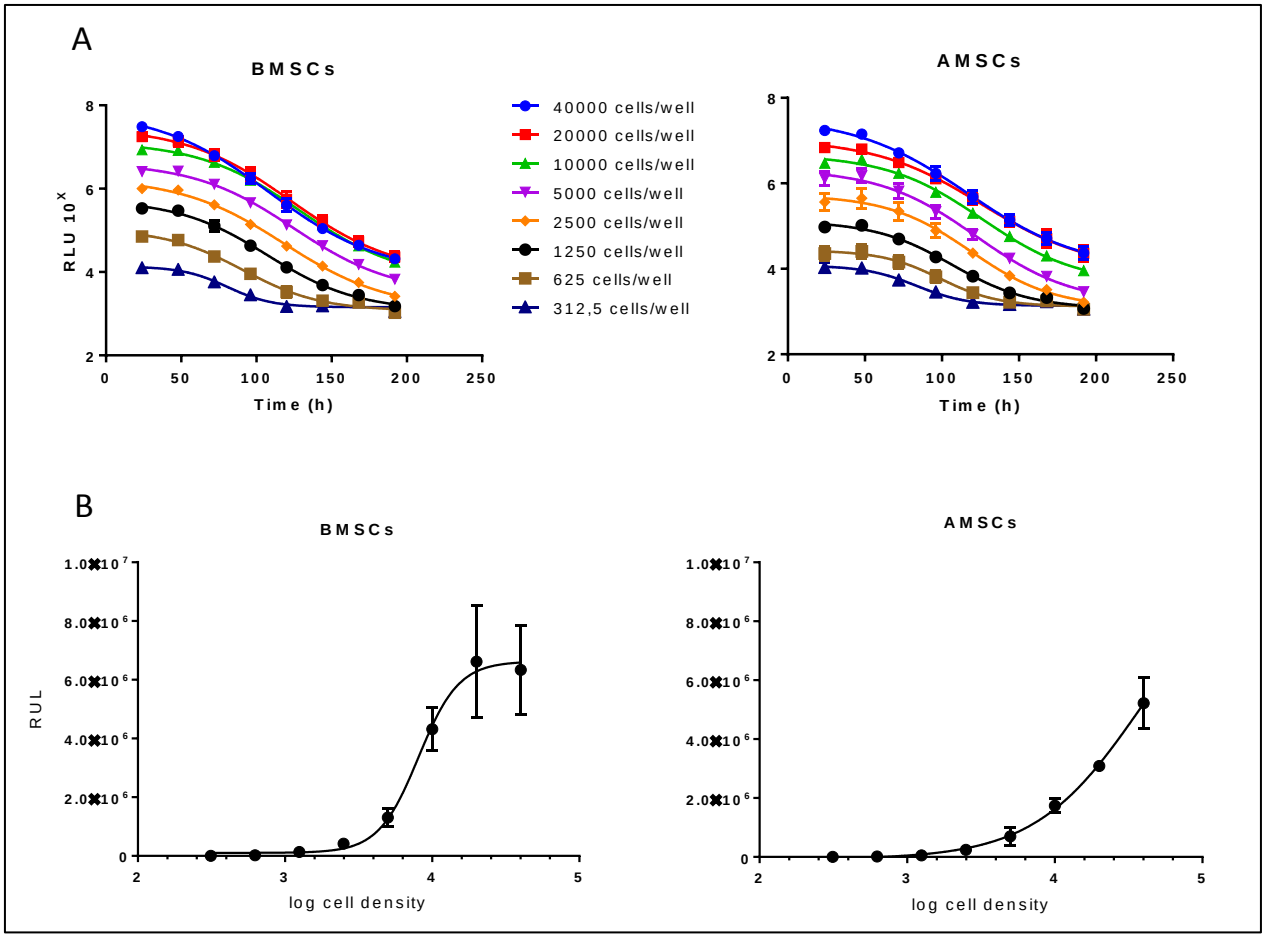

Figure 39 Kinetics of Metridia luciferase translation on TAMs, using MSCs at different cell densities. mRNA doses were calculated as 50 pg/cell. Supernatants were collected every 24 h after transfection, and kept at -20 °C. After 8 days, expression of Metridia luciferase was measured for all time points. (A) Kinetics of protein production in different cell densities. Y-axis is in logarithmic scale. (B) Expression of Met luc cmRNA 72 h after transfection in different cell densities. X-axis is in logarithmic scale. Data shown are mean ± SD from the values of three replicates.

3.2.8 *In vitro* osteogenic differentiation using hBMP2-encoding TAMs

To validate the performance of the sustained cmRNA delivery system for a physiological effect, two *in vitro* osteogenic differentiation experiments were designed with two different cell types, namely MC3T3-E1 and MSCs, using hBMP2 cmRNA lipoplexes [81, 82, 98].

3.2.8.1 In vitro cell differentiation using MC3T3-E1 cells

First, expression of BMP2 protein was detected using immunohistochemistry (IHC) of collagen sponges. 10,000 of osteoblast-like cells (MC3T3-E1) were seeded on the hBMP2-encoding TAM. Cells on the empty sponges were used as a negative control. Five days later, the sponges were assessed for the expression of BMP2 using immunohistochemistry, following by counter-staining of the cells' nuclei with hematoxylin (Figure 40).

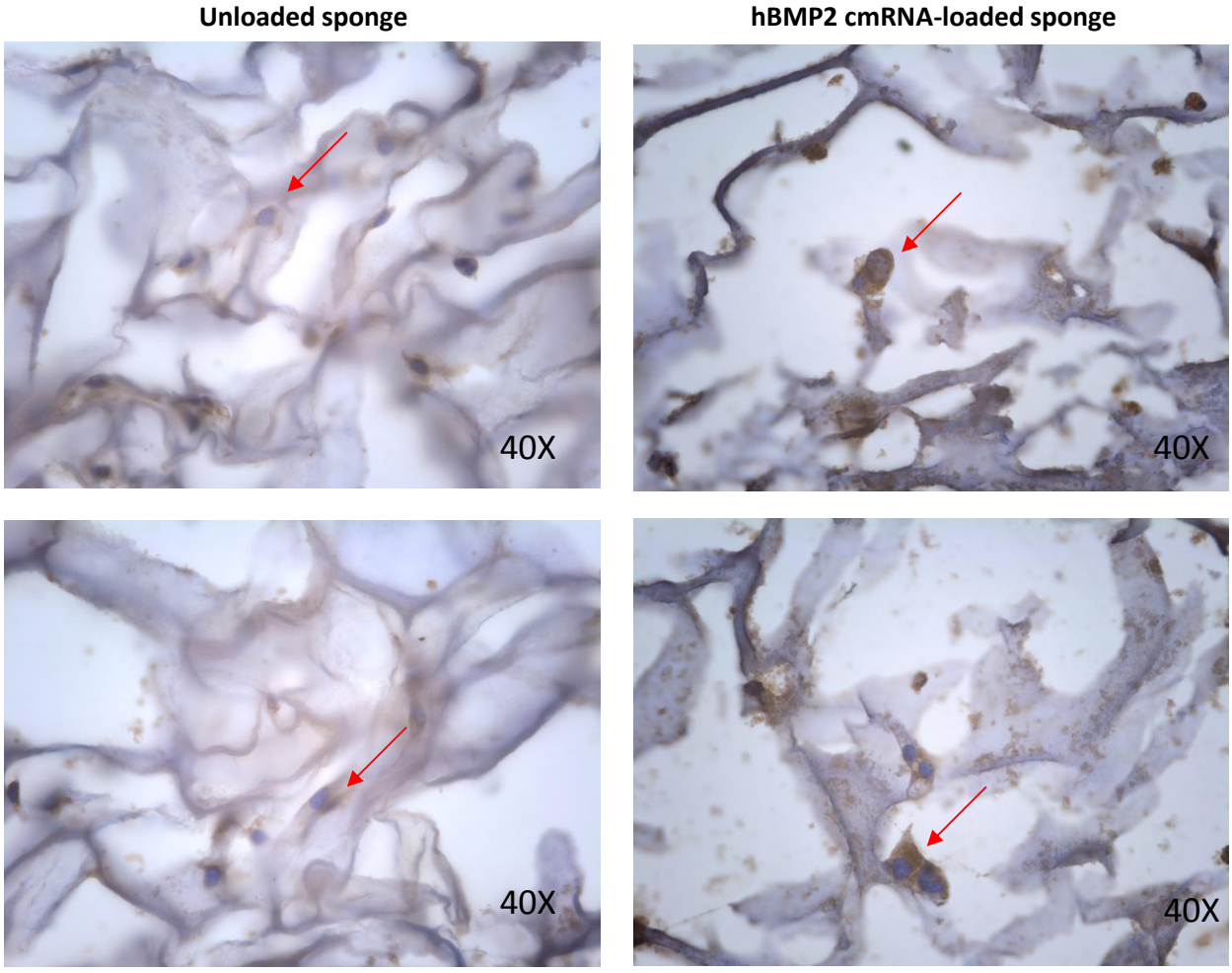

Figure 40 IHC of collagen sponges for the detection of hBMP2 five days after seeding MC3T3-E1. hBMP2 proteins were stained in dark brown. The nuclei of the cells were counter-stained with Hematoxylin in dark blue. Red arrows show some examples of hBMP2 positive cells.

Although some of the substrate solutions were absorbed by the collagen sponges and gave a brownish background, dark brown spots indicating BMP2 protein were more intense and widely dispersed in the sponges loaded with hBMP2 cmRNA, especially close to the locations of the cells (stained in dark blue).

To confirm osteogenic differentiation in MC3T3-E1 cells, 7 and 14 days after seeding the cells on hBMP2-encoding TAMs, reverse transcription polymerase chain reaction (RT-qPCR) was performed to quantify the expression of osteogenic markers (OCN and ALP). Untransfected cells, seeded on unloaded collagen sponges, were used as a negative control. As shown in Figure 41, both markers strongly expressed in both time points, and the expressions increased by day 14.

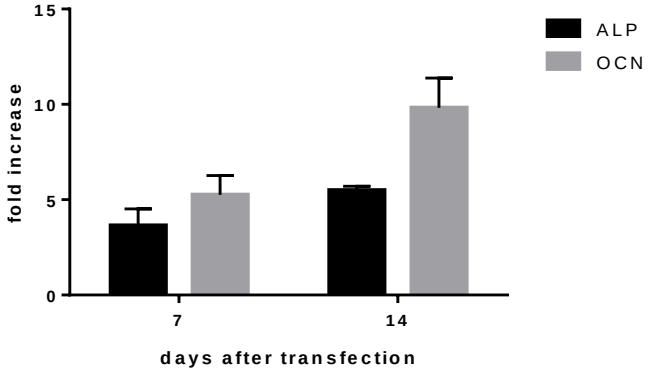

Figure 41 In vitro bone differentiation using MC3T3-E1 cells. RT-qPCR results: fold increase of expression of osteoblast markers at 7 and 14 days after seeding MC3T3-E1 cells on hBMP2-encoding TAMs. Values are mean ± SD from of three replicates, and normalized to the expression of GAPDH. Data expressed as fold increase to untransfected cells in 3D.

3.2.8.2 In vitro cell differentiation using Mesenchymal stem cells (MSCs)

In the next step, the same setting was used to perform *in vitro* osteogenic differentiation using MSCs. First, freshly isolated cells were evaluated for the positive and negative surface markers of MSCs, using FACS analysis (Figure 42). As expected, cells were expressing CD90 and CD29, which are identifiers for MSCs. On the other hand, the cells did not express markers of

differentiated cells, such as CD45 (expressed in all hematopoietic cells except erythrocytes and platelets), CD106 (found on endothelial or vascular cells, upon inflammation), and CD31 (found on platelets, monocytes, neutrophils) [99]. Negative results obtained with isotype controls, i.e. IgM K-FITC, IgG1 K-FITC and IgG1 K-PE, ensured specific binding of applied antibodies.

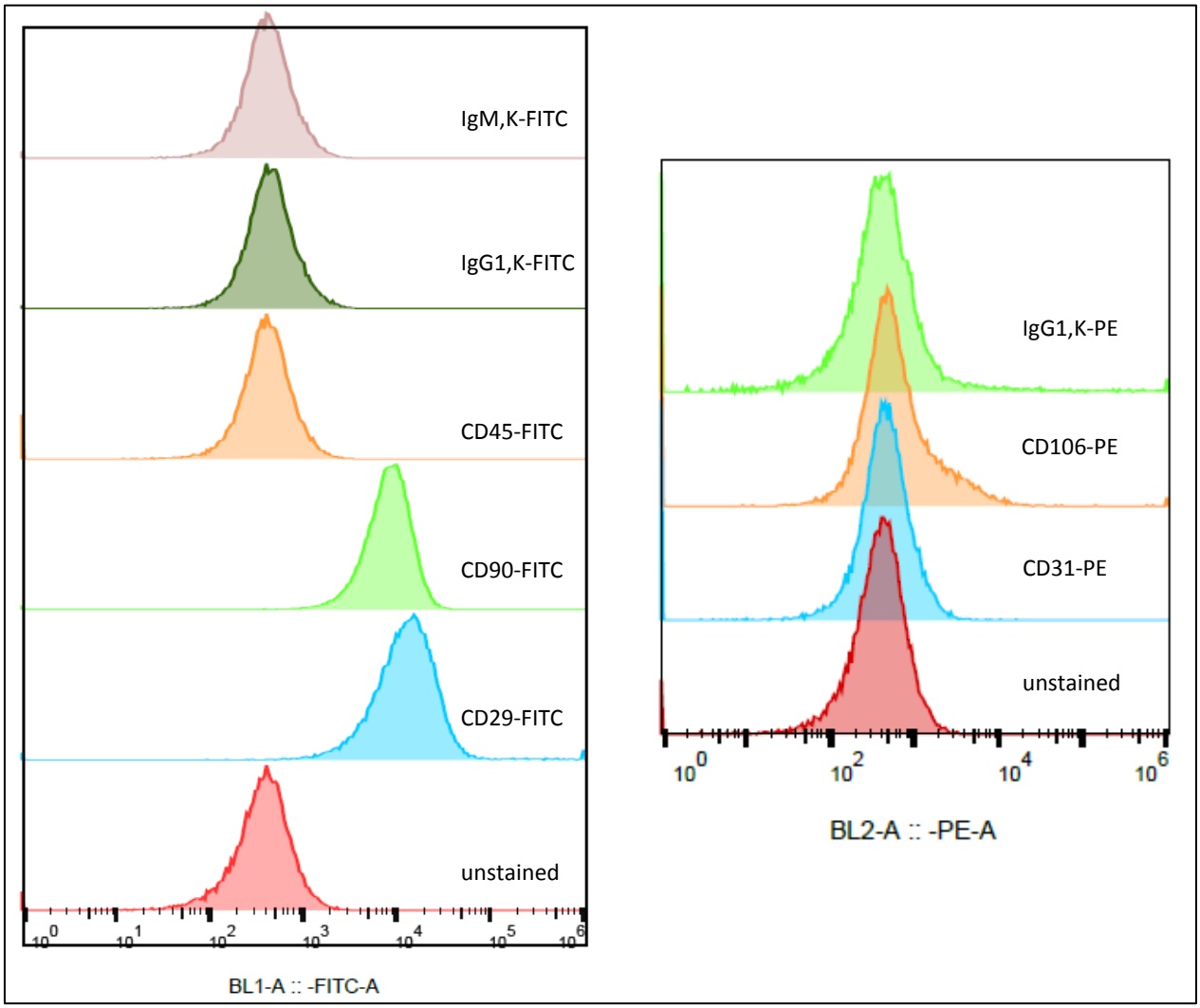

Figure 42 FACS analysis: investigation of positive (CD90 and CD29), and negative (CD45, CD106 and CD31) markers for MSCs after isolation from fat tissue of rat. IgM K-FITC, IgG1 K-FITC, and IgG1 K-PE have been used as isotype controls.

Thereafter, MSCs were seeded on the hBMP2-endocing TAMs. At 24 h post transfection, hBMP2 translation was quantified in the supernatant, using ELISA (Figure 43).

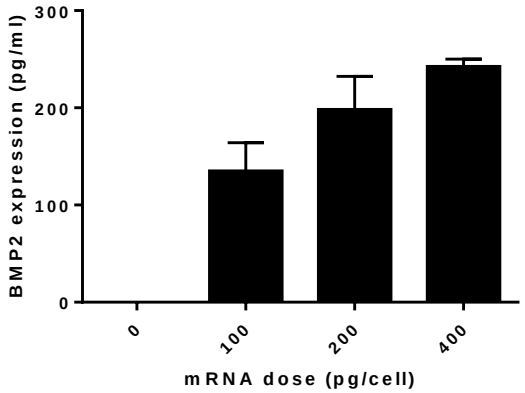

Figure 43 ELISA: production of hBMP2 by MSCs seeded on hBMP2-encoding TAMs. Data shown are mean ± SD from the values of three replicates.

7 and 14 days later, expression of osteogenic markers (RUNX2, OSX, OCN, and ALP) were detected, using RT-qPCR. Unexpectedly, all markers were highly expressed, not only in transfected but also in untransfected MSCs seeded on the 3D collagen scaffold. Therefore, an untransfected MSCs culture in a conventional 2D setting (standard cell culture cultivation in a petri-dish), treated exactly like cells in 3D (with respect to medium and washes), was chosen as the negative control to normalize the expression of osteogenic markers observed in cells in 3D. As presented in Figure 44 A, the cultivation in a 3D collagen matrix alone significantly upregulated the expression of osteogenic markers in MSCs. In addition to the quantification of osteogenic markers via real time PCR, sponges were visualized for macroscopic changes during the course of the differentiation experiment. The images are shown in Figure 44 B. By day 7, sponges loaded with hBMP2 appeared fluffier and had expanded in size, while unloaded sponges condensed and shrank over time.

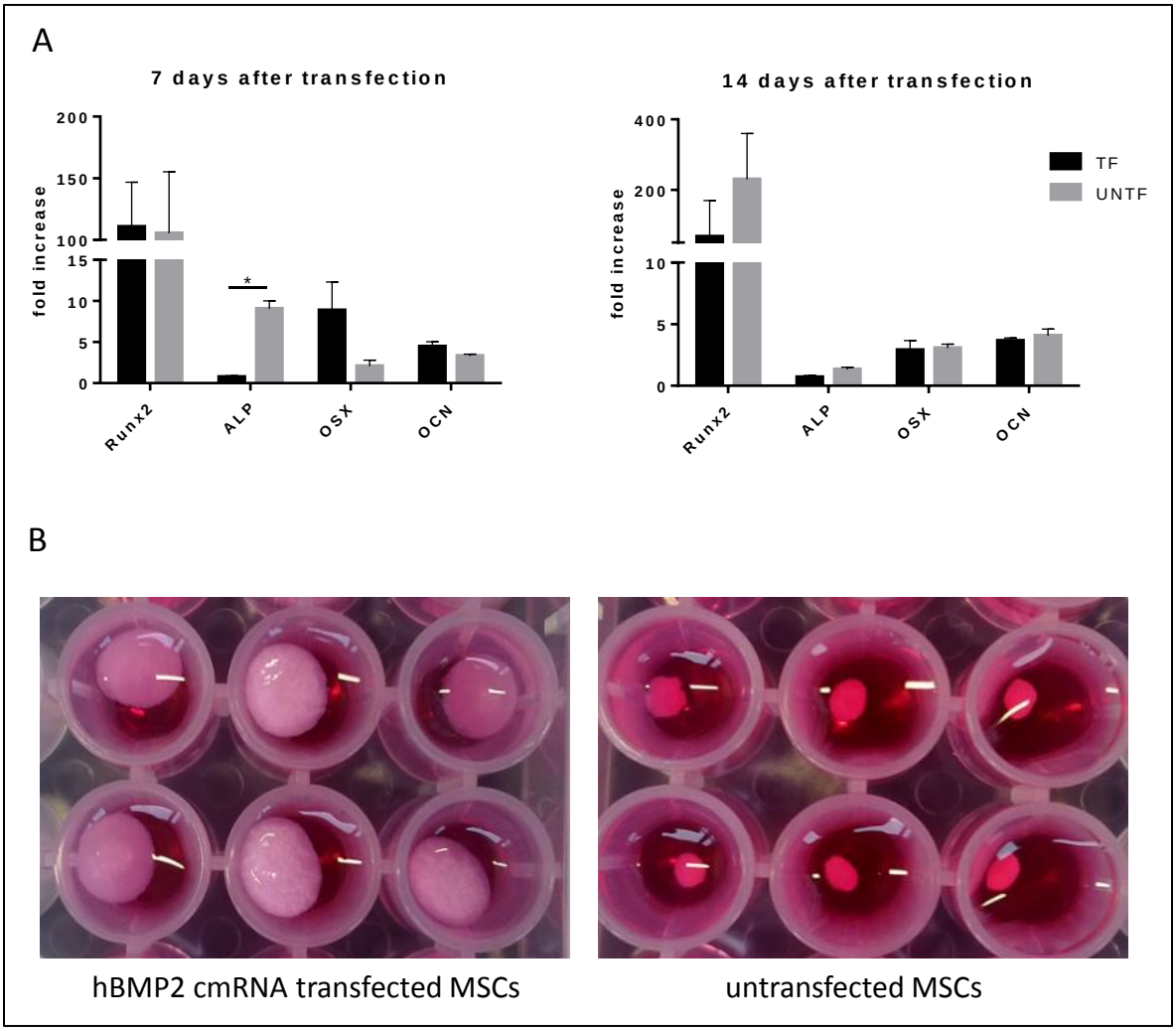

Figure 44 . In vitro bone differentiation, using MSCs. (A) RT-qPCR results: fold increase of expression of osteoblast markers at 7 and 14 days after seeding MSCs on hBMP2-encoding TAMs. Values are mean ± SD from of three replicates, and normalized to the expression of β-tubulin. Data expressed as fold increase to untransfected cells in 2D, and compared using multiple t-test. (B) Macroscopic changes in sponges' morphologies during differentiation. Pictures were taken from the 96-well-plate 7 days after seeding MSCs on the sponges.

3.2.9 *In vivo* bone regeneration using hBMP2-encoding TAMs

In vivo bone regeneration activity was evaluated in a non-critical rat femur defect model. hBMP2-encoding TAMs as well as empty collagen sponges were applied to nine femur defects for each group. In details, the sponges were implanted in to 2-mm diameter bone defects, created in the central part of rat femur bones. To visualize and quantify bone healing, a micro-computed tomography (μ-CT) scan was taken two weeks after surgery. As presented in Figure 45 A and B,

significantly more newly formed bone was found in the defects treated with hBMP2-encoding TAMs than the ones treated with empty sponges.

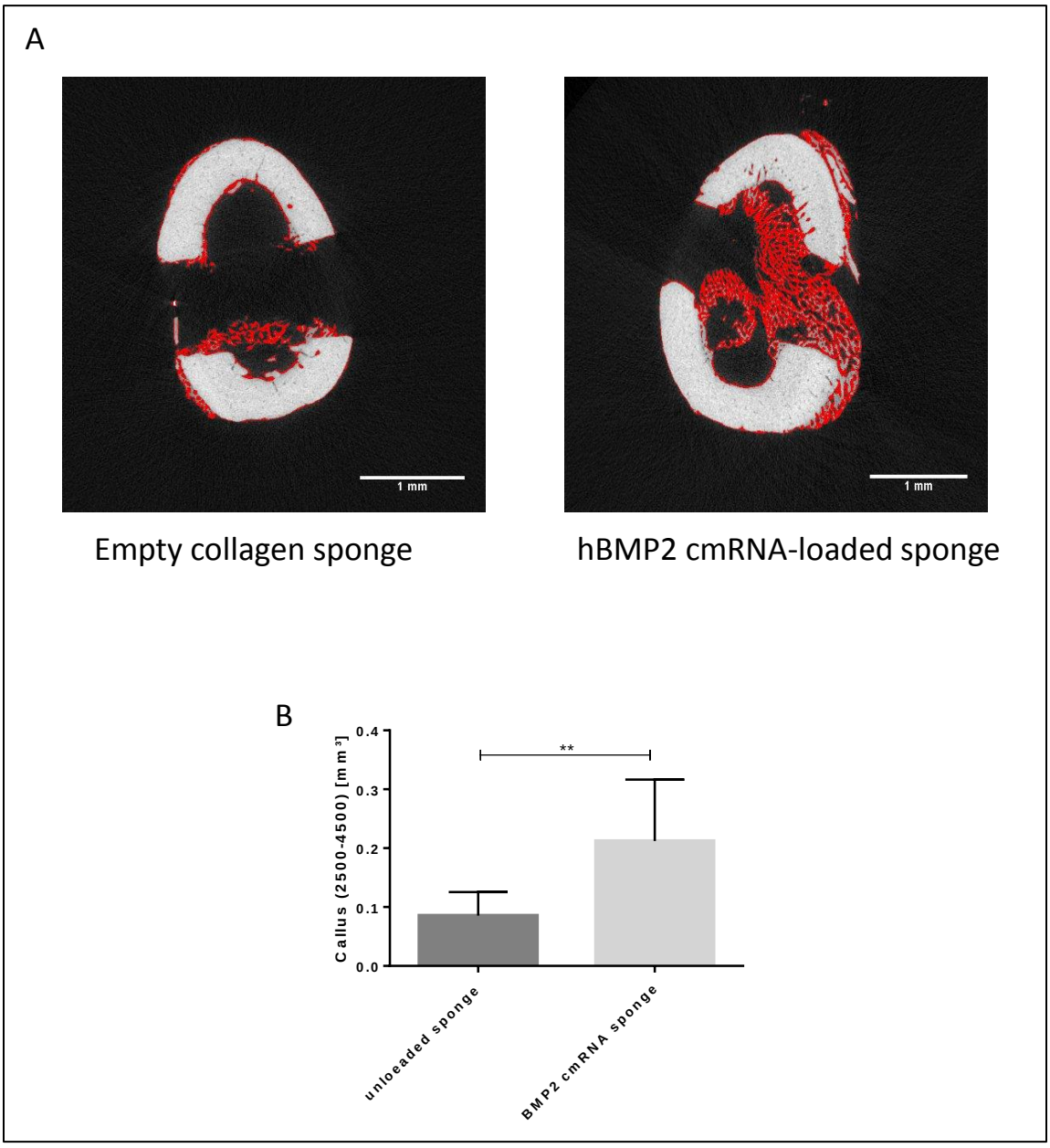

Figure 45 In vivo bone regeneration. (A) µ-CT images of rat femur bone at 2 weeks after implantation. Red parts represent newly formed bone. (B) µ-CT analysis for evaluation of bone formation areas at 2 weeks after implantation. Values compared using t-test (n= 9).

Further analysis with µ-CT in different parts of the bone (periosteal, cortical, and medulla) revealed the highest bone regeneration in the medullary area (Figure 46), where lots of bone marrow stem cells do exist.

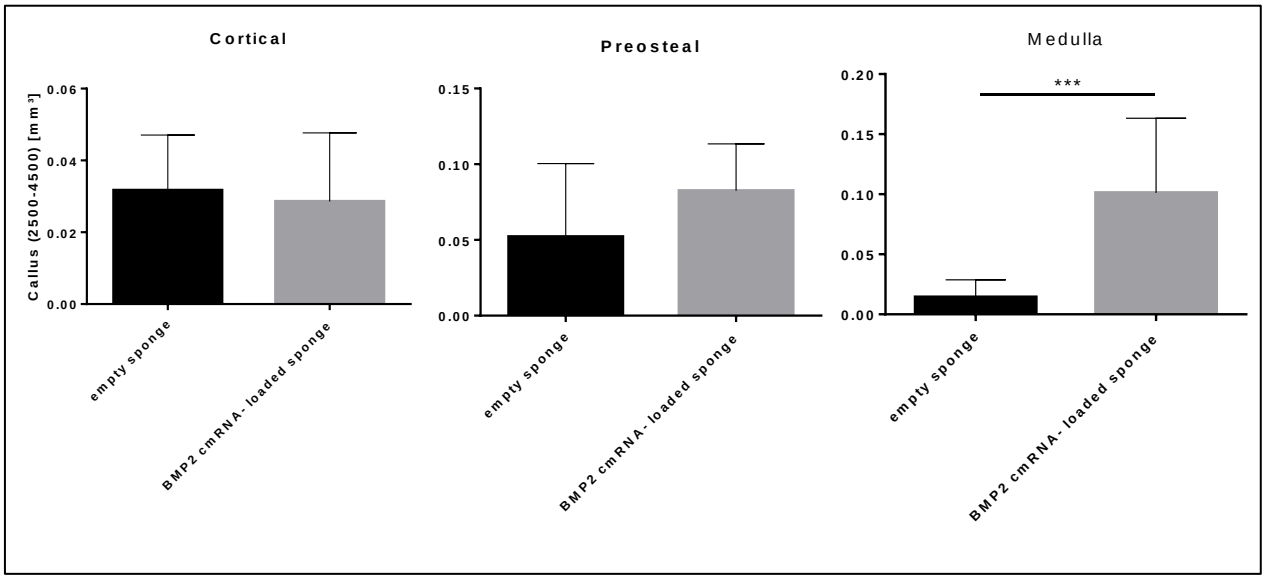

Figure 46 In vivo osteogenic effect of collagen sponges loaded with hBMP2 cmRNA lipoplexes in different parts of bone. Values compared using T-test.

To analyze the newly formed callus tissue in defects treated with hBMP2-encoding TAMs, histomorphometry was carried out at week 2 by Professor Reinhold Erben in the University of Veterinary Medicine Vienna. Similar to the µ-CT results, more mineralized callus formation was found in the hBMP2 cmRNA-treated group relative to controls (Figure 47 A and B). The newly formed callus within the defect contained a higher amount of fibrous tissue in the defects treated with hBMP2-encoding TAMs compared to those treated with empty sponges (Figure 47 C). In the bone healing process, fibrous tissue can trigger osteoid formation and bone regeneration [100]. Accordingly, a trend towards a higher osteoid volume was observed in the hBMP2 cmRNA-treated defects (Figure 47 D).

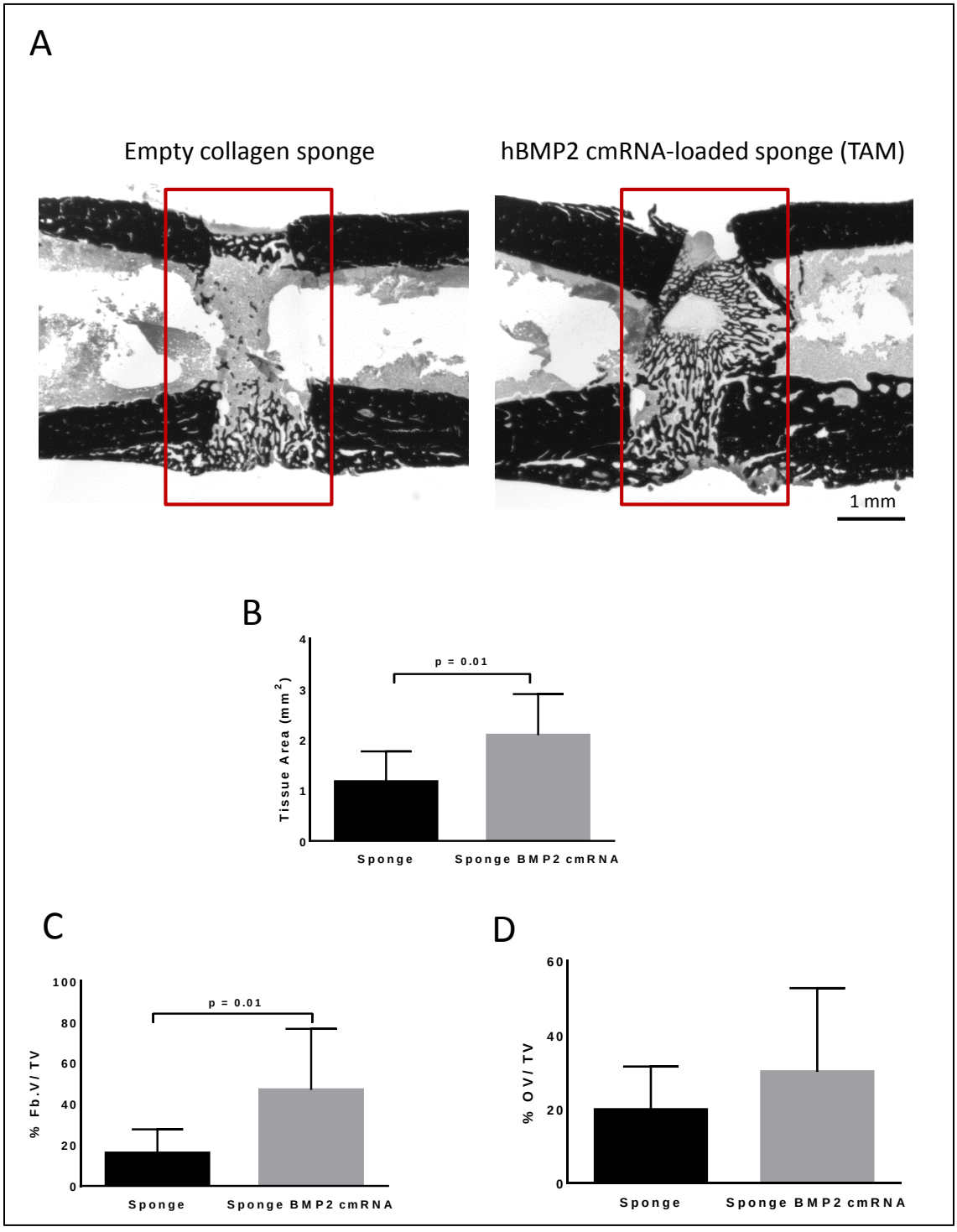

Figure 47 Histomorphometric analysis of in vivo bone regeneration (A) Von Kossa/McNeal staining of 5-µm-thick, longitudinal femoral bone sections. Rectangles show where the sponges were placed in the defect. Mineralized tissue is stained in black. (B) Area of periosteal mineralized callus. (C) Relative amount of fibrous tissue (Fb.V/TV) within the callus in the defect. (D) Osteoid volume (OV/BV) within the callus tissue. Data represent means ± SD for n= 9 animals each. P values were calculated by t-test. Histological evaluations were carried out in the University of Veterinary Medicine Vienna by Prof. Reinhold Erben.

3.2.10 Stability assay of vacuum-dried cmRNA lipoplexes on TAMs

Long-term stability assessment was performed to estimate the shelf life of vacuum-dried cmRNA lipoplexes on TAMs as ready-to-use bioproducts. For this purpose, 96-well-plates containing Met luc-encoding TAMs were vacuum-sealed and stored at room temperature (RT). At regular intervals, one of the plates was used to seed NIH3T3 cells on. 24 h post cell seeding, expression of *Metridia* luciferase was measured. The expressions from plates stored for different time points were then compared to that of a plate which had been used directly after vacuum-drying (time point= 0). As shown in Figure 48, regardless of the applied cmRNA doses, vacuum-dried cmRNA complexes on the TAMs were stable at least for 6 months at RT. After 12 months of storage at RT the TAMs were still active and could transfect the cells; however, the transfection efficacies were reduced to some extent.

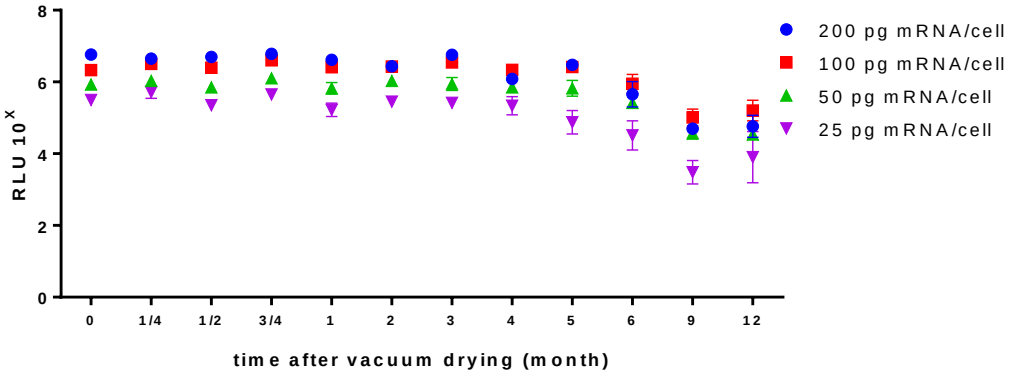

Figure 48 Stability of vacuum-dried cmRNA lipoplexes on TAMs. Metridia luciferase cmRNA-loaded collagen sponges vacuum-dried for 2 h, then vacuum sealed and kept at RT. In different time points after vacuum-drying, plates opened and NIH3T3 cells were seeded on the sponges. Expression of Met luc was measured 24 h after cell seeding. All data shown are mean ± SD from the values of three replicate. Y-axis is in logarithmic scale.

4 Discussion

The future prospects of regenerative medicine and tissue engineering include the regeneration or even replacement of damaged tissues or organs in order to restore their normal functions [101]. To do this, differentiation and dedifferentiation of the cells have been used as strong tools in regenerative medicine, when a cell can be reprogrammed to the desired state [102]. To date, most of work in this area has been performed using gene or protein delivery [63, 101, 103-105]. In this thesis, we take advantage of cmRNAs, which have remarkable benefits over gene and recombinant protein therapy [17, 18, 21], but rarely have been used for cell fate conversion [86, 96].

To successfully design robust systems for genetic modifications of cells, we attempted to combat the most critical difficulties seen in cell fate conversion. One major problem in cell reprogramming is low efficacy [86, 106]. The other difficulty in this area is that normally cell fate conversion needs a prolonged protein expression for a defined time [86, 107, 108], and thus requires repetitive retransfection regime [86]. To address the first problem, magnetofection was introduced as an enhanced cmRNA delivery method. Considering the latter, collagen sponges as "transcript-activated matrices" have been used for sustained cmRNA delivery.

4.1 Safety aspects of mRNA therapeutics over gene and protein therapies

Remarkable advantages of mRNA over DNA make the former a superior choice for gene transfer and protein expression. These advantages include the lack of necessity of nuclear delivery, and no risk of insertional mutagenesis [109]. mRNAs also surpass recombinant protein therapies in safety aspects as the translated proteins are produced by the host protein machinery and undergo all post

translational modifications of the host. Therefore, the immune response, which is normally associated with recombinant protein delivery, might be eliminated [17, 18, 20].

Until very recently mRNA applications were limited to genetic vaccines [110, 111]. This was primarily due to difficulties along with mRNA handling and delivery. Unmodified mRNA is very sensitive to the ubiquitous presence of nucleases, and thus degrade quickly compared to DNAs. Furthermore, mRNA can be detected with a family of pattern-recognition receptors (PRCs), known as Toll-like receptors (TLRs), and activate inflammatory reactions which play an important role in antiviral response in the body [109].

These problems have been recently overcome by using nucleotide modifications that hinder binding mRNA molecules to PRR, and thus reduced the immune reaction. These modification included replacement of 5-50% uridine and cytidine with 2-thiouridine and 5-methylcytidine, respectively [21, 22].

The final cmRNAs, with less immunogenicity and higher stability, have become the focus of intense research in molecular medicine and biotechnology [20, 112].

Thanks to these scientific endeavors, starting with the first preclinical exploration of mRNA in 1990s, mRNAs and cmRNAs are currently being investigated for many therapeutic approaches, from which mRNA-based cancer immunotherapies and infectious disease vaccines are now in their clinical phases [112]. Figure 49 illustrates the current preclinical and clinical studies involving mRNA therapeutics.

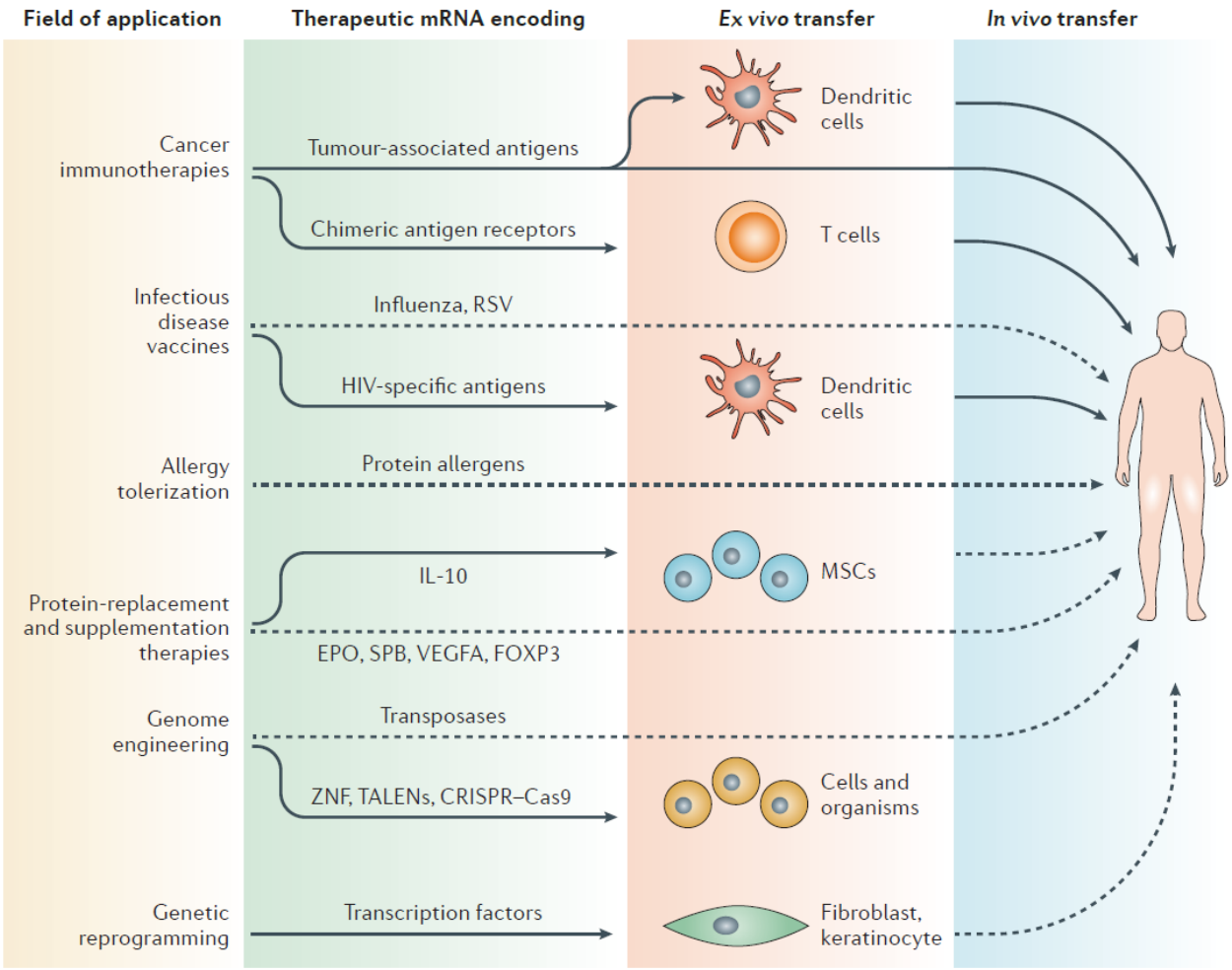

Figure 49 Current therapeutics investigation of mRNA. Figure taken from Sahin et al,/ Nat Rev Drug Discov., (2014) [112]

Despite remarkable achievements in the mRNA therapeutics field, robust systems for efficient mRNA delivery are in early development only [109, 113]. This study established two kinds of delivery methods for cmRNAs: magnetofection for enhanced cmRNA delivery, and using transcript-activated matrices (TAMs) for sustained cmRNA delivery.

4.2 Magnetofection: enhanced cmRNA delivery

Since its discovery in 2000, magnetofection has been widely investigated for enhanced and targeted delivery of DNA, siRNA, shRNA, and antisense oligodesoxynucleotides, as well as of viral vectors [30, 46, 47, 114]. Even though more scientific efforts are necessary to establish efficient magnetofection methods for *in vivo* applications [45], its enhancing effect on nucleic acid delivery *in vitro* has been well established [36]. Consequently, the *in vitro* effect of magnetofection for enhanced mRNA delivery has also been expected, but not guaranteed. Indeed, despite high similarity in the structures, different vectors are suitable for DNA and mRNA delivery [15, 92]. In other words, suitable magnetic nanoparticles that function for enhanced DNA delivery, may not do the same for mRNA delivery. Therefore, magnetofection of cmRNA has been in fact evaluated for the first time in this thesis. The final goal of this *in vitro* optimization was to simplify and improve the efficacy of the current complex protocol for reprogramming somatic cells to pluripotency [86, 87]. However, reprogramming to pluripotency itself stood beyond the scope and objectives of this thesis.

PMEFs have been chosen for all magnetofection screening experiments, as these cells are widely used for reprogramming to iPSCs [86, 106, 115, 116]. Since these cells are not cancerous cell lines, being sensitive to contact inhibition [1], their optimum density was determined prior to all screening assays (Figure 12). The experimental range of cell densities was chosen close to that of recommended in commercially available resources of MEF, i.e. 1 X 10^4 cells/cm2, (product sheet of MEF (C57BL/6) [MEFBL/ 61], (ATCC® SCRC1008 ™)), and further experiments were performed according to the determined optimum cell density (4000 cells/well in a 96-well-plate format). In the next step, a suitable vector for magnetofection of cmRNA was identified, considering transfection efficiency and cell toxicity. DreamFect™ Gold (Df-Gold), as an example

of cationic lipid vectors, was compared to PAA20k-EPE, a cationic polymer. The vectors were compared in their efficacy for cmRNA delivery, either alone (in form of lipofection and polyfection), or in combination with magnetic nanoparticles (magnetofection). On the other hand, two types of magnetic nanoparticles with different surface charges (PEI Mag2 positively and SO-Mag5 negatively charged) were tested to see the possible effects of surface charge in cmRNA delivery.

Before comparing the vectors, each of them has been optimized considering lipid to nucleic acid (L:N) ratio for cationic lipids, and N:P ratio for cationic polymers. Different L:N and N:P ratios have great influence on the efficacy of nucleic acid, namely mRNA, delivery [16, 117].

In this study L:N=4:1 (V:W) was chosen as the optimum ratio for cmRNA delivery resulting in high transfection efficacy and low cytotoxicity (Figure 13). L:N ratio of 4:1 for Df-Gold has been previously used for the delivery of other nucleic acids [118, 119]. Although a higher L:N ratio like 6:1 enhanced cell viability, transfection efficacy with this ratio was not satisfactory.

Among cationic polymers, a proprietary molecule from Ethris GmbH, PAA20k-EPE, was tested for its efficacy. This polymer contains several secondary amino groups, which help in endosomal escape of the mRNA cargo via proton sponge mechanisms (see Figure 14) [120]. Comparing different N:P ratios of PAA20k-EPE proved that a higher N:P ratio (32 instead of 16) increased cell toxicity, but not the transfection efficacy (Figure 15). This is in line with previous studies that have shown higher N:P ratios do not guarantee higher transfection efficacy in nucleic acid delivery [121], and optimal N:P ratio is specific for every cationic polymer [122].

Although magnetofection improved the transfection efficacy regardless of the type of magnetic nanoparticles, Fe:N ratios of the nanoparticles (Figure 17), and type and amount of non-viral vectors (Figure 15, Figure 13), Df-Gold led to a higher transfection efficacy than PAA20k-EPE

(Figure 16). This is in agreement with findings of Bettinger *et al*., who claimed that usually cationic lipids work better than polymers for mRNA delivery [15].

To find the best type of magnetic nanoparticle for cmRNA delivery, SO-Mag5 (negatively charged) and PEI Mag2 (Positively charged) were compared for different Fe:N ratios. No matter whether SO-Mag5 or PEI Mag2 were used, all resulting magnetic lipoplexes were positively charged (Table 3), indicating that the positive charge of the cationic lipid more than neutralized the charge of the magnetic nanoparticles. Although the zeta potential was almost the same for magnetic lipoplexes composing SO-Mag5 or PEI Mag2, the size measurements showed dramatic differences. Magnetic lipoplexes containing SO-Mag5 were approximately five times bigger than those with PEI Mag2. However, they showed no significant differences in transfection efficacy of Luc cmRNA in PMEFs (Figure 17). These data disagree with other findings for conventional DNA-based gene delivery, where Baichao *et al*., for example, showed that bigger lipoplexes had higher efficiency, as the large particles facilitated membrane fusion [123]. The relation between size and transfection efficiency of nucleic acids is reported in other studies as well [124-126]. Concerning magnetic lipoplexes however, Plank, *et al*. claimed no direct relationship between size and transfection efficacy [36]. Based on these findings, magnetic nanoparticles in different size ranges are forced to the surface of target cells and thus accelerate the endocytosis rates. This phenomenon can eclipse the efficiency derived from time-dependent aggregation and sedimentation of larger particles.

Regarding the toxicity assays, applied magnetic nanoparticles not only were biocompatible and non-toxic for the cells, but also enhanced cell proliferation and viability (Figure 17). Other studies also confirmed the ability of iron nanoparticles coated with different materials to promote cell proliferation [127, 128].

Next, kinetics studies were performed post cmRNA lipofection and magnetofection, where dramatic enhanced delivery was obtained using magnetofection (Figure 19). Kinetics of expression is a key point to modify the current protocol for reprogramming fibroblasts to iPSCs that needs 14 consecutive days of transfection [87]. In this experiment, magnetofection did not prolong the cmRNA translation. However, it did accelerate the translation of cmRNA, compared to lipofection (peak of translation was at 12 h and 24 h for magnetofection and lipofection, respectively). Based on the enhanced and accelerated cmRNA delivery, by using magnetofection a shorter and more concise protocol for reprogramming to iPSC is expected (probably 7 days instead of 14 days).

One other important requirement for reprogramming to iPSC is the simultaneous cotransfection of four different cmRNAs to fibroblast [84, 86]. In this study, various ways of mixing complex components have been examined to determine the optimal strategy for complex preparations of up to three reporter cmRNAs (Figure 21, and Figure 22). Based on the findings, adding different cmRNAs, sequentially, to the tube containing MNPs and Df-Gold (Strategy 1 in Figure 22 A) led to the highest cotransfection efficacy. In this way, the number of positive cells as well as the intensity of transfected cells is higher than using a cocktail of cmRNAs (see strategy 1 and 3 in Figure 22 B and C). Nevertheless, magnetofection could even further improve the efficacy in each strategy of complex preparation. To date, for reprogramming to iPSC with cmRNAs, a cocktail of cmRNAs has been used [87]. Therefore, our protocol, which benefits not only from an optimized strategy for complex preparation but also enhanced delivery with magnetofection, is likely to improve the efficacy of reprogramming fibroblasts to iPSC (Figure 50).

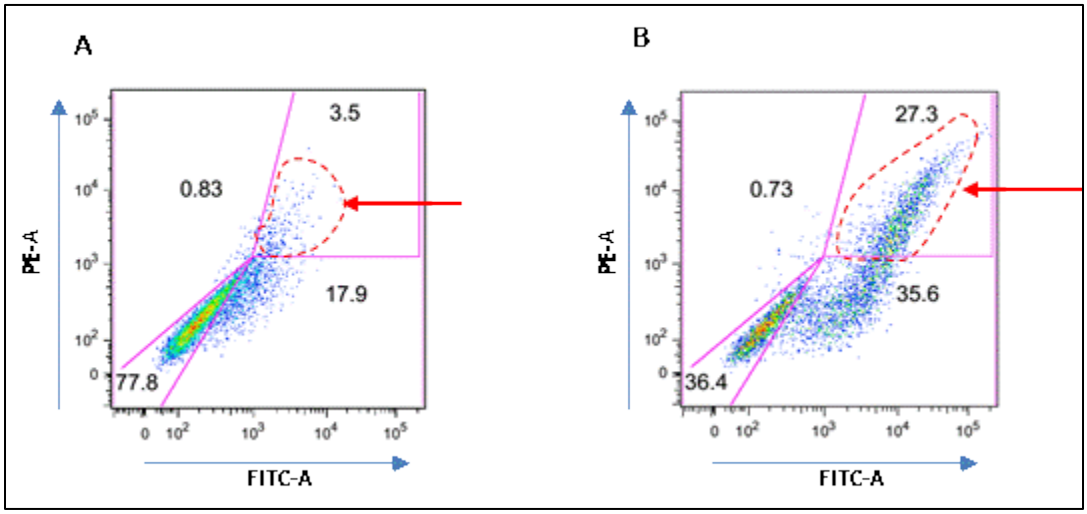

Figure 50 Expected improvement in efficiency of iPSC reprogramming using the optimized magnetofection protocol. FACS analysis: dot plots show the number and intensity of double positive cells after cotransfection of Luc, eGFP and RFP cmRNAs. (A) Current method (lipofection, using a cocktails of cmRNAs), and (B) optimized method in this thesis (magnetofection, adding cmRNAs sequentially to the complex of lipid and MNPs). Arrows show populations of cotransfected cells.

Furthermore, magnetofection significantly improved cotransfection efficiency in coculture of different primary fibroblasts (see Figure 28). In current setup, PMEFs and PFFs were cocultured and transfected following Mandal's protocol (Figure 26) [87], and higher transfection efficacies were obtained, both in single cmRNA transfections (eGFP or RFP) and in cotransfections of different cmRNAs (Luc, eGFP and RFP) (see Figure 27, and Figure 28).

The final protocol for magnetofection of cmRNA is relevant in research and therapeutic applications when simultaneous translations of several cmRNA-encoded proteins are required, such as reprogramming to iPSCs with cmRNAs encoding Yamanaka factors.

4.3 Transcript-activated matrix (TAM): sustained cmRNA delivery

As mentioned previously, mRNA delivery results in rapid and transient protein production. Therefore, a sustained cmRNA delivery system will be useful when a prolonged production of protein is required. The conversion of cells' fates, for instance differentiation to osteoblasts or dedifferentiation to pluripotency, are good examples of such a situation [81, 106]. In this dissertation, a kind of transcript-activated matrix, consisting of collagen sponges loaded with lipoplexes of cmRNAs, has been established for retard cmRNA delivery (Figure 51).

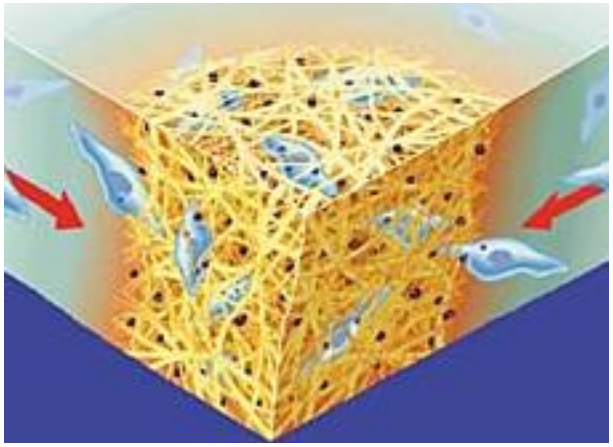

Figure 51 Transcript-activated matrix: vacuum-dried cmRNA complex loaded collagen sponges serve as TAMs, in which cells can grow and proliferate (Source: http://pubs.acs.org/cen/coverstory/7948/print/7948dnadelivery.html)

Firstly, we showed that cells can grow on and in the 3D matrix of a collagen TAM. Collagen sponges have been known for a long time to be suitable 3D scaffods for cell culturing, which can in turn improve cell signaling and cellular behavior, and influence gene expression in the cells [60]. Furthermore, collagen sponges are approved for clinical use as wound dressings or for filling bone defects [129], and have been used to form gene-activated matrices (GAMs) in preclinical research for gene therapy-supported tissue regeneration [60, 130, 131]. GAMs, as described in the literature, are mostly comprised of recombinant adenoviruses and retroviruses [131], or polymer-based

plasmid DNA delivery systems [132]. Here a lipid-base cmRNA delivery system using collagen sponges was applied to prepare ready-to-use TAMs.

A uniform distribution of cmRNA lipoplexes and cells on TAMs was observed (Figure 31, Figure 33, and Figure 34). The quantification of eGFP cmRNA transfection efficacy on the TAMs by FACS analysis demonstrated the remarkably high efficacy of this technology, which approached 100% (Figure 35 B and C). To validate the TAMs for clinical approaches, cell viability was also assessed, and a very high cell viability, around 90%, was observed even for high doses of cmRNA (up to 100 pg/cell), which was acceptable for both *in vitro* and *in vivo* applications. (Figure 30 B). The high cell-viability could be the result of the uniform cell distribution within the 3D matrix, which can closely resemble an *in vivo* situation and improve cell signaling and proliferation [49], and consequently the cells were able to tolerate even high doses of cmRNA complexes. This high cell viability will be particularly beneficial if the general efficacy is low and higher doses of cmRNAs are needed.

In the next step, kinetics of translation of *Metridia* luciferase cmRNA were measured to assess the ability of collagen sponges to provide sustained cmRNA delivery, using NIH3T3 cell line (Figure 36) and primary cells with various cell densities (Figure 39), as well as modified and unmodified mRNAs (Figure 37). Based on the kinetics results, TAMs provide a robust sustained delivery system for cmRNAs, which is independent of mRNA modifications, cell type and cell density, even for primary cells which are more sensitive to contact inhibition and cell density [90]. Such a system will be very advantageous if there is a lack of a source of cells and patient samples, when a switch to a low cell density would also be feasible.

To have such a retard delivery system, vacuum-drying seems to play a critical role, whereas the translation of cmRNAs in non-dried sponges decreased faster than in dried ones. In addition, the translation of cmRNAs on the non-dried sponges had a shorter half-life (18 h) than that of cmRNAs

on the dried sponges (23 h) (Figure 38). The prolonged cmRNA delivery after vacuum-drying might be due to the closed structure of TAMs (Figure 32), where imprisoned lipoplexes need time to either reach the cells or be released from the matrix [81]. The uniform distribution of the vacuum-dried cmRNA lipoplexes on the TAMs (Figure 33) could be another reason for the steady state protein production for several days, without peaks of transfection efficacy or a burst release [81].

Vacuum-drying had another substantial influence, stabilizing cmRNA complexes on the TAMs for at least 6 months at RT (Figure 48). This considerable shelf life for the very sensitive mRNA molecules [133] can in turn increase the availability and ease of use of potential cmRNA therapeutics, especially in developing countries with minimum storage conditions, and bring cmRNAs closer to the clinical applications.

When TAM had been well optimized for delivery of reporter cmRNAs into the cell line as well as the primary cells, the system was tested for potential delivery of a physiological cmRNA, namely hBMP2.

First, TAMs indeed prolonged delivery of physiological cmRNA, where translation of the hBMP2 cmRNA was detected five days after seeding the cells on the hBMP2-encoading TMAs (Figure 40).

Then, the system was tested at the preclinical level, and hBMP2-encoding TAMs were applied to induce bone formation *in vitro,* and *in vivo*.

Indeed, the bone-inducing effect of BMP2 cmRNA complexes with PEI has been very recently published [96]. In our study, however, we proved that dried cmRNA-PEI polyplexes on TAM were not able to transfect the cells, and thus were not suitable vectors for our delivery system. cmRNA lipoplexes, on the other hand, showed very high transfection efficiencies (Figure 30 A). In addition, cmRNA-PEI polyplexes were more toxic than cmRNA lipoplexes (Figure 30 B), which can be the result of their high positive surface charges (Table 4) [134]. Moreover, the size of hBMP2 cmRNA

lipoplexes in this study was half that of cmRNA polyplexes that Elangovan *et. al* used (Table 4) [96]. The smaller particle size here (around 50 nm) can improve *in vitro* cellular uptake as well as *in vivo* pharmacokinetics and biodistribution [135].

Various studies have proven the effect of BMP2 protein in bone tissue engineering, using different carriers [81, 82, 136]. However, currently collagen is the only FDA approved carrier for recombinant hBMP2. Consequently, the efficiency of collagen as a carrier for stabilized hBMP2 cmRNAs was investigated in this thesis. Just recently, Balmayor *et. al* indicated that hBMP2 cmRNAs can trigger bone formation using fibrin matrices [137]. However, collagen sponges are easier to handle, especially considering *in vivo* applications, and also provide stable and ready-to-use bioproducts for clinical applications in tissue engineering.

In vitro bone differentiation was performed using the osteoblast-like cell line (MC3T3-E1) (Figure 41) and MSCs (Figure 44), seeded on the hBMP2-encoding TAMs [81, 98]. With MC3T3-E1 cells, hBMP2 cmRNA had a significant effect in triggering bone formation, as expression of osteogenic markers was several fold higher in transfected cells than in untransfected cells seeded on 3D collagen scaffolds (Figure 41).

On the contrary, there was almost no significant difference in expression of osteogenic markers between hBMP2 transfected MSCs and untransfected MSCs on the collagen sponges (Figure 44 A). However, expression of hBMP2 from MSCs seeded on the hBMP2 cmRNA-loaded collagen sponge was previously detected, using ELISA (Figure 43). According to this data, collagen sponges themselves can trigger bone regeneration in MSCs *in vitro*. Previously, it also had been shown that collagen itself could be used as bone substitutes due to its osteoinductive activity [67].

Another explanation for this phenomenon may be the dramatic macroscopic changes in transfected and untransfected collagen sponges containing MSCs (Figure 44 B). By day 7, sponges loaded with hBMP2 appeared fluffier and had expanded in size, while unloaded sponges condensed and shrank

over time. Since MSCs were too confluent in the unloaded shrunken sponges, they would probably lose their multipotency and start to program to the terminally differentiated cells [138, 139], and as they were growing in the osteogenic medium, an osteogenic differentiation would be most likely. To perform the *in vivo* experiment, loaded and unloaded collagen sponges were implanted into the rat femur defects. Two weeks later, rats were sacrificed and bone formation was evaluated using µ-CT and histomorphometry. The obtained results were similar to those of *in vitro* osteogenic differentiation. Both µ-CT results and histomorphometry showed significantly higher bone formation in the defects treated with hBMP2-encoding TAMs, compared to empty collagens (Figure 45, Figure 47). µCT analysis showed that the maximum bone formation took place in the medullary area (Figure 46). Although for an ideal tissue engineering strategy, new bones should be created mostly in the cortical area, the predominantly medullary bone formation seen in this study may be due to placement of collagen sponges in the bone defects. In our study, the collagen sponges were placed in the whole bone defect (and not just in the cortical part). Since the marrow cavity contains more BMSCs compared to other parts of the bone, maximum hBMP2 cmRNA-induced bone formation may have happened there. In other words, to see a cortical bone formation, hBMP2-encoading TAMs should be placed just in the cortical area, which is not feasible in a rat model, due to the small size of rat bones. Other publications treating the same animal model with recombinant BMP2 protein also showed more bone formation in the medullary than in the cortical area at 2 weeks post-surgery. However, more cortical bone formation was observed at 4 weeks post-surgery [140]. Therefore, additional experiments at later time points would be useful for investigation of bone regeneration in the cortical area.

These results were different from what had been seen in the *in vitro* osteogenic differentiation using MSCs, where hBMP2 cmRNA-loaded and unloaded collagen sponges were equally effective (Figure 44 A). This difference could be due to differences in the *in vitro* and *in vivo* circumstances,

as many factors could influence the effect of BMPs and collagen sponges for bone regeneration *in vivo*, such as the presence of small molecules, growth factors and cytokines [141-143]. Such factors are missing in the *in vitro* situation, and thus *in vivo* results may not exactly follow *in vitro* results. Accordingly, for future studies, collagen sponges can be pre-loaded not only with desired cmRNA lipoplexes, but also with small molecules and cytokines, which can enhance the immigration of MSCs inside the sponges [144, 145], and thus improve the transfection efficacy.

Overall, this project revealed the safety, efficiency, and stability of transcript-activated matrices as ready-to-use bioproducts. The virus-free and gene-free technology provides a cmRNA-based sustained delivery system, which is independent from RNA modification, cell type and cell density. Investigating bone differentiation *in vitro* and *in vivo* with this technology confirmed the usefulness of TAMs for clinical applications, when a prolonged protein delivery meets the aim of therapy. This study opens new ways for easier yet promising applications of messenger RNA which surpass DNA-based gene therapy in safety aspects.

5 References

[1] Alberts B, Bray D, Hopkin K, Johnson A, Lewis J, Raff M, et al. Essential cell biology: Garland Science; 2013.
[2] Barrett LW, Fletcher S, Wilton SD. Regulation of eukaryotic gene expression by the untranslated gene regions and other non-coding elements. Cellular and molecular life sciences. 2012;69:3613-34.
[3] Pichon X, Wilson LA, Stoneley M, Bastide A, King HA, Somers J, et al. RNA binding protein/RNA element interactions and the control of translation. Current protein & peptide science. 2012;13:294.
[4] Penalva LO, Sánchez L. RNA binding protein sex-lethal (Sxl) and control of Drosophila sex determination and dosage compensation. Microbiology and molecular biology reviews. 2003;67:343-59.
[5] Malone RW, Felgner PL, Verma IM. Cationic liposome-mediated RNA transfection. Proceedings of the National Academy of Sciences. 1989;86:6077-81.
[6] Lewis JD, Izaurflde E. The role of the cap structure in RNA processing and nuclear export. European Journal of Biochemistry. 1997;247:461-9.
[7] Burkard KT, Butler JS. A nuclear 3′-5′ exonuclease involved in mRNA degradation interacts with Poly (A) polymerase and the hnRNA protein Npl3p. Molecular and cellular biology. 2000;20:604-16.
[8] Shatkin A. Capping of eucaryotic mRNAs. Cell. 1976;9:645-53.
[9] Guhaniyogi J, Brewer G. Regulation of mRNA stability in mammalian cells. Gene. 2001;265:11-23.
[10] Schellekens H. Immunogenicity of therapeutic proteins: clinical implications and future prospects. Clinical therapeutics. 2002;24:1720-40.
[11] Pollard H, Remy J-S, Loussouarn G, Demolombe S, Behr J-P, Escande D. Polyethylenimine but not cationic lipids promotes transgene delivery to the nucleus in mammalian cells. Journal of Biological Chemistry. 1998;273:7507-11.
[12] Brunner S, Sauer T, Carotta S, Cotten M, Saltik M, Wagner E. Cell cycle dependence of gene transfer by lipoplex, polyplex and recombinant adenovirus. Gene therapy. 2000;7:401-7.
[13] Howe SJ, Mansour MR, Schwarzwaelder K, Bartholomae C, Hubank M, Kempski H, et al. Insertional mutagenesis combined with acquired somatic mutations causes leukemogenesis following gene therapy of SCID-X1 patients. The Journal of clinical investigation. 2008;118:3143.
[14] Baum C, von Kalle C, Staal FJ, Li Z, Fehse B, Schmidt M, et al. Chance or necessity? Insertional mutagenesis in gene therapy and its consequences. Molecular Therapy. 2004;9:5-13.
[15] Bettinger T, Carlisle RC, Read ML, Ogris M, Seymour LW. Peptide-mediated RNA delivery: a novel approach for enhanced transfection of primary and post-mitotic cells. Nucleic acids research. 2001;29:3882-91.
[16] Mitchell DA, Nair SK. RNA-transfected dendritic cells in cancer immunotherapy. Journal of Clinical Investigation. 2000;106:1065.
[17] Yamamoto A, Kormann M, Rosenecker J, Rudolph C. Current prospects for mRNA gene delivery. European Journal of Pharmaceutics and Biopharmaceutics. 2009;71:484-9.
[18] Tavernier G, Andries O, Demeester J, Sanders NN, De Smedt SC, Rejman J. mRNA as gene therapeutic: how to control protein expression. Journal of Controlled Release. 2011;150:238-47.
[19] Esteller M. Non-coding RNAs in human disease. Nature Reviews Genetics. 2011;12:861-74.

[20] Van Tendeloo VF, Ponsaerts P, Berneman ZN. mRNA-based gene transfer as a tool for gene and cell therapy. Current opinion in molecular therapeutics. 2007;9:423-31.
[21] Kormann MS, Hasenpusch G, Aneja MK, Nica G, Flemmer AW, Herber-Jonat S, et al. Expression of therapeutic proteins after delivery of chemically modified mRNA in mice. Nature biotechnology. 2011;29:154-7.
[22] Karikó K, Buckstein M, Ni H, Weissman D. Suppression of RNA recognition by Toll-like receptors: the impact of nucleoside modification and the evolutionary origin of RNA. Immunity. 2005;23:165-75.
[23] Qiu P, Ziegelhoffer P, Sun J, Yang N. Gene gun delivery of mRNA in situ results in efficient transgene expression and genetic immunization. Gene therapy. 1996;3:262-8.
[24] Van Tendeloo VF, Ponsaerts P, Lardon F, Nijs G, Lenjou M, Van Broeckhoven C, et al. Highly efficient gene delivery by mRNA electroporation in human hematopoietic cells: superiority to lipofection and passive pulsing of mRNA and to electroporation of plasmid cDNA for tumor antigen loading of dendritic cells. Blood. 2001;98:49-56.
[25] Nair SK, Boczkowski D, Morse M, Cumming RI, Lyerly HK, Gilboa E. Induction of primary carcinoembryonic antigen (CEA)-specific cytotoxic T lymphocytes in vitro using human dendritic cells transfected with RNA. Nature biotechnology. 1998;16:364-9.
[26] Lu D, Benjamin R, Kim M, Conry R, Curiel D. Optimization of methods to achieve mRNA-mediated transfection of tumor cells in vitro and in vivo employing cationic liposome vectors. Cancer gene therapy. 1994;1:245-52.
[27] Glenn JS, Ellens H, White JM. Delivery of liposome-encapsulated RNA to cells expressing influenza virus hemagglutinin. Methods in enzymology. 1992;221:327-39.
[28] Anderson DM, Hall LL, Ayyalapu AR, Irion VR, Nantz MH, Hecker JG. Stability of mRNA/cationic lipid lipoplexes in human and rat cerebrospinal fluid: methods and evidence for nonviral mRNA gene delivery to the central nervous system. Human gene therapy. 2003;14:191-202.
[29] Strobel I, Berchtold S, Götze A, Schulze U, Schuler G, Steinkasserer A. Human dendritic cells transfected with either RNA or DNA encoding influenza matrix protein M1 differ in their ability to stimulate cytotoxic T lymphocytes. Gene therapy. 2000;7:2028-35.
[30] Plank C, Scherer F, Schillinger U, Anton M. Magnetofection: enhancement and localization of gene delivery with magnetic particles under the influence of a magnetic field. J Gene Med. 2000;2:S24.
[31] Chan L, Nesbeth D, MacKey T, Galea-Lauri J, Gäken J, Martin F, et al. Conjugation of lentivirus to paramagnetic particles via nonviral proteins allows efficient concentration and infection of primary acute myeloid leukemia cells. Journal of virology. 2005;79:13190-4.
[32] Hughes C, Galea-Lauri J, Farzaneh F, Darling D. Streptavidin paramagnetic particles provide a choice of three affinity-based capture and magnetic concentration strategies for retroviral vectors. Molecular Therapy. 2001;3:623-30.
[33] Isalan M, Santori MI, Gonzalez C, Serrano L. Localized transfection on arrays of magnetic beads coated with PCR products. Nature methods. 2005;2:113-8.
[34] Mah C, Fraites TJ, Zolotukhin I, Song S, Flotte TR, Dobson J, et al. Improved method of recombinant AAV2 delivery for systemic targeted gene therapy. Molecular Therapy. 2002;6:106-12.
[35] Pandori MW, Hobson DA, Sano T. Adenovirus–Microbead Conjugates Possess Enhanced Infectivity: A New Strategy for Localized Gene Delivery. Virology. 2002;299:204-12.
[36] Plank C, Zelphati O, Mykhaylyk O. Magnetically enhanced nucleic acid delivery. Ten years of magnetofection—Progress and prospects. Advanced drug delivery reviews. 2011;63:1300-31.

[37] Huth S, Lausier J, Gersting SW, Rudolph C, Plank C, Welsch U, et al. Insights into the mechanism of magnetofection using PEI-based magnetofectins for gene transfer. The journal of gene medicine. 2004;6:923-36.
[38] Plank C, Scherer F, Schillinger U, Bergemann C, Anton M. Magnetofection: enhancing and targeting gene delivery with superparamagnetic nanoparticles and magnetic fields. Journal of liposome research. 2003;13:29-32.
[39] Plank C, Schillinger U, Scherer F, Bergemann C, Rémy J-S, Krötz F, et al. The magnetofection method: using magnetic force to enhance gene delivery. Biological chemistry. 2003;384:737-47.
[40] Plank C, Anton M, Rudolph C, Rosenecker J, Krötz F. Enhancing and targeting nucleic acid delivery by magnetic force. Expert opinion on biological therapy. 2003;3:745-58.
[41] Weissleder Ra, Stark D, Engelstad B, Bacon B, Compton C, White D, et al. Superparamagnetic iron oxide: pharmacokinetics and toxicity. American Journal of Roentgenology. 1989;152:167-73.
[42] Dobson J. Gene therapy progress and prospects: magnetic nanoparticle-based gene delivery. Gene therapy. 2006;13:283-7.
[43] Mykhaylyk O, Zelphati O, Rosenecker J, Plank C. siRNA delivery by magnetofection. Current opinion in molecular therapeutics. 2008;10:493-505.
[44] Mykhaylyk O, Vlaskou D, Tresilwised N, Pithayanukul P, Möller W, Plank C. Magnetic nanoparticle formulations for DNA and siRNA delivery. Journal of Magnetism and Magnetic materials. 2007;311:275-81.
[45] Scherer F, Anton M, Schillinger U, Henke J, Bergemann C, Kruger A, et al. Magnetofection: enhancing and targeting gene delivery by magnetic force in vitro and in vivo. Gene therapy. 2002;9:102-9.
[46] Wang C, Ding C, Kong M, Dong A, Qian J, Jiang D, et al. Tumor-targeting magnetic lipoplex delivery of short hairpin RNA suppresses IGF-1R overexpression of lung adenocarcinoma A549 cells in vitro and in vivo. Biochemical and biophysical research communications. 2011;410:537-42.
[47] Krötz F, de Wit C, Sohn H-Y, Zahler S, Gloe T, Pohl U, et al. Magnetofection--a highly efficient tool for antisense oligonucleotide delivery in vitro and in vivo. Molecular therapy: the journal of the American Society of Gene Therapy. 2003;7:700-10.
[48] Haycock JW. 3D cell culture: a review of current approaches and techniques. 3D Cell Culture: Springer; 2011. p. 1-15.
[49] Mueller-Klieser W. Three-dimensional cell cultures: from molecular mechanisms to clinical applications. American Journal of Physiology-Cell Physiology. 1997;273:C1109-C23.
[50] Huh D, Hamilton GA, Ingber DE. From 3D cell culture to organs-on-chips. Trends in cell biology. 2011;21:745-54.
[51] Pampaloni F, Reynaud EG, Stelzer EH. The third dimension bridges the gap between cell culture and live tissue. Nature reviews Molecular cell biology. 2007;8:839-45.
[52] Toda S, Watanabe K, Yokoi F, Matsumura S, Suzuki K, Ootani A, et al. A new organotypic culture of thyroid tissue maintains three-dimensional follicles with C cells for a long term. Biochemical and biophysical research communications. 2002;294:906-11.
[53] Holopainen IE. Organotypic hippocampal slice cultures: a model system to study basic cellular and molecular mechanisms of neuronal cell death, neuroprotection, and synaptic plasticity. Neurochemical research. 2005;30:1521-8.
[54] Ivascu A, Kubbies M. Rapid generation of single-tumor spheroids for high-throughput cell function and toxicity analysis. Journal of biomolecular screening. 2006;11:922-32.
[55] Griffith LG, Swartz MA. Capturing complex 3D tissue physiology in vitro. Nature reviews Molecular cell biology. 2006;7:211-24.

[56] Lee J, Cuddihy MJ, Kotov NA. Three-dimensional cell culture matrices: state of the art. Tissue Engineering Part B: Reviews. 2008;14:61-86.
[57] Carletti E, Motta A, Migliaresi C. Scaffolds for tissue engineering and 3D cell culture. 3D cell culture: Springer; 2011. p. 17-39.
[58] Langer R, Tirrell DA. Designing materials for biology and medicine. Nature. 2004;428:487-92.
[59] Lee CH, Singla A, Lee Y. Biomedical applications of collagen. International journal of pharmaceutics. 2001;221:1-22.
[60] Chevallay B, Herbage D. Collagen-based biomaterials as 3D scaffold for cell cultures: applications for tissue engineering and gene therapy. Medical and Biological Engineering and Computing. 2000;38:211-8.
[61] Negri S, Fila C, Farinato S, Bellomi A, Pagliaro PP. Tissue engineering: chondrocyte culture on type 1 collagen support. Cytohistological and immunohistochemical study. Journal of tissue engineering and regenerative medicine. 2007;1:158-9.
[62] Cen L, Liu W, Cui L, Zhang W, Cao Y. Collagen tissue engineering: development of novel biomaterials and applications. Pediatric research. 2008;63:492-6.
[63] Dang JM, Leong KW. Natural polymers for gene delivery and tissue engineering. Advanced drug delivery reviews. 2006;58:487-99.
[64] Hansbrough JF, Boyce ST, Cooper ML, Foreman TJ. Burn wound closure with cultured autologous keratinocytes and fibroblasts attached to a collagen-glycosaminoglycan substrate. Jama. 1989;262:2125-30.
[65] Harriger MD, Supp AP, Warden GD, Boyce ST. Glutaraldehyde crosslinking of collagen substrates inhibits degradation in skin substitutes grafted to athymic mice. Journal of biomedical materials research. 1997;35:137-45.
[66] Takaoka K, Nakahara H, Yoshikawa H, Masuhara K, Tsuda T, Ono K. Ectopic bone induction on and in porous hydroxyapatite combined with collagen and bone morphogenetic protein. Clinical orthopaedics and related research. 1988;234:250-4.
[67] Murata M, Huang BZ, Shibata T, Imai S, Nagai N, Arisue M. Bone augmentation by recombinant human BMP-2 and collagen on adult rat parietal bone. International Journal of Oral & Maxillofacial Surgery. 1999;28:232-7.
[68] Flanagan TC, Wilkins B, Black A, Jockenhoevel S, Smith TJ, Pandit AS. A collagen-glycosaminoglycan co-culture model for heart valve tissue engineering applications. Biomaterials. 2006;27:2233-46.
[69] Auger F, Rouabhia M, Goulet F, Berthod F, Moulin V, Germain L. Tissue-engineered human skin substitutes developed from collagen-populated hydrated gels: clinical and fundamental applications. Medical and Biological Engineering and Computing. 1998;36:801-12.
[70] Pitaru S, Tal H, Soldinger M, Grosskopf A, Noff M. Partial Regeneration of Periodontal Tissues Using Collagen Barriers: Initial Observations in the Canine*. Journal of Periodontology. 1988;59:380-6.
[71] Ceballos D, Navarro X, Dubey N, Wendelschafer-Crabb G, Kennedy WR, Tranquillo RT. Magnetically aligned collagen gel filling a collagen nerve guide improves peripheral nerve regeneration. Experimental neurology. 1999;158:290-300.
[72] Friess W. Collagen–biomaterial for drug delivery. European Journal of Pharmaceutics and Biopharmaceutics. 1998;45:113-36.
[73] Unterman SR, Rootman DS, Hill JM, Parelman JJ, Thompson HW, Kaufman HE. Collagen shield drug delivery: therapeutic concentrations of tobramycin in the rabbit cornea and aqueous humor. Journal of Cataract & Refractive Surgery. 1988;14:500-4.

[74] Seeherman H, Wozney J, Li R. Bone morphogenetic protein delivery systems. Spine. 2002;27:S16-S23.
[75] McKay WF, Peckham SM, Badura JM. A comprehensive clinical review of recombinant human bone morphogenetic protein-2 (INFUSE® Bone Graft). International orthopaedics. 2007;31:729-34.
[76] Bartus RT, Tracy MA, Emerich DF, Zale SE. Sustained delivery of proteins for novel therapeutic products. Science. 1998;281:1161.
[77] Khan A, Benboubetra M, Sayyed PZ, Wooi Ng K, Fox S, Beck G, et al. Sustained polymeric delivery of gene silencing antisense ODNs, siRNA, DNAzymes and ribozymes: in vitro and in vivo studies. Journal of drug targeting. 2004;12:393-404.
[78] Zuk PA, Zhu M, Mizuno H, Huang J, Futrell JW, Katz AJ, et al. Multilineage cells from human adipose tissue: implications for cell-based therapies. Tissue engineering. 2001;7:211-28.
[79] Segers VF, Lee RT. Stem-cell therapy for cardiac disease. Nature. 2008;451:937-42.
[80] Laurencin C, Attawia M, Lu L, Borden M, Lu H, Gorum W, et al. Poly (lactide-co-glycolide)/hydroxyapatite delivery of BMP-2-producing cells: a regional gene therapy approach to bone regeneration. Biomaterials. 2001;22:1271-7.
[81] Lee JW, Kang KS, Lee SH, Kim J-Y, Lee B-K, Cho D-W. Bone regeneration using a microstereolithography-produced customized poly (propylene fumarate)/diethyl fumarate photopolymer 3D scaffold incorporating BMP-2 loaded PLGA microspheres. Biomaterials. 2011;32:744-52.
[82] Meinel L, Hofmann S, Betz O, Fajardo R, Merkle HP, Langer R, et al. Osteogenesis by human mesenchymal stem cells cultured on silk biomaterials: comparison of adenovirus mediated gene transfer and protein delivery of BMP-2. Biomaterials. 2006;27:4993-5002.
[83] Cai S, Fu X, Sheng Z. Dedifferentiation: a new approach in stem cell research. Bioscience. 2007;57:655-62.
[84] Takahashi K, Yamanaka S. Induction of pluripotent stem cells from mouse embryonic and adult fibroblast cultures by defined factors. cell. 2006;126:663-76.
[85] Yamanaka S, Gurdon JB. The Nobel Prize in Physiology or Medicine 2012. 2012.
[86] Warren L, Manos PD, Ahfeldt T, Loh Y-H, Li H, Lau F, et al. Highly efficient reprogramming to pluripotency and directed differentiation of human cells with synthetic modified mRNA. Cell stem cell. 2010;7:618-30.
[87] Mandal PK, Rossi DJ. Reprogramming human fibroblasts to pluripotency using modified mRNA. Nature protocols. 2013;8:568-82.
[88] Jesorka A, Orwar O. Liposomes: technologies and analytical applications. Annu Rev Anal Chem. 2008;1:801-32.
[89] Wolbank S, Peterbauer A, Fahrner M, Hennerbichler S, Van Griensven M, Stadler G, et al. Dose-dependent immunomodulatory effect of human stem cells from amniotic membrane: a comparison with human mesenchymal stem cells from adipose tissue. Tissue engineering. 2007;13:1173-83.
[90] Klug WS, Cummings MR, Spencer CA, Palladino MA. Concepts of genetics: Benjamin Cummings; 2014.
[91] Corish P, Tyler-Smith C. Attenuation of green fluorescent protein half-life in mammalian cells. Protein engineering. 1999;12:1035-40.
[92] Dohmen C, Plank C, Rudolph C, Koch C. Compositions for introducing rna into cells. Google Patents; 2014.
[93] Anderson M, Omri A. The effect of different lipid components on the in vitro stability and release kinetics of liposome formulations. Drug delivery. 2004;11:33-9.

[94] Liang X, Mao G, Ng KS. Mechanical properties and stability measurement of cholesterol-containing liposome on mica by atomic force microscopy. Journal of colloid and interface science. 2004;278:53-62.
[95] Milla P, Dosio F, Cattel L. PEGylation of proteins and liposomes: a powerful and flexible strategy to improve the drug delivery. Current drug metabolism. 2012;13:105-19.
[96] Elangovan S, Khorsand B, Do A-V, Hong L, Dewerth A, Kormann M, et al. Chemically modified RNA activated matrices enhance bone regeneration. Journal of Controlled Release. 2015;218:22-8.
[97] Kannan V, Balabathula P, Thoma LA, Wood GC. Effect of sucrose as a lyoprotectant on the integrity of paclitaxel-loaded liposomes during lyophilization. Journal of liposome research. 2014:1-9.
[98] Kim J, Kim IS, Cho TH, Lee KB, Hwang SJ, Tae G, et al. Bone regeneration using hyaluronic acid-based hydrogel with bone morphogenic protein-2 and human mesenchymal stem cells. Biomaterials. 2007;28:1830-7.
[99] Balmayor ER, van Griensven M. Stem Cell Therapy for Bone Disorders. Mesenchymal Stem Cell Therapy, Chase LG, Vemuri MC (eds) Humana Press: New York. 2012:101-16.
[100] Lüllmann-Rauch R. Histologie: De Boeck Supérieur; 2008.
[101] Eguizabal C, Montserrat N, Veiga A, Izpisua BJ. Dedifferentiation, transdifferentiation, and reprogramming: future directions in regenerative medicine. Seminars in reproductive medicine2013. p. 82-94.
[102] Jopling C, Boue S, Belmonte JCI. Dedifferentiation, transdifferentiation and reprogramming: three routes to regeneration. Nature reviews Molecular cell biology. 2011;12:79-89.
[103] Jin Q, Anusaksathien O, Webb S, Rutherford R, Giannobile W. Gene therapy of bone morphogenetic protein for periodontal tissue engineering. Journal of periodontology. 2003;74:202-13.
[104] Bonadio J, Smiley E, Patil P, Goldstein S. Localized, direct plasmid gene delivery in vivo: prolonged therapy results in reproducible tissue regeneration. Nature medicine. 1999;5:753-9.
[105] Reddi AH. Role of morphogenetic proteins in skeletal tissue engineering and regeneration. Nature biotechnology. 1998;16:247-52.
[106] Wernig M, Meissner A, Foreman R, Brambrink T, Ku M, Hochedlinger K, et al. In vitro reprogramming of fibroblasts into a pluripotent ES-cell-like state. Nature. 2007;448:318-24.
[107] Petite H, Viateau V, Bensaid W, Meunier A, de Pollak C, Bourguignon M, et al. Tissue-engineered bone regeneration. Nature biotechnology. 2000;18:959-63.
[108] Lin Y, Tang W, Wu L, Jing W, Li X, Wu Y, et al. Bone regeneration by BMP-2 enhanced adipose stem cells loading on alginate gel. Histochemistry and cell biology. 2008;129:203-10.
[109] McIvor RS. Therapeutic Delivery of mRNA: The Medium Is the Message. Molecular Therapy. 2011;19:822.
[110] Pascolo S. Messenger RNA-based vaccines. Expert opinion on biological therapy. 2004;4:1285-94.
[111] Cannon G, Weissman D. RNA based vaccines. DNA and cell biology. 2002;21:953-61.
[112] Sahin U, Karikó K, Türeci Ö. mRNA-based therapeutics [mdash] developing a new class of drugs. Nature Reviews Drug Discovery. 2014.
[113] Fenton OS, Kauffman KJ, McClellan RL, Appel EA, Dorkin JR, Tibbitt MW, et al. Bioinspired Alkenyl Amino Alcohol Ionizable Lipid Materials for Highly Potent In Vivo mRNA Delivery. Advanced materials. 2016.

[114] Mykhaylyk O, Zelphati O, Hammerschmid E, Anton M, Rosenecker J, Plank C. Recent advances in magnetofection and its potential to deliver siRNAs in vitro. siRNA and miRNA Gene Silencing: Springer; 2009. p. 1-36.
[115] Woltjen K, Michael IP, Mohseni P, Desai R, Mileikovsky M, Hämäläinen R, et al. piggyBac transposition reprograms fibroblasts to induced pluripotent stem cells. Nature. 2009;458:766-70.
[116] Wernig M, Meissner A, Cassady JP, Jaenisch R. c-Myc is dispensable for direct reprogramming of mouse fibroblasts. Cell stem cell. 2008;2:10-2.
[117] Gary DJ, Min J, Kim Y, Park K, Won YY. The Effect of N/P Ratio on the In Vitro and In Vivo Interaction Properties of PEGylated Poly [2-(dimethylamino) ethyl methacrylate]-Based siRNA Complexes. Macromolecular bioscience. 2013;13:1059-71.
[118] Mykhaylyk O, Steingötter A, Perea H, Aigner J, Botnar R, Plank C. Nucleic acid delivery to magnetically-labeled cells in a 2D array and at the luminal surface of cell culture tube and their detection by MRI. Journal of biomedical nanotechnology. 2009;5:692-706.
[119] Sanchez-Antequera Y, Mykhaylyk OM, Thalhammer S, Plank C. Gene delivery to Jurkat T cells using non-viral vectors associated with magnetic nanoparticles. International Journal of Biomedical Nanoscience and Nanotechnology. 2010;1:202-29.
[120] Liang W, Lam JK. Endosomal escape pathways for non-viral nucleic acid delivery systems: INTECH Open Access Publisher; 2012.
[121] Lee C-H, Ni Y-H, Chen C-C, Chou C-K, Chang F-H. Synergistic effect of polyethylenimine and cationic liposomes in nucleic acid delivery to human cancer cells. Biochimica et Biophysica Acta (BBA)-Biomembranes. 2003;1611:55-62.
[122] Sizovs A, McLendon PM, Srinivasachari S, Reineke TM. Carbohydrate polymers for nonviral nucleic acid delivery. Nucleic Acid Transfection: Springer; 2010. p. 131-90.
[123] Ma B, Zhang S, Jiang H, Zhao B, Lv H. Lipoplex morphologies and their influences on transfection efficiency in gene delivery. Journal of Controlled Release. 2007;123:184-94.
[124] Ross P, Hui S. Lipoplex size is a major determinant of in vitro lipofection efficiency. Gene therapy. 1999;6:651-9.
[125] Almofti MR, Harashima H, Shinohara Y, Almofti A, Li W, Kiwada H. Lipoplex size determines lipofection efficiency with or without serum. Molecular membrane biology. 2003;20:35-43.
[126] Li W, Ishida T, Okada Y, Oku N, Kiwada H. Increased gene expression by cationic liposomes (TFL-3) in lung metastases following intravenous injection. Biological and Pharmaceutical Bulletin. 2005;28:701-6.
[127] Shi S-F, Jia J-F, Guo X-K, Zhao Y-P, Chen D-S, Guo Y-Y, et al. Biocompatibility of chitosan-coated iron oxide nanoparticles with osteoblast cells. International journal of nanomedicine. 2012;7:5593.
[128] Gholami A, Rasoul-amini S, Ebrahiminezhad A, Seradj SH, Ghasemi Y. Lipoamino Acid Coated Superparamagnetic Iron Oxide Nanoparticles Concentration and Time Dependently Enhanced Growth of Human Hepatocarcinoma Cell Line (Hep-G2). Journal of Nanomaterials. 2015;2015.
[129] Domb AJ, Kumar N. Biodegradable polymers in clinical use and clinical development: John Wiley & Sons; 2011.
[130] Scherer F, Schillinger U, Putz U, Stemberger A, Plank C. Nonviral vector loaded collagen sponges for sustained gene delivery in vitro and in vivo. The journal of gene medicine. 2002;4:634-43.
[131] De Laporte L, Shea LD. Matrices and scaffolds for DNA delivery in tissue engineering. Advanced drug delivery reviews. 2007;59:292-307.

[132] Tierney EG, Duffy GP, Cryan S-A, Curtin CM, O'Brien FJ. Non-viral gene-activated matrices: next generation constructs for bone repair. Organogenesis. 2013;9:22-8.
[133] Belasco JG, Brawerman G. Control of messenger RNA stability: Elsevier; 2012.
[134] Fröhlich E. The role of surface charge in cellular uptake and cytotoxicity of medical nanoparticles. Int J Nanomedicine. 2012;7:5577-91.
[135] Albanese A, Tang PS, Chan WC. The effect of nanoparticle size, shape, and surface chemistry on biological systems. Annual review of biomedical engineering. 2012;14:1-16.
[136] Kempen DH, Lu L, Heijink A, Hefferan TE, Creemers LB, Maran A, et al. Effect of local sequential VEGF and BMP-2 delivery on ectopic and orthotopic bone regeneration. Biomaterials. 2009;30:2816-25.
[137] Balmayor ER, Geiger JP, Aneja MK, Berezhanskyy T, Utzinger M, Mykhaylyk O, et al. Chemically modified RNA induces osteogenesis of stem cells and human tissue explants as well as accelerates bone healing in rats. Biomaterials. 2016.
[138] Sekiya I, Larson BL, Smith JR, Pochampally R, Cui JG, Prockop DJ. Expansion of human adult stem cells from bone marrow stroma: conditions that maximize the yields of early progenitors and evaluate their quality. Stem cells. 2002;20:530-41.
[139] Colter DC, Class R, DiGirolamo CM, Prockop DJ. Rapid expansion of recycling stem cells in cultures of plastic-adherent cells from human bone marrow. Proceedings of the National Academy of Sciences. 2000;97:3213-8.
[140] Keibl C, Fügl A, Zanoni G, Tangl S, Wolbank S, Redl H, et al. Human adipose derived stem cells reduce callus volume upon BMP-2 administration in bone regeneration. Injury. 2011;42:814-20.
[141] Lynch SE, Buser D, Hernandez RA, Weber H, Stich H, Fox CH, et al. Effects of the platelet-derived growth factor/insulin-like growth factor-I combination on bone regeneration around titanium dental implants. Results of a pilot study in beagle dogs. Journal of Periodontology. 1991;62:710-6.
[142] Wan C, Gilbert SR, Wang Y, Cao X, Shen X, Ramaswamy G, et al. Activation of the hypoxia-inducible factor-1α pathway accelerates bone regeneration. Proceedings of the National Academy of Sciences. 2008;105:686-91.
[143] Mountziaris PM, Mikos AG. Modulation of the inflammatory response for enhanced bone tissue regeneration. Tissue Engineering Part B: Reviews. 2008;14:179-86.
[144] Xu F, Shi J, Yu B, Ni W, Wu X, Gu Z. Chemokines mediate mesenchymal stem cell migration toward gliomas in vitro. Oncology reports. 2010;23:1561-7.
[145] Wu Y, Zhao RC. The role of chemokines in mesenchymal stem cell homing to myocardium. Stem Cell Reviews and Reports. 2012;8:243-50.

6 Abbreviations

ATP	Adenosine triphosphate
cmRNA	Chemically modified mRNA
CTP	Cytidine triphosphate
DNA	Deoxyribonucleic acid
Df-Gold	DreamFect Gold
DMEM	Dulbecco's Modified Eagle's Medium
eGFP	Enhanced green fluorescent protein
GAM	Gene-activated matrix
GTP	Guanosine-triphosphate
hBMP2	Human bone morphogenetic proteine2
HE	Hematoxylin eosin
ICH	Immunohistochemistry
iPSC	Induced pluripotent stem cell
IVT	In vitro transcription
L:N	Lipid: Nucleic acid
Luc	Luciferase
MNP	Magnetic nanoparticles
mRNA	Messenger Ribonucleic acid
MSC	Mesenchymal stem cell
N:P	Nitrogen: phosphate
ORF	Open reading frame
PEI	Plyethylenimine

PFF	Porcine fetal fibroblasts
PI	Propidium Iodide
PMEF	Primary mouse embryonic fibroblast
PRR	Pattern recognition receptor
RFP	Red fluorescent protein
RLU	Relative light unit
RT	Room temperature
RTqPCR	Reverse transcription quantitative polymerase chain reaction
SEM	Scanning electron microscopy
shRNA	Small hairpin RNA
siRNA	Small interfering RNA
SNIM RNA	Stabilized non-immunogenic messenger RNA
TAM	Transcript-activated matrix
TLR	Toll-like receptor
UTP	Uridine triphosphate
UTR	Untranslated region
WFI	Water for injection
α-MEM	Alpha Minimum essential medium